FUNCTIONAL ANALYSIS OF FAM83D AND DUPD1 – TWO NOVEL

NERUOGENIC SKELETAL MUSCLE ATROPHY-INDUCED GENES

By Lisa Michelle Cooper

A thesis submitted to the Department of Biology

in partial fulfillment of the requirements for the degree of

Master of Science in Biology

UNIVERSITY OF NORTH FLORIDA

COLLEGE OF ARTS AND SCIENCES

April 2020

CERTIFICATE OF APPROVAL

The thesis "Functional Analysis of Fam83d and Dupd1 – Two Novel Neurogenic Skeletal Muscle Atrophy-Induced Genes" submitted by Lisa Michelle Cooper

Approved by the thesis committee: Date

_____   _____

Dr. David Waddell, Ph.D.
Committee Chair Person

_____   _____

Dr. Frank Smith, Ph.D.

_____   _____

Dr. Joy Wolfram, Ph.D.

Table of Contents

List of Figures

List of Tables

Abstract

Fam83d and Dupd1 have been identified as novel genes in skeletal muscle that are upregulated in response to neurogenic atrophy in a mouse model. qPCR analysis reveaed both genes are expressed in skeletal muscle with Fam83d expression being highest during myoblast proliferation, while Dupd1 expression is highest during myotube differentiation. Overexpression of either protein results in inhibition of proper muscle cell differentiation as evidenced by repression of both myosin heavy chain and myogenin expression. Characterization of transcriptional activity revealed both genes are modulated by myogenic regulatory factors and additionally, Dupd1 expression is enhanced by dexamethasone treatment. Assessment of subcellular localization revealed that Fam83d localizes in a punctate manner in the cytoplasm, while the expression of Dupd1 showed ubiquitous distribution throughout the cell. To assess function, Fam83d or Dupd1 were ectopically overexpressed in cultured muscle cells. Overexpression of Fam83d resulted in significant repression of phosphorylated ERK and AKT. Interestingly, inhibition of the 26S proteasome and the MAP kinase signaling pathway both resulted in stabilization of Fam83d during muscle cell differentiation. Finally, Fam83d has a putative phospholipase D-like domain that appears to be necessary for destabilizing casein kinase Iα and inhibiting ERK phosphorylation in cultured myoblasts. Overexpression of Dupd1 resulted in significant repression of phosphorylated ERK and AMPK. Additionally, Dupd1 overexpression resulted in dramatic increases in GR protein as well as phosphorylated GR, while attenuating activity of a GRE reporter gene. The discovery that Fam83d and Dupd1 are expressed in skeletal muscle combined with the observation that they are induced in response to neurogenic atrophy helps further our understanding of the molecular and cellular events of skeletal muscle wasting

Chapter 1: Background on skeletal muscle atrophy, MuRF1 and cell signaling

Skeletal Muscle Atrophy

Muscle atrophy is identified as the reduction in muscle mass and strength. Muscle mass is maintained by a balance between protein synthesis and protein degradation. When protein degradation outpaces synthesis, atrophy occurs (1). Atrophy can result from a variety of conditions including aging, spinal cord injury, immobilization, corticosteroid exposure, and denervation (2). Many molecular pathways contribute to muscle degradation, but the full scope of these pathway interactions is still unclear. Additional research into muscle degradation mechanisms, such as the ubiquitin proteasome system, will help further elucidate these pathways and may identify possible targets for future therapeutic intervention.

The Ubiquitin Proteasome System

The ubiquitin proteasome system (UPS) is one pathway that participates in muscle degradation. This pathway consists of three proteins, the E1 ubiquitin activating enzyme, the E2 ubiquitin conjugating enzyme and the E3 ubiquitin ligase. A ubiquitin molecule first binds to a cysteine residue on the E1 enzyme. The ubiquitin is then transferred to a cysteine residue on the E2 enzyme. The E2 enzyme transfers the ubiquitin to the target substrate to tag it for degradation. This transfer is regulated by the E3 ubiquitin ligase which has a binding site for both the E2 enzyme and a binding site that is substrate specific (3). The E3 enzyme is crucial as it provides selectivity and specificity to the UPS. The conjugation and ubiquitin transfer continues until the substrate accumulates a chain of four or more molecules of ubiquitin which initiates degradation by the 26s proteasome (Fig. 1).
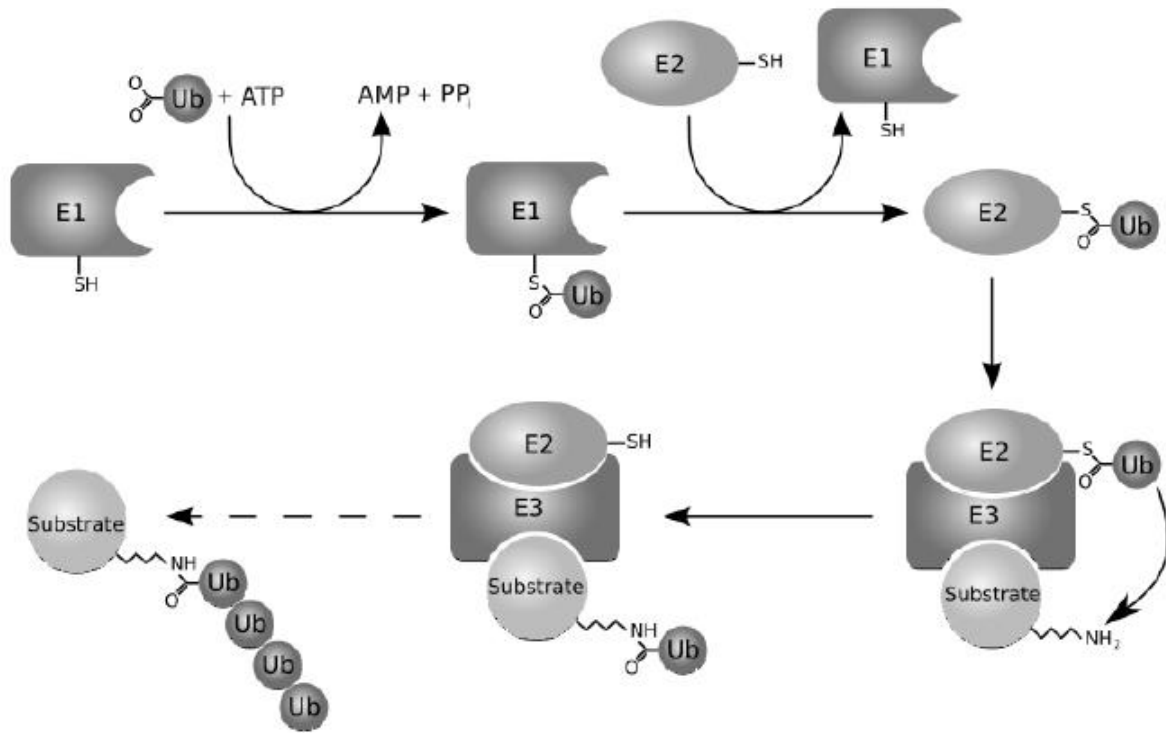
Figure 1. Schematic of the ubiquitin proteasome system. The E1 ubiquitin activating enzyme, E2 ubiquitin conjugating enzyme and E3 ubiquitin ligase form a pathway to ubiquinate substrates for degradation by the 26s proteasome (4).

MuRF1 and MAFbx

Since E3 ubiquitin ligases provide specificity for the ubiquitin proteasome system, identifying muscle specific E3 ubiquitin ligases is a critical component of understanding muscle atrophy pathways. In 2001, a study by Bodine et al identified muscle RING finger 1 (MuRF1) and muscle atrophy F-box (MAFbx) as universal markers of muscle atrophy (2). In the study, rats were subjected to denervation, hind limb suspension, and immobilization. Muscle tissue was then isolated and analyzed for genes showing differential expression between atrophy and control conditions in wild-type animals (2). Many genes showed differential regulation in one or two of the conditions but only MuRF1 and MAFbx were upregulated in all three conditions (Fig.

2). Knockout mice were produced to further examine the role of these two genes and in both cases the knockout mice were atrophy resistant compared to control animals (2). MuRF1 knockouts exhibited 36% muscle sparing and MAFbx knockouts exhibited 56% muscle sparing as compared to control (2). While MAFbx knockouts showed a greater percentage of muscle sparing, the MuRF1 knockouts showed greater muscle integrity making MuRF1 the preferred subject for further study (2). The structure of MuRF1 suggests its role as an E3 ubiquitin ligase but to date there has been a lack of clearly identified protein targets (1), which leads to further questions about MuRF1's role in muscle atrophy.
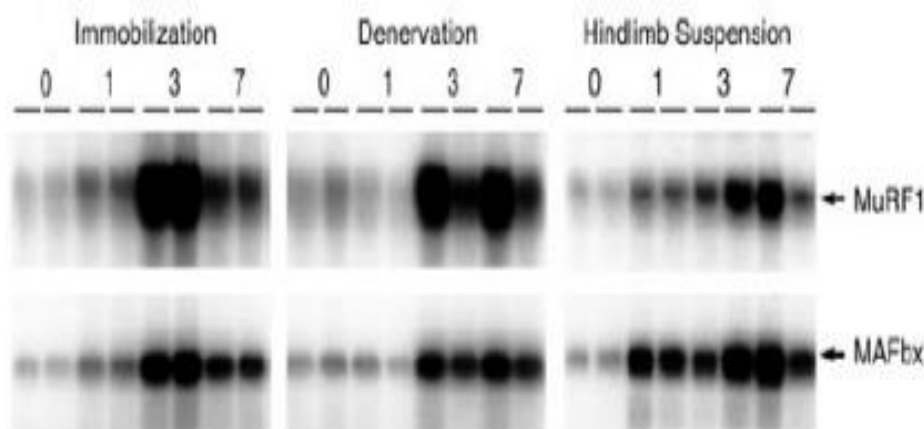
Figure 2. Northern blot displaying mRNA expression of MuRF1 and MAFbx in muscle tissue of rats subjected to atrophy induction by immobilization, denervation, and hind limb suspension. Expression is observed at day 1 and reaches a peak at day 3 post denervation (2).

MuRF1 as a Transcriptional Regulator

In 2013, Furlow et al. investigated MuRF1's role in muscle atrophy more closely using genome-wide microarray analysis (5). Knockout mice were produced by inserting a β-galactosidase lacZ cassette into the MuRF1 gene (2). This insert disrupted the function of the MuRF1 gene and produced β-galactosidase when the MuRF1 promoter is active. This construct allowed researches to assess endogenous MuRF1 promoter activity without the effect of the functional MuRF1 gene.

They compared MuRF1 knockout and control mice under neurogenic atrophy conditions and control conditions by harvesting gastrocnemius muscle at 3 and 14 days post-denervation (5). A microarray analysis was then performed on harvested muscles to identify genes with differential expression at early (3 days) and late (14 days) stages of denervation. In the wild-type (WT) mice, MuRF1 expression was elevated at day 3 post-denervation but returned to baseline by day 14. In the knockout KO) animals, β-galactosidase expression was also elevated at day 3 but remained elevated at day 14, suggesting that MuRF1 may be negatively regulating its own expression (Fig. 3).
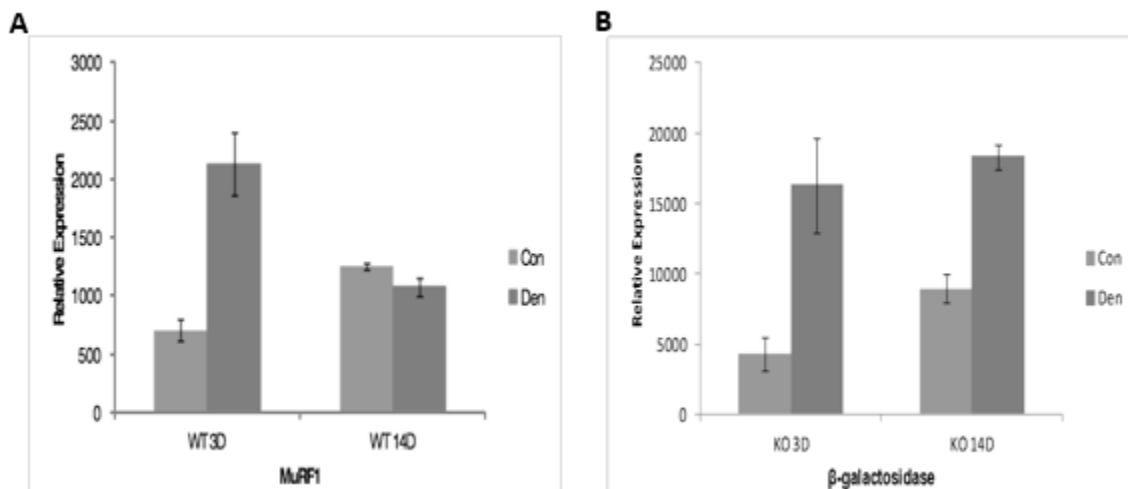
Figure 3. Transcriptional activity of the MuRF1 gene locus in WT and MuRF1 KO mice following sciatic nerve transection. (A) Denervated WT mice showed an increase in MuRF1 gene expression at day 3 (3D), but returned to baseline at day 14 (14D) post-denervation. (B) Denervated KO mice showed at increase in β-galactosidase expression, which is under the control of the MuRF1 promoter, at day 3 and expression remained elevated at day 14 post-denervation (5).

In addition, MAFbx expression varied between the wild-type and MuRF1 knockout mice. Denervated wild-type mice showed increased MAFbx expression at day 3 and expression returned to baseline by day 14 (Fig. 4). However, in the MuRF1 knockout mice, MAFbx

expression was elevated at day 3 and remained elevated at day 14 (Fig. 4). This suggests that

MuRF1 may also be negatively regulating MAFbx expression (5).
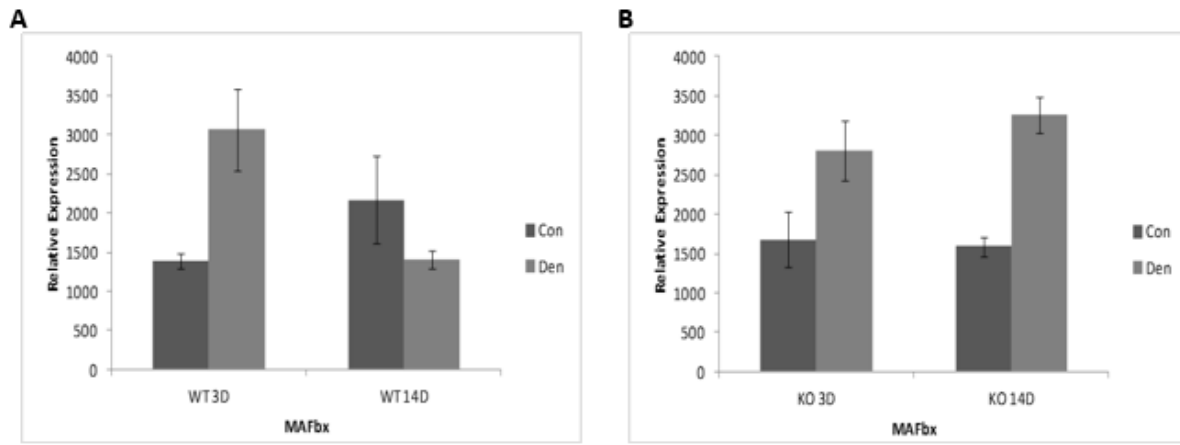
Figure 4. Transcriptional activity of MAFbx in wild-type and MuRF1 KO mice following sciatic nerve transection. (A) Denervated WT mice showed an increase in MAFbx gene expression at day 3 (3D), but expression returned to baseline at day 14 (14D) post-denervation. (B) Denervated MuRF1 KO mice showed an increase in MAFbx gene expression at day 3 and it remained elevated at day 14 post-denervation (5).

Differences in expression were shown for a wide variety of genes when comparing the wild-type

and MuRF1 knockout mice subjected to atrophy conditions. One of these genes, Family with

Sequence Similarity 83 D (Fam83d) is the subject of chapter 2, while Dual specificity

phosphatase and pro isomerase domain containing 1 (Dupd1), is the focus of chapter 3 of this

thesis.

Myogenic Regulatory Factors (MRFs)

Myogenic Regulatory Factors (MRF) are transcription factors important to the development of

muscle tissue and are dramatically upregulated in response to neurogenic atrophy. MRFs

function by interacting with co-activators and co-repressors within the promoter region of

muscle-specific genes (6,7). MRFs are characterized by the presence of a basic helix-loop-helix

motif, which promotes binding to a canonical E-box consensus sequence of 5'-CANNTG-3' (where N can be any nucleotide). These E-box sequences are found in the promoter regions of most muscle-specific genes, which includes MuRF1 and MAFbx. MRFs can bind directly to these E-boxes and modulate the transcriptional activity of genes that possess these enhancers (6,7).

MyoD and myogenin are two such MRFs that have previously been shown to be upregulated during neurogenic skeletal muscle atrophy (7). MyoD acts as a marker of myogenic commitment to skeletal muscle and is important in maintaining the differentiated state of the cells. It is also required for the expression of myogenin, which plays a significant role in muscle cell differentiation and viability (7). Myogenin is also required for full induction of MuRF1 and MAFbx under neurogenic atrophy conditions (8). In fact, previous studies have shown that deletion of myogenin leads to a reduction of MuRF1 and MAFbx and subsequent resistance to muscle wasting in mice following denervation (8).

Signal Transduction Pathways Involved in Muscle Growth and Development
Atrophy is an active process, requiring transcriptional activation and differential regulation of a wide variety of genes (9). This can occur through regulation by one or more signaling pathways that regulate myogenesis, protein synthesis, and protein degradation (9). MAP kinase signaling is an important pathway involved in cell growth, proliferation, and differentiation in a wide variety of tissue types (10). The pathway consists of four main branches including, the ERK1/2, p38, JNK and ERK5 arms (10). Within each of these branches, growth factor binding to receptor tyrosine kinases triggers a signaling cascade that leads to phosphorylation and activation of MAP kinase kinase kinases (MAP3Ks), which in turn phosphorylate MAP2Ks to activate them,

6

which then in turn activates MAPKs by phosphorylation as well (10). Each branch triggers a unique terminal kinase to translocate to the nucleus to act as a transcription factor to modulate the activity of a subset of genes (11). ERK signaling plays a critical role in muscle cell proliferation and repression of premature differentiation through prevention of early cell cycle exit (11). While ERK signaling is reduced as muscle cells differentiate, ERK1/2 activity has been shown to increase again during terminal differentiation and has been found to be critical for proper myocyte fusion and survival (12). ERK1/2 signaling likely has a role to play in skeletal muscle atrophy as evidenced by improved myogenesis and reduced muscle wasting in cachexic mice following treatment with PD98059, an ERK-specific inhibitor (13).
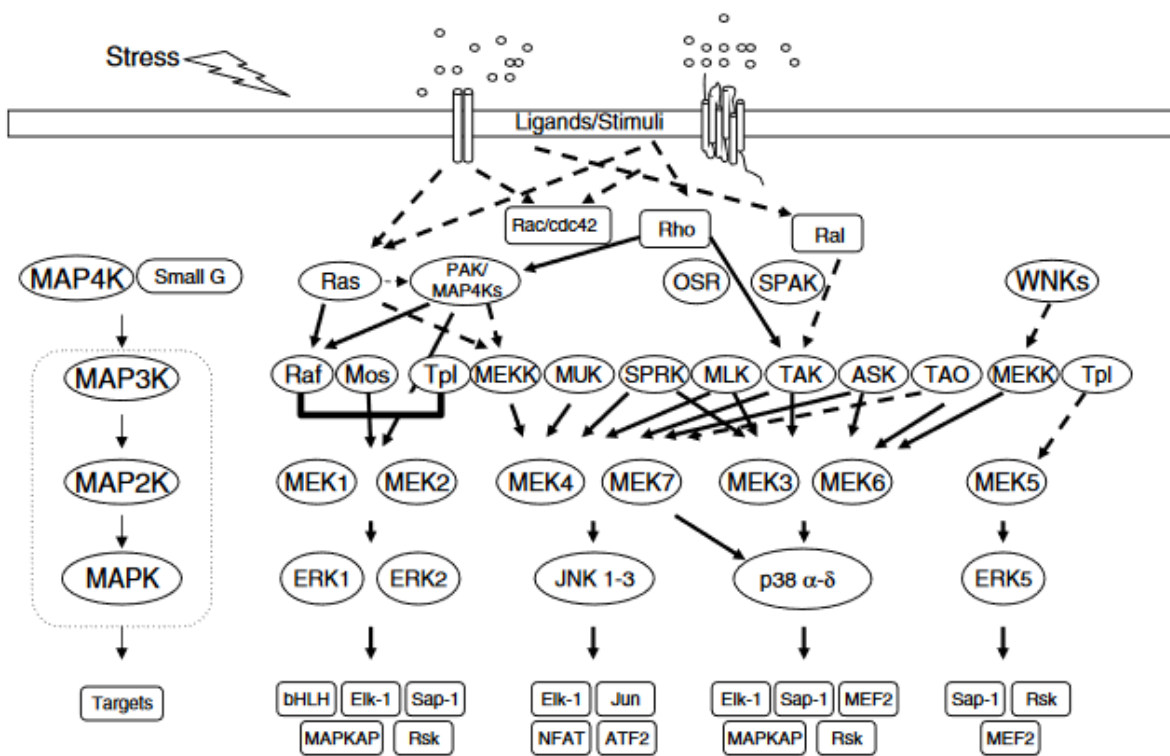
Figure 5. Illustration of MAPK cascades for ERK1/2, JNK, p38, and ERK5. (14).

Previous research also suggests that the AKT signaling pathway is important in muscle atrophy and hypertrophy depending on the state of the tissue (11). Activated by insulin-like growth factor (IGF), AKT functions to activate expression of pro-survival proteins, such as mTOR, and

suppresses expression of apoptotic proteins, such as those in the FoxO family (15). AKT is capable of phosphorylating mTOR which increases activity of downstream targets involved in protein synthesis (16). Dephosphorylation of FoxO proteins leads to FoxO translocation to the nucleus where it binds to FoxO binding elements (FBE) in the promoter region of various genes related to skeletal muscle atrophy (17). AKT phosphorylation of FoxO proteins leads to cytoplasmic sequestration and blockage of the activation of atrophy-inducing genes, such as MuRF1 (17).
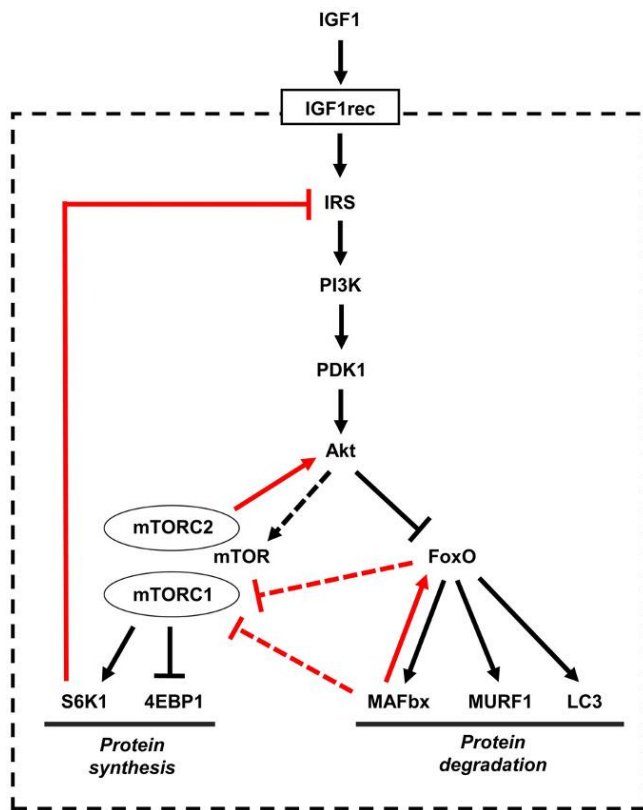
Figure 6. The insulin-like growth factor 1 (IGF1)-Akt pathway controls muscle growth via mammalian target of rapamycin (mTOR) and FoxO proteins. (16)

Glucocorticoid (GC) signaling is known to play a role in skeletal muscle atrophy (18,19).

Increases in GCs lead to decreases in protein synthesis and increases in protein degradation (19).

The inactive glucocorticoid receptor is found in the cytoplasm bound to a chaperone complex containing several proteins including heat shock protein 90 (HSP90) (20). As a ligand-dependent

transcription factor, binding of GCs result in the cytoplasmic glucocorticoid receptor (GR) to translocate to the nucleus where it may bind to glucocorticoid response elements (GRE) (19). GR possesses multiple phosphorylation sites and a dynamic interplay between phosphorylation and dephosphorylation events determines its precise role following nuclear translocation (20). In addition to transcriptional enhancement though GR homodimer binding to GRE consensus elements, ligand-bound GR may translocate to the nucleus and bind to other transcription factors, such as AP-1 and KF-κB, and interfere with their ability to function as transcription factors (20). GR activation of catabolic pathways including the ubiquitin proteasome system and autophagy pathways are thought to play a major role in the molecular mechanisms responsible for skeletal muscle atrophy resulting from increased glucocorticoid exposure (18). In fact, both MuRF1 and MAFbx contain glucocorticoid response elements that enhance their expression in the presence of GCs (17,18)
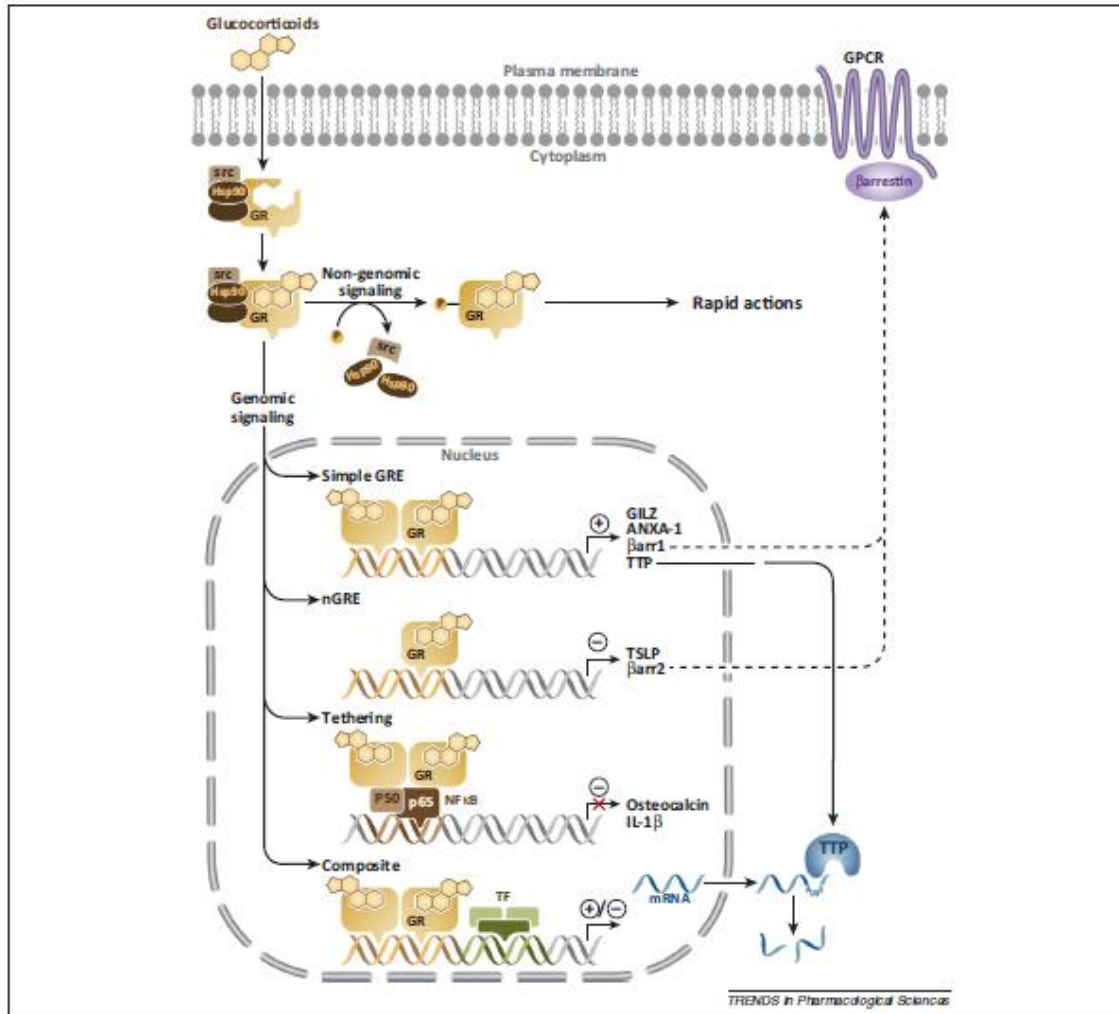
Figure 7. Glucocorticoid receptor (GR) signaling. Following glucocorticoid binding, GR becomes phosphorylated and translocates to the nucleus where it may influence transcription of target genes in a multitude of ways (20).

Chapter 2: Identification and Functional Analysis of Family with sequence similarity 83 D (Fam83d) in Skeletal Muscle

Introduction

Overview of Fam83d

Fam83d is one of 8 members of a family of proteins related by a highly conserved domain of unknown function, DUF1669, found at the N-terminus of each protein (21). This group of proteins shares little homology outside of the DUF1669 region. Endogenous expression of this family of proteins varies across tissue types but all members have been shown to be upregulated in one or more tumor types (21). Indeed, several studies have examined the function of Fam83d in cancer, including its role in breast cancer (22, 23), hepatocellular carcinoma (24) (25) lung cancer (26, 27) ovarian cancer (28, 29) and colorectal cancer (30). While its precise role in oncogenesis remains unclear, previous studies have demonstrated its involvement in several cell signaling pathways involved in cell proliferation and differentiation, including the MAP kinase, AKT/mTOR, and Wnt/β-catenin signaling cascades (22, 23, 24, 25, 26, 27, 28, 29, 30).

Materials and Methods

Cell Culture

The C_2C_{12} immortalized mouse myoblast cell line was obtained from the American Type Culture Collection (Manassas, VA) and maintained in DMEM (Life 163 Technologies, Grand Island, NY) supplemented with 10% fetal bovine serum (FBS) (GE164 Healthcare HyClone Laboratories, Logan, UT), non-essential amino acids, gentamicin, penicillin and streptomycin (all from Life Technologies, Grand Island, NY). Cells were grown in a humidified chamber at 37ºC at 5% CO2. Cells were switched to DMEM supplemented with 2% FBS, non-essential

amino acids, gentamicin, penicillin and streptomycin 48 hours post plating to stimulated

myotubes differentiation.

RNA Isolation and cDNA synthesis

Total RNA was isolated from C_2C_{12} myoblast cells using the RNeasy Mini Kit (Qiagen,

Valencia, CA) according to the manufacturer's protocol. Purified RNA (1µg) was reverse-

transcribed using Oligo-dT primers and Moloney Murine Leukemia Virus (M-MLV) Reverse

Transcriptase according to the manufacturer's protocol (Life Technologies, Grand Island, NY)

Amplification and cloning of the full length Fam83d cDNA

For the amplification of Fam83d cDNA, gene-specific primer pairs were designed (Table 1)

using the gene sequences from *Mus musculus* (GenBank accession number: NM_027975). PCR

was performed according to the manufacturer's protocol (Life Technologies, Grand Island, NY)

using Taq DNA polymerase, template prepared by reverse transcription of RNA isolated from

C_2C_{12} cells as described above and gene specific primer pairs (Table 1). Amplicons were cloned

into the pGEM-T Easy vector (Promega, Madison, WI) according the manufacturer's protocol

and sequenced using the Big Dye Sanger terminator sequencing method (Eurofins MWG

Operon, Huntsville, AL) to confirm amplification of the expected target and the absence of

mutations. The Fam83d cDNA was sub-cloned into the Xho1 and Xba1 restriction sites of

pcDNA3.1 (+) (Life Technologies, Grand Island, NY) and sequenced to confirm correct

orientation. The Fam83d cDNA was also sub-cloned into the Xho1 and Xba1 restriction sites of

the pEGFP-C3 expression plasmid (Clontech, Mountain View, CA) and sequenced to confirm

correct orientation and in frame fusion with GFP. The Fam83d cDNA fused to myc and DDDDK

tags in the PS100001 vector was purchased from OriGene Technologies (Rockville, MD) catalog number MR209141.

Promoter cloning of the Fam83d gene

For the amplification of the proximal regulatory region of Fam83d, genomic DNA was isolated from C_2C_{12} cells using the DNeasy Blood and Tissue Kit (Qiagen, Valencia, CA) according to the manufacturer's protocol. PCR was performed using Fam83d promoter region-specific primer pairs (Table 1) developed using mouse genomic sequences obtained from the Ensembl database (www.ensembl.org). PCR reactions were performed using Taq DNA polymerase and genomic mouse DNA according to the manufacturer's protocol (Life Technologies, Grand Island, NY). The PCR amplicons were cloned into the pGEM-T Easy vector (Promega, Madison, WI) according to the manufacturer's protocol and sequenced to confirm amplification of the predicted target region and the absence of mutations. The Fam83d promoter fragments (~500 and ~1000 base pairs) were sub-cloned into the HindIII and Xho I sites of the pSEAP2-Basic reporter plasmid (Clontech, Mountain View, CA) to create the pSEAP-Fam83d-Pro500 and the pSEAP-Fam83d-Pro1000 reporter plasmids and sequenced to confirm correct orientation.

Site-directed mutagenesis

The putative phospholipase D-like catalytic domain sequence located in exon 3 of Fam83d was mutated (H239N and K241Q) using the primer pairs listed in Table 1. The Fam83d-F280A mutant was generated using the primers listed in Table 1. The QuikChange II Site Directed Mutagenesis protocol utilizing PfuTurbo DNA polymerase was performed according to the manufacturer's protocol (Agilent Technologies, Santa Clara, CA). The mutagenesis PCR

reactions were digested with DpnI (New England BioLabs, Ipswich, MA) and then transformed

into heat competent DH5α *E.coli* cells (Life Technologies, Grand Island, NY). Clones were

isolated and plasmids were purified via alcohol precipitation and sequenced to confirm

successful mutation of the phospholipase D-like domain catalytic pocket.

Transfections

C_2C_{12} myoblast cells were plated into 12 well plates at a density of 75,000 cells/well with

DMEM + 10% FBS (proliferation media) and cultured overnight. All conditions assessed were

conducted in triplicate. Transfections were performed utilizing Turbofect Transfection Reagent

(Thermo Scientific, Rockford, IL) following manufacturer protocol. One hour prior to

transfection, media was refreshed and 1 μg of total DNA (250 ng/well of reporter plasmid, 125

ng/well of β -galactosidase (β-gal) as the internal control plasmid, and empty pBluescript vector

as filler DNA to 1 μg DNA/well) was allowed to complex with transfection reagent for 20

minutes prior to overlaying the cells. Following 24-hour incubation with the transfection

reaction, the proliferation media was replaced with differentiation media (DMEM + 2% FBS)

and incubated for an additional 24-72 hours until reporter assays were performed.

Reporter gene assay

Growth media was collected from C_2C_{12} mouse myoblasts at 24–72 hr after the switch to

differentiation media post transfection and tested for SEAP levels using the Phospha-Light SEAP

Reporter Gene Assay Kit and following the manufacturer's instructions (Life Technologies,

Grand Island, NY). The level of SEAP generated luminescence was assessed with a Synergy 2

microplate reader programmed for an endpoint read and a 2 s integration time. At the conclusion

of the experiment, cells were lysed with Passive Lysis Buffer (Promega, Madison, WI), lysates were centrifuged to clear cell debris and assessed for β-galactosidase (β-gal) activity. The SEAP activity numbers were corrected with β-gal activity numbers to adjust for any variation in transfection levels between wells.

Bioinformatic analysis of Fam83d

DNA sequences corresponding to the promoter regions of human, rat, and mouse Fam83d (Ensembl Transcript ID: ENST00000619850.2, ENSRNOT00000021308.4, and ENSMUST00000029183.2, respectively) starting at -2000 and including the first exon were taken from the Ensembl database (www.ensembl.org) and analyzed using the Clustal Omega multiple sequence alignment tool available on the EMBL-EBI website (https://www.ebi.ac.uk/Tools/msa/clustalo/). The Clustal Omega alignment data was then analyzed using Boxshade version 3.21 (http://www.ch.embnet.org/software/BOX_form.html) that is available on the ExPASy (www.expasy.org) website. The polypeptide sequences for human, mouse, and rat Fam83d were also downloaded from Ensembl and aligned using the Clustal Omega alignment tool and shaded with Boxshade as described for the promoter sequences above.

Quantitative PCR

Total RNA was isolated from proliferating and differentiated C_2C_{12} cells as described above. Purified total RNA (1.0 μg) was reverse-transcribed using the iScript cDNA Synthesis Kit according to the manufacturer's protocol (Bio- Rad, Hercules, CA). cDNA amplification was conducted using the iTaq Universal SYBR Green Reaction Supermix and gene specific primers

(Table 1) according to the manufacturer's protocol (Bio-Rad, Hercules, CA) and the CFX

Connect Real-Time PCR Detection System (Bio-Rad, Hercules, CA) was used to analyze

quantitative gene expression of Fam83d at PD2, DD2 and DD7. Each timepoint was performed

in biological triplicates, each individual biological replicate was used for cDNA synthesis in

duplicate, and each cDNA synthesis replicate plated and analyzed in technical triplicates (three

biological replicates × two cDNA synthesis replicates × three technical replicates = 18 individual

reads per biological sample) and the experiment was repeated at least twice. Relative gene

expression was calculated using the $2-\Delta\Delta Ct$ Livak method and GAPDH as the reference gene.

Protein purification and Western blot analysis

C_2C_{12} cells were cultured in 10 cm culture dishes and Fam83d was exogenously expressed by

transfecting the cells with the PS100001-Fam83d-myc-DDK or pcDNA3.1-Fam83d expression

plasmid 24 h post-plating. The Fam83d overexpression time course was collected by harvesting

cells 48 h post-plating (PD2), as well as cells cultured for an additional 1,3 or 5 days in

differentiation media (DD1, DD3, DD5). The collected cells were spun down and kept at −80°C

until cell homogenization and protein isolation was performed.

The harvested cells were incubated on ice for 30 min, with agitation every 10 minutes, in

Universal Lysis Buffer (50mM Tris, pH 7.5, 150mM NaCl, 50mM NaF, 0.5% NP-40), plus

additions (1mM PMSF, 1mM DTT, 10mM β-glycerophosphate, 2mM sodium molbydate, and a

protease inhibitor cocktail; ULB(+)). Cell homogenates were centrifuged to clear cellular debris

and protein concentrations were determined using the Quick Start Bradford 1× Dye Reagent

(Bio-Rad, Hercules, CA) following the manufacturer's instructions.

Western blots were conducted using 75-100 μg of protein on a 10% sodium dodecyl sulfate polyacrylamide gel electrophoresis denaturing gel and then transferring overnight to polyvinylidene fluoride membrane (EMD Millipore, Billerica, MA). Membranes were stained with Ponceau S to visualize equal protein loading and successful transfer and then incubated with blocking solution (5% w/v dry milk in tris-buffered saline with 0.05% Tween-20). Western blots were probed with anti-Fam83d (gift from Dr. Gopal Sapkota, University of Dundee, United Kingdom), anti-myosin heavy chain (MYH1/2/4/6; sc-32732; Santa Cruz Biotechnology Dallas, TX), anti-myogenin (F5D; sc-12732; Santa Cruz Biotechnology, Dallas, TX), anti-p-ERK (E4; sc-7383; Santa Cruz Biotechnology, Dallas, TX), anti-ERK1 (K-23; sc-94; Santa Cruz Biotechnology, Dallas, TX), anti-Fbxw7 (28424-1-AP; ProteinTech, Rosemont, IL), anti-CSNK1α1 (55192-1-AP; ProteinTech, Rosemont, IL), anti-MEK1/2 (11049-1-AP; ProteinTech, Rosemont, IL), anti- Calcoco1 (19843-1-AP; ProteinTech, Rosemont, IL), anti-HMMR (15820-1-AP; ProteinTech, Rosemont, IL), anti-AKT-phospho-S473 (66444-1-lg; ProteinTech, Rosemont, IL). Anti-AKT (60203-2-lg; ProteinTech, Rosemont, IL), anti-phospho-mTOR-Ser2448 (D9C2; #5536; Cell Signaling Technology, Danvers, MA), anti-phospho-mTORSer2481 (#2974; Cell Signaling Technology, Danvers, MA), antiphospho-MEK1/2 (9154T; Cell Signaling Technology, Danvers, MA), anti-phospho-GSK-3β (5558 T; Cell Signaling Technology, Danvers, MA), anti- GSK-3β (22104–1-AP; ProteinTech, Rosemont, IL), antimTOR (66888–1-lg; ProteinTech, Rosemont, IL) anti-myc (60003–2-lg; ProteinTech, Rosemont, IL), anti-DDDDK (FLAG equivalent) (20543–1- AP; ProteinTech, Rosemont, IL) anti-GAPDH (60004–1-lg; ProteinTech, Rosemont, IL) and anti-α tubulin (DM1A; sc-32293; Santa Cruz Biotechnology, Dallas, TX) primary antibodies followed by probing with an

appropriate HRP-conjugated secondary antibody (Santa Cruz Biotechnology, Dallas, TX) (Table 2). Western blots were visualized using ECL substrate according to the manufacturer's instructions (Pierce/Thermo Fisher Scientific, Rockford, IL). PVDF membranes were stripped by incubating for 20–30 min in stripping buffer (10%SDS, 0.5 M tris-HCl pH 6.8 and β-mercaptoethanol) at 50 °C, and then blocked, re-probed, and visualized as described above. Western blot band intensity quantifications were conducted using the open access ImageJ software.

Confocal Fluorescence Microscopy

C_2C_{12} cells were plated using Cellvis (Sunnyvale, CA) 35mm glass bottom dishes and transfected 24 h after cells were plated with either the pEGFP-C3 or pEGFP-Fam83d plasmids duplexed with TurboFect Reagent (Thermo Fisher Scientific, Rockford, IL) as per manufacturer's instructions. Before imaging, the cells were washed with phosphate buffered saline, fixed with paraformaldehyde, dissolved in sodium cacodylate, and stained with DRAQ5 fluorescent DNA dye (Biostatus, Leicestershire, UK). The images were acquired using an Olympus Fluoview FV-1000 confocal fluorescent microscope equipped with Super Apochromat UPLSAPO 20X and Super Apochromat UPLSAPO 60XW objectives. Open access ImageJ software combined with the Open Microscopy Environment Bio-Formats plugin was used to analyze, merge, and save all images.

Co-immunoprecipitation

C_2C_{12} cells were grown in 10% FBS DMEM media and transfected with Fam83d-myc-DDK expression plasmid and harvested 24 hours post transfection. Cells were lysed on ice for 30

minutes in ULB(+) (50mM Tris, pH 7.5, 150mM NaCl, 50mM NaF, 0.5% NP-40, 1mM PMSF, 1mM DTT, 10mM β-glycerophosphate, 2mM sodium molbydate and a protease inhibitor cocktail). Protein was isolated by centrifugation and protein concentrations were quantified using the Quick Start Bradford 1X Dye Reagent (Bio-Rad, Hercules, CA) according to the manufacturer's protocol. 500μg protein was diluted in ULB and precleared with protein A/G agarose beads (Pierce/Thermo Scientific, Rockford, IL) for 1 hour at 4°C with constant end-over-end rotation. Beads were cleared from solution via centrifugation and the supernatant was incubated with 2μg anti-myc (60003-2-lg; Proteintech, 318 Rosemont, IL) antibody for 4 hours at 4°C with constant end-over-end rotation. Protein A/G agarose beads were added to solution and incubation was continued for 6 additional hours. Beads were cleared from solution via centrifugation and pelleted beads were washed 3X with ULB, and then boiled for 5 mins at 95°C. 50μg of protein lysate was used for input control and SDS-PAGE was performed. Separated proteins were then transferred to a PVDF membrane and probed using the antibodies described above.

Statistics

Data are presented as the mean ± standard deviation (SD). Statistical analysis was conducted using a two-tailed t-test and a difference was considered statistically significant at a P value < 0.05.

Table 1. List of primers used in the Fam83d study

Primer	Sequence (5'-3')
Fam83d-cDNA-F	GCAAGCTTGCCATGGCTGCTCGCTTCGAGC
Fam83d-cDNA-R	GCGAATTCCGGCAGTCACTGATAGGGAGGG
Fam83d-cDNA-Mut-F	CGGGAAGGTTAATGAGCAGTTCACACTG
Fam83d-cDNA-Mut-R	CAGTGTGAACTGCTCATTAACCTTCCCG
Fam83d-pro500-F	GCCTCGAGGATGCAGGGTGGAGTGGCAATGAGGC

Fam83d-pro1000-F	GCCTCGAGCCTCCCATGTGCTGGGAGTGTGCCACC
Fam83d-pro5000-R	GCAAGCTTGCCCAGAACCGATCCACTTGTCTACG
Fam83d-qpcr-F	GATCTGAGAGTTCATCCTGAGC
Fam83d-qpc-R	CAACCTTTGTTCCTGACCTTGC

Table 2. List of antibodies used in the Fam83d study

Antibody	Source	Catalog #	Dilution
anti-Fam83d	University of Dundee, Scotland		WB: 1:500
anti-Calcoco1	ProteinTech, Rosemont, IL	19843-1-AP	WB: 1:2000
anti-myc	ProteinTech, Rosemont, IL	60003-2-lg	WB: 1:2000 IF: 1:50
anti-α-tubulin	Santa Cruz Biotechnology, Dallas, TX	sc-32293	WB: 1:1000
anti-Myosin Heavy Chain (MYH1/2/4/6)	Santa Cruz Biotechnology, Dallas, TX	sc-32732	WB: 1:1000
anti-myogenin	Santa Cruz Biotechnology, Dallas, TX	sc-12732	WB: 1:1000
anti-GAPDH	ProteinTech, Rosemont, IL	60004-1-lg	WB: 1:5000
anti-phospho-ERK	Santa Cruz Biotechnology, Dallas, TX	sc-7383	WB: 1:1000
anti-ERK	Santa Cruz Biotechnology, Dallas, TX	sc-94	WB: 1:1000
anti-phospho-MEK1/2 (Ser217/221)	Cell Signaling Technology, Danvers, MA	9154	WB: 1:2000
anti-MEK1/2	ProteinTech, Rosemont, IL	11049-1-AP	WB: 1:5000
anti-Akt1-phospho-S473	ProteinTech, Rosemont, IL	66444-I-lg	WB: 1:2000
anti-Akt	ProteinTech, Rosemont, IL	60203-2-lg	WB: 1:5000
anti-phospho-mTOR-Ser2448	Cell Signaling Technology, Danvers, MA	5536	WB: 1:2000
anti-mTOR	ProteinTech, Rosemont, IL	66888-1-lg	WB: 1:10000
anti-phospho-GSK3β (Ser9)	Cell Signaling Technology, Danvers, MA	5558	WB: 1:1000
anti-GSK3β	ProteinTech, Rosemont, IL	22104-1-AP	WB: 1:2000
anti-CSNK1A1	ProteinTech, Rosemont, IL	55192-1-AP	WB: 1:2000
anti-FBXW7	ProteinTech, Rosemont, IL	28424-1-AP	WB: 1:5000
anti-HHMR	ProteinTech, Rosemont, IL	15820-1-AP	WB: 1:1000
anti-DDK	ProteinTech, Rosemont, IL	20543-1-AP	WB: 1:5000
Mouse anti-rabbit IgG-HRP	Santa Cruz Biotechnology, Dallas, TX	sc-2357	WB: 1:5000
Rabbit anti-mouse IgG-HRP (H+L)	Thermo Scientific, Rockford, IL	PI31450	WB: 1:5000
Donkey anti-Sheep IgG-HRP (H+L)	Jackson Immuno Research, West Grove, PA	713-035-147	WB: 1:10000
Goat anti-mouse IgG (H+L), FITC conjugate	ProteinTech, Rosemont, IL	SA00003-1	IF: 1:100

Results

Fam83d is upregulated during neurogenic skeletal muscle atrophy

RNA was isolated from control and denervated mouse gastrocnemius and soleus muscles and an Illumina mouse-6 v1.1 microarray was performed at 3 days and 14 days post denervation as previously described (5). Analysis of the microarray data submitted to the NCBI Gene Expression Omnibus (GEO) revealed a significant number of genes that show differential expression patterns in response to neurogenic muscle atrophy (5). Many of these genes have not previously been implicated in atrophy and have not been characterized in skeletal muscle. Fam83d shows low basal levels of expression in control gastrocnemius and soleus muscles and there was no significant difference in expression between control and denervated tissue at 3 days post-denervation; however, Fam83d was shown to be significantly upregulated by day 14 post-denervation compared to control muscles (Fig. 8A). Fam83d is found on chromosome 2 in mice and is composed of four exons and three introns (Fig. 8B). The Fam83d gene locus shows architectural conservation between mouse and human and lies immediately downstream of Ppp1r16b and immediately upstream of Dhx35 in both species (Fig. 8C).

A.
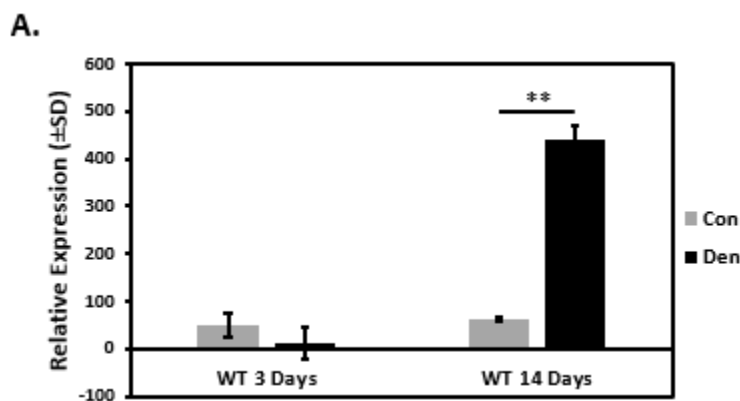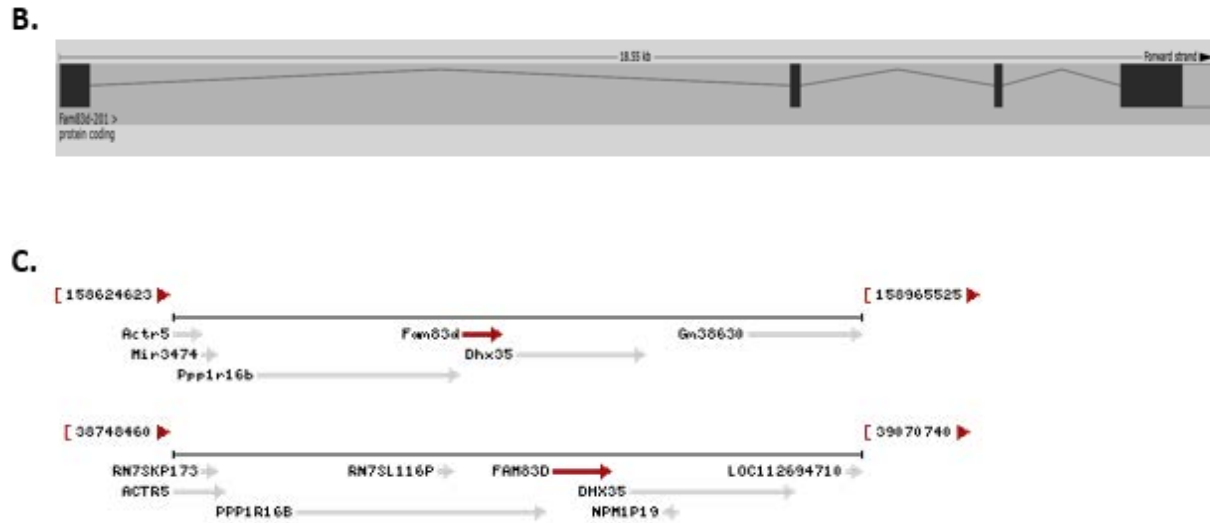
Figure 8. Fam83d is upregulated during neurogenic atrophy. (A) Whole genome expression analysis was conducted on triceps surae muscle from wild-type (WT) mice after 3 days (3D) and 14 days (14D) of denervation. Each condition represents the average expression from three animals and error bars represent ± SD. White bars, controls (Con); black bars, denervated (Den). Significant difference between denervated mice and control mice in the same group (**:P < .01). (B) Schematic of the Fam83d transcript in mouse. Darkened rectangles represent the exons containing the translated region, open rectangles represent exons containing the untranslated regions, and the lines connecting these rectangles represent introns. (C) Schematic of the mouse and human Fam83d gene loci on Chromosomes 2 and 20, respectively and the relative positions of adjacent genes.

Fam83d is expressed during muscle cell proliferation but is rapidly degraded as cells differentiate

To measure the transcriptional activity of Fam83d, total RNA was harvested from C_2C_{12} mouse myoblasts during proliferation (PD2), as well as, from myotubes at early (DD2) and late (DD7) differentiation timepoints. cDNA synthesized from isolated RNA was used to conduct RT-qPCR using Fam83d specific primers (Table 1). The qPCR analysis demonstrated that Fam83d mRNA levels are significantly higher during proliferation when compared to both early and late differentiation timepoints (Fig. 9A). To validate the ability of a Fam83d antibody, generously

provided by Dr. Gopal Sapkota at the University of Dundee, United Kingdom, to detect mouse Fam83d, NIH3T3 cells were transfected with either a pcDNA3-Fam83d or pEGFP-Fam83d expression plasmid. Protein homogenates isolated from control cells and transfected cells were then analyzed by Western blot and the Fam83d antibody was able to successfully detect both the untagged and GFP-tagged Fam83d proteins (Fig. 9B). Protein homogenates from C_2C_{12} cells isolated from proliferating myoblasts (PD2) and cells differentiated for 1, 3, and 5 days were analyzed by Western blot using the validated anti-Fam83d antibody to assess endogenous Fam83d protein levels. In agreement with the qPCR data, Western blot analysis revealed that Fam83d protein levels are higher during proliferation and then rapidly decrease as muscle cells differentiate (Fig. 9C). Myosin Heavy Chain (MyHC) was analyzed as a marker of muscle cell differentiation, Calcoco1 was used as a control for protein stability during differentiation, and α-tubulin was used as a loading control.

To determine if this decrease in protein level was due to degradation through the 26S proteasome pathway, C_2C_{12} cells were transfected with a Fam83d-myc expression plasmid and treated with increasing concentrations of the proteasome inhibitor MG132. Cells were harvested 12 h post-MG132 treatment and protein lysates were analyzed by Western blot. The levels of myc-tagged Fam83d were found to be much higher at differentiation day one compared to DMSO treated control cells (Fig. 9D).
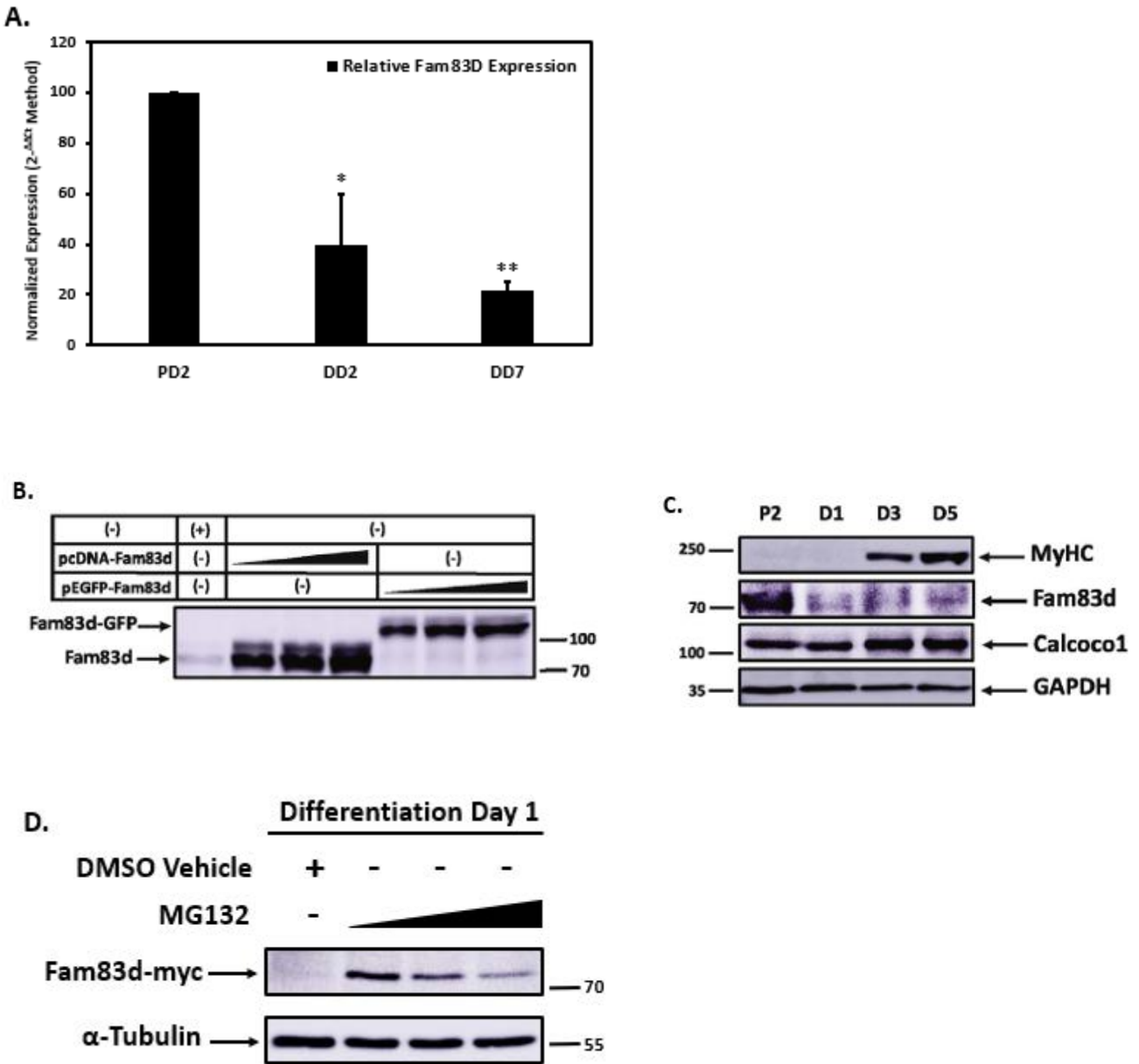
Figure 9. Fam83d expression in mouse myoblasts. (A) Fam83d mRNA is expressed highly during proliferation and then decreases significantly during differentiation. Quantitative polymerase chain reaction (qPCR) utilizing cDNA generated from RNA isolated from C_2C_{12} cells harvested at proliferation day 2 (PD2), differentiation day 2 (DD2) and differentiation day 7 (DD7). Cells were maintained in proliferation media (10% serum) and harvested at 2 days post-plating and the remaining cells were switched to differentiation media (2% serum) and harvested at 2- and 7-days post-media change. Significant difference between Fam83d expression in differentiated cells compared to Fam83d expression in proliferating cells (*:P < .05, **:P < .01). (B) Validation of a Fam83d antibody to detect murine Fam83d using protein lysates from NIH3T3 cells ectopically expressing mouse Fam83d. NIH3T3 cells were transiently transfected with pcDNA3-Fam83d, or pEGFP-Fam83d and 25 μg, 50 μg or 75 μg of protein lysate was

loaded and analyzed by Western blot. (C) Western blot analysis was performed with the validated Fam83d antibody using protein homogenates from proliferating [P] and differentiated [D] C_2C_{12} cells harvested over a 5-day differentiation time course to assess endogenous Fam83d protein levels. Cells were maintained in proliferation media (10% serum) and harvested at 2-days post-plating and the remaining cells were then switched to differentiation media (2% serum) and harvested at 1, 3, and 5 days post-media change. Myosin Heavy Chain (MyHC) was analyzed as a marker of differentiation, Calcoco1 was analyzed as a protein that is not affected by muscle cell differentiation, and α-tubulin was analyzed to confirm equal protein loading. (D) Western blot analysis using lysates from C_2C_{12} cells transfected with a Fam8d3-myc-Flag expression plasmid, treated with MG132 (0.625, 1.25, and 2.5 μM), harvested after 1 day of differentiation, and probed using an anti-myc antibody. α-tubulin was analyzed to confirm equal protein loading.

Fam83d Expression Is Regulated by Myogenic Regulatory Factors

To gain insight into how Fam83d is regulated transcriptionally in muscle cells, 416 and 785 base

pairs of the promoter were amplified using the primers listed in Table 1. The fragments were

then fused to a secreted alkaline phosphatase (SEAP) reporter plasmid to create the pSEAP-

Fam83d-Pro416 and pSEAP-Fam83d-Pro785 reporter constructs. The Fam83d reporter gene

constructs were transfected into C_2C_{12} mouse myoblasts and SEAP assays were performed 48 h

after the switch to differentiation media. The 416 and 785 bp fragments both showed

significantly higher expression compared to the empty plasmid alone (Fig. 10A). Bioinformatic

analysis of the promoter region of Fam83d revealed three canonical E-Box elements within the

first 400 bps upstream of the start of transcription (Fig. 10B). Myogenic regulatory factors, such

as MyoD, are known to regulate gene transcription through interaction with E-box consensus

elements (5′- CANNTG-3′) found in the promotors of muscle-specific genes. Therefore, to

determine if the Fam83d reporter genes are responsive to ectopic expression of MyoD, cells were

transfected with a MyoD expression plasmid in combination with the reporter gene constructs.

Overexpression of MyoD significantly repressed the transcriptional activity of both the pSEAP-

Fam83d-Pro416 and pSEAP-Fam83d-Pro785 reporter constructs (Fig. 10C and D).

A.
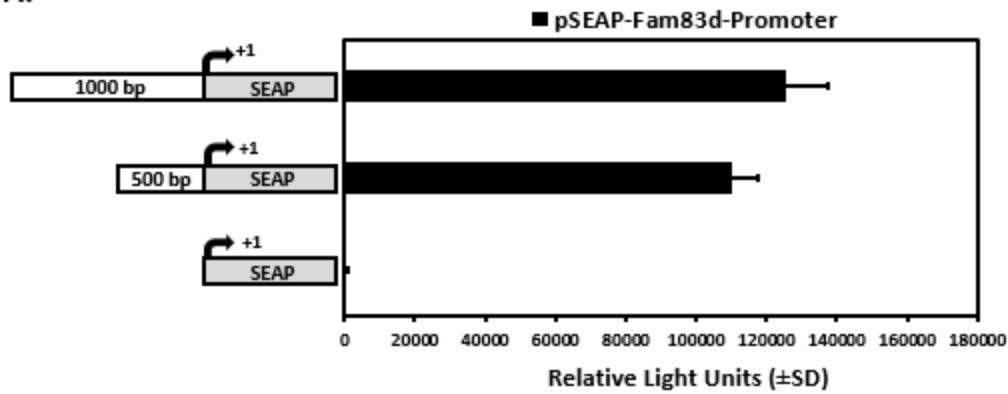
B.
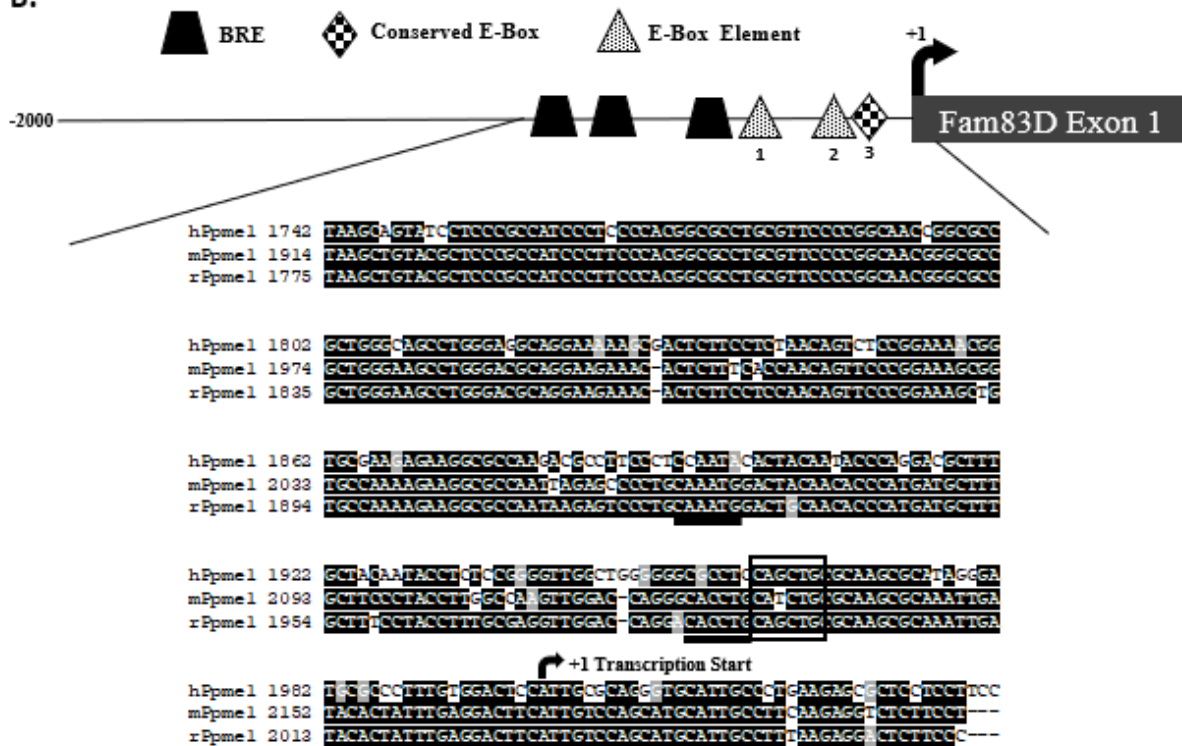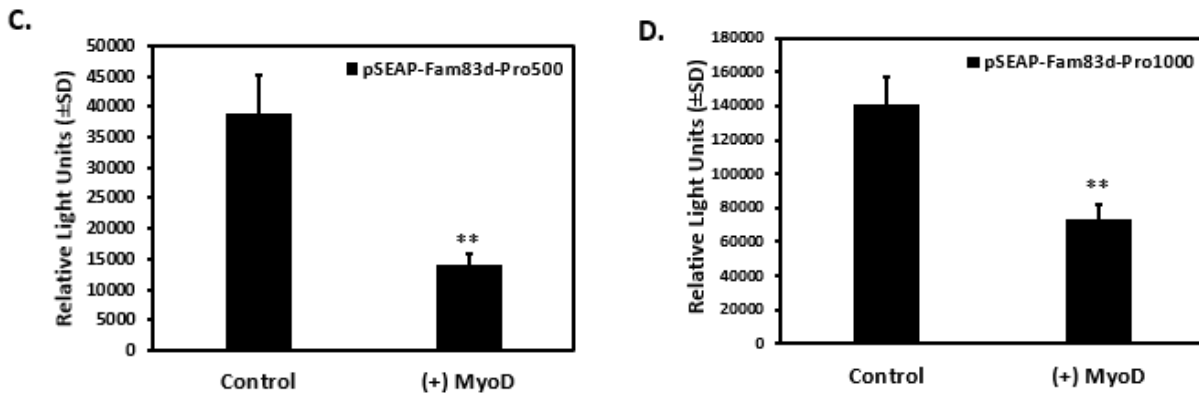
Figure 10. Cloning and analysis of the proximal regulatory region of the Fam83d gene locus. (A) C_2C_{12} myoblasts were transfected with either an empty reporter plasmid or reporter plasmids containing 416 bp or 785 bp of the Fam83d promoter fused to the Secreted Alkaline Phosphatase (SEAP) reporter gene. Each condition was performed in triplicate and each experiment was repeated at least three times (n = 3). The graphs are of a representative experiment and values correspond to the mean relative light unit (RLU) values ±SD. Significant difference between the empty control reporter plasmid (pSEAP2-Basic) and the pSEAP2-Fam83d reporter constructs, (*: P < .0001). (B) Schematic and sequence alignment of the Fam83d regulatory region. Promoter sequences from mouse, rat, and human Fam83d (2000 base pairs upstream of the transcription start site (+1) through the first exon) were downloaded from the Ensembl database (www.ensembl.org) and aligned using the ClustalW algorithm. Approximate positions of putative transcription factor binding sites are indicated in the schematic of the Fam83d regulatory region at the top. Putative TFIIB Response Element (BRE) 5′-(G/C)(G/C(G/A)CGCC-3′ (black trapezoids) and putative consensus E-box elements 5′-CANNTG-3′ (checkered diamond and dotted triangle) are indicated. N represents any nucleotide. Conserved nucleotides are highlighted in black, transitions are highlighted in gray, and transversions are highlighted in white. C_2C_{12} myoblasts were transfected with either the (C) pSEAP2-Fam83d-Pro416 reporter or the (D) pSEAP2-Fam83d-Pro785 reporter with or without a MyoD expression plasmid. The media was then assayed for SEAP activity 48 h (DD2) following the switch to differentiation media and SEAP numbers were normalized to β-galactosidase activity to correct for variations in transfection efficiency. Each condition was performed in triplicate and each experiment was repeated at least three times (n = 3). The graphs are of a representative experiment and values correspond to the mean relative light unit (RLU) values ±SD. Significant differences between the activities of the pSEAP2-Fam83d-Pro reporter constructs with and without MyoD ectopic expression, (**: P < .01).

Subcellular localization of Fam83d

The Fam83d gene is located on chromosome 2 in mouse and encodes a 585 amino acid

polypeptide with a predicted molecular weight of approximately 56 kDa, although the observed

molecular weight appears closer to 70 kDa (Fig. 9C). The Fam83d protein contains a

putative domain of unknown function (DUF) located at the N-terminus of the polypeptide (highlighted in red in the alignment), which is conserved among all members of the Fam83 family (Fig. 11A). Further analysis utilizing the NCBI conserved domain database identified a putative phospholipase D-like (PLD-like) catalytic motif (highlighted in green in the alignment) within this DUF region (Fig. 11A). As this is the first study to describe Fam83d in skeletal muscle, there are no other reports describing its localization in muscle cells. Therefore, Fam83d was fused with GFP and the fusion protein was ectopically expressed in cultured myoblasts to determine subcellular localization by confocal fluorescent microscopy. C_2C_{12} cells were transfected with either an empty GFP expression plasmid or a Fam83d-GFP expression plasmid and analyzed 24 h post-transfection. The control cells transfected with the empty GFP expression plasmid showed uniform GFP localization throughout the cell (Fig. 11B, Panels 1–3), while cells transfected with the Fam83d-GFP fusion plasmid showed accumulation in puncta located in the cytoplasm of cultured myoblasts (Fig. 11B, Panels 4–12). Since GFP has been known to affect localization of proteins it is fused with, we also overexpressed myc-tagged Fam83d in C2C12 myoblasts and performed immunofluorescence using an anti-myc antibody and a FITC-conjugated secondary and found that the localization pattern matched the GFP-Fam83d localization pattern (Fig. 11C)

A.

```
hFam83d   1   MALLSEGLDEVPAACLSPCGPPNPTELFSESRRLALEELVAGGPEAEAAFLRRERLARFL
mFam83d   1   MAARFELLDDLPAACLSPCGPPNPTELFSEARRLALEQLLAGGPLAWAAFLRRERLGRFI
rFam83d   1   MAARCELLDDLPAACLSPCGPPNPTELFSEARRLALEQLLAGGRNAVDAFLRRERLGRFI

hFam83d  61   NPDEVHAIRRAAERPGEERAEAAAARED SFGSSHDCSSGTYFPEQSDLEPELRLELGWRAE
mFam83d  61   NADEVREVLGAAERPGEDGAA---VAEDSFGSSHECSSGTYFPEQSDLEPPALELGWPSP
rFam83d  61   NTDEVREVLGAAERPGEDGAV---VTEESFGSSHDCSSGTYFPEQSDLEPPALELGWPSP

hFam83d  121  YQGAYRGATRVETHFQPRGAGEGGPYGCKDALRQQLRSAREVIAVVMDVETDIDIFRDLQ
mFam83d  118  YQGAYRGATRVEAHFQPRGAGAGGPYGCKDALRQQLRSAREVIAVVMDVFSDIDIFRDLQ
rFam83d  118  HRGAYRGATRVEAHFQPRGAGAGGPYGCKDALRQQLRSAREVIAVVMDVFSDIDIFRDLQ
                    Domain of Unknown Function 1669 (DUF1669)

hFam83d  181  EICRNQGVAVYILLDQALLSQFLDMCMDLKVHPEQEKLMTVRTITGNIYYARSGTRIISK
mFam83d  178  FSCRKRGVAVYILLDQTLIPHFLDMCMDLRVHPEQEKLMTVRTITGNIYYARSGTKVVGP
rFam83d  178  ETCRKRGVAVYILLDQALLSHFLDMCMDLKVHPEQEKLMTVRTITGNIYYARSGTKVVGK

                *  *
hFam83d  241  VHEKFTLIDGIRVATGSYSFTWTDGKLNSSNLVILSGQVVEHFDLEFRILYAQSKPISPK
mFam83d  238  VHEKFTLIDGIRVATGSYSFTWTDGKLNSSNLVILSGQVVEHFDLEFRILYAQSEPISSK
rFam83d  238  VHEKFTLIDGIRVATGSYSFTWTDGKLNSSNLVILSGQVVEHFDLEFRILYAQSEPISSK
                Putative Phospholipase D-like Domain Catalytic Pocket

hFam83d  301  LLSHFQSSNKFDHLTNRKPQSKELTLGNLLRMRLARLSSTPRKADLDPEMEAEGNAERKP
mFam83d  298  LLSNFQINSKFDHLADRKPQSKEPTLGNLLRMRLARLSSTPRKSNLGPPEPPKDRAKPKR
rFam83d  298  LLSNFQISGKFDHLADQKPQSKEPTLGNLLRTRLARLSSTPKKTGLDPEVPPKDRDKTKR

hFam83d  361  HDCESSTVSEEDYFSSHRDELQSRKAIDAATQTEPGEEMPGLSVSEVGTQTSIATACAGT
mFam83d  358  PDSEASTISDEDYFHSHKDQLEISKVADAATQTEPREEMAAVSLSEVGTQTSSSMMCVGT
rFam83d  358  HDSETSTISDEDYFCSHKDQLESKVVDAATQTEPGEEMAAVSLSEVGTQTSSSMMCAGT

hFam83d  421  QTAVITRIASSQTTIWSRSTTTQTDMDENILFPRGTQSTEGSPVSKMSVSRSSSLKSSSS
mFam83d  418  QTTVVTRAASSQATVWSKSTTTQTEADES-FLPQGAQSKEGSPASKMSVSRSSSVRSSSS
rFam83d  418  QTTVVTRAASSQATVWSKSTTTQTEADES-FLPQGAQSKEESPASKMSVSRSSSLRSSSS

hFam83d  481  VSSQGSVASSTGSPASIRTTDFHNPGYPKYL--GTPHLELYLSDSLRNLNKERQFHFAGI
mFam83d  477  VSSQGSLASSVSSHVSLTAADLHTPAYPKYLGLGTPHLDLCLRDSFRNLSKERQVHFTGI
rFam83d  477  VSSQGSLASSVSSHVSLSGTDLHTPGYPKYLGLGTPHLDLCLRDSFRNLSKERQVHFTGI

hFam83d  539  RSRLNHMLAVLSRRTLFTENHLGLHSGNFSR--VNLLAVRDVALYPSYQ
mFam83d  537  RSRLTQMLTVLSRRTLFTEHYLSYSPGSFTRASTNLVSVRDIALYPPYQ
rFam83d  537  RSRLTQMLTVLSRRTLFTEHYLSYSPGSFTRASTNLVSVRDIALYPPYQ
```

29

B.

	GFP	Draq5	Merged
Control 20X			
Fam83D 20X			
Fam38D 60X			
Fam38D 100X			
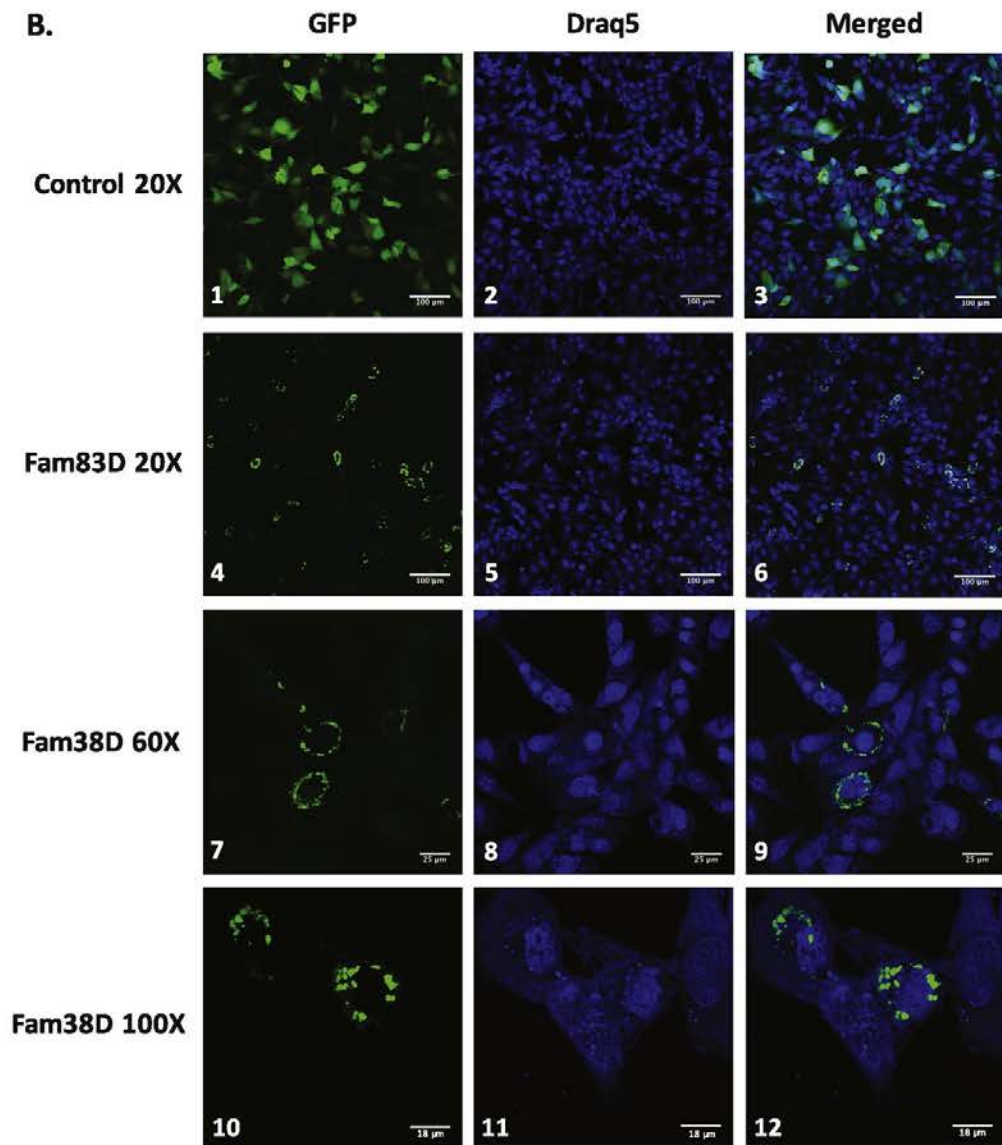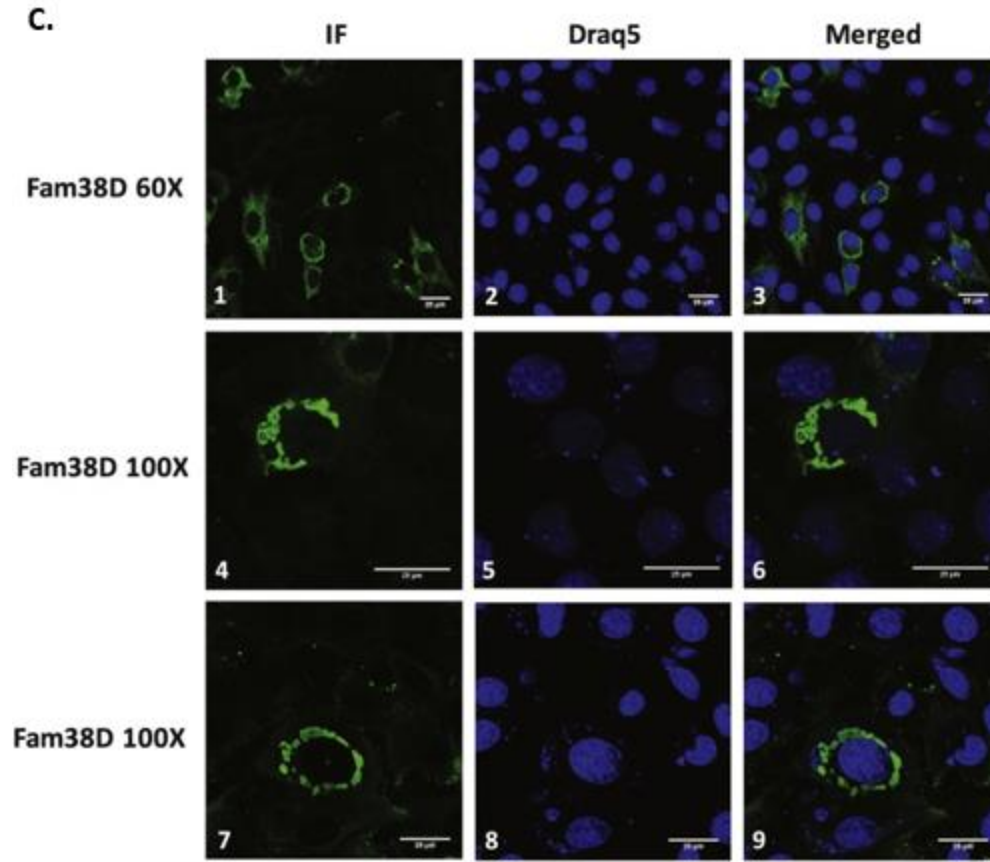
Figure 11. Fam83d localizes to the cytoplasm of myoblast cells. (A) Sequences of the mouse, rat, and human Fam83d protein were downloaded from the Ensembl database and aligned using the ClustalW2 algorithm. Approximate position of the domain of unknown function 1669 (DUF1669) is highlighted in red and the putative phospholipase D-like motif catalytic pocket is highlighted in greed in the alignment. (B) Proliferating C_2C_{12} cells (PD2) transfected with the empty pEGFP-C3 expression vector were imaged at 20× (Panels 1–3) and uniform cellular localization of GFP was observed. Representative C_2C_{12} cells transfected with a pEGFP-Fam83d expression plasmid were imaged at proliferation day 2 (PD2) at 20× (Panels 4–6), 60× (Panels 7–9, and 100× (Panels 10–12) and punctate cytoplasmic fluorescence was observed. Draq5, a cell permeable fluorescent DNA dye, was used to visualize cell nuclei. (C) Immunofluorescent detection of Fam83d-myc-Flag was performed using C_2C_{12} myoblast cells. C_2C_{12} cells were transfected with a Fam83d-myc-Flag expression plasmid and then incubated with a myc primary antibody and a FITC-conjugated secondary antibody revealing punctate cytoplasmic fluorescence at 60× (Panels 1–3) and 100× (Panels 4–9) magnification. Draq5, a cell permeable fluorescent DNA dye, was used to visualize cell nuclei and merged images were generated using ImageJ.

Ectopic expression of Fam83d inhibits muscle cell differentiation

To evaluate if Fam83d impacts muscle cell differentiation, C_2C_{12} cells were transfected with a myc-tagged Fam83d expression plasmid. Cells were then harvested over a time course that included 2 days of proliferation (PD2) and 1, 3 and 5 days of differentiation (DD1, DD3 and DD5, respectively). Protein was isolated from cells and evaluated for the level of expression of the canonical makers of muscle cell differentiation, skeletal muscle myosin heavy chain (MyHC) and myogenin. Western blot analysis showed significantly lower levels of both myogenin and MyHC at all differentiation time points (Fig. 12A). To quantify the amount of inhibition, Fam83d was overexpressed in biological quadruplicates and harvested at 3 days of differentiation. Lysates were evaluated by Western blot and myogenin and MyHC expression levels and were found to be significantly repressed in lysates isolated from cells ectopically expressing Fam83d (Fig. 12B and C). Fam83d protein levels were analyzed to confirm overexpression and GAPDH was analyzed to confirm equal loading and to correct for variations in protein levels between individual lanes (Fig. 12A and B).
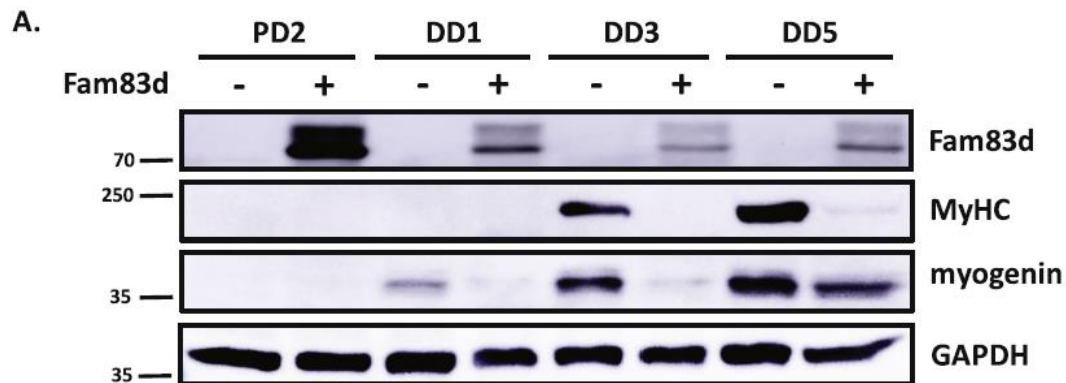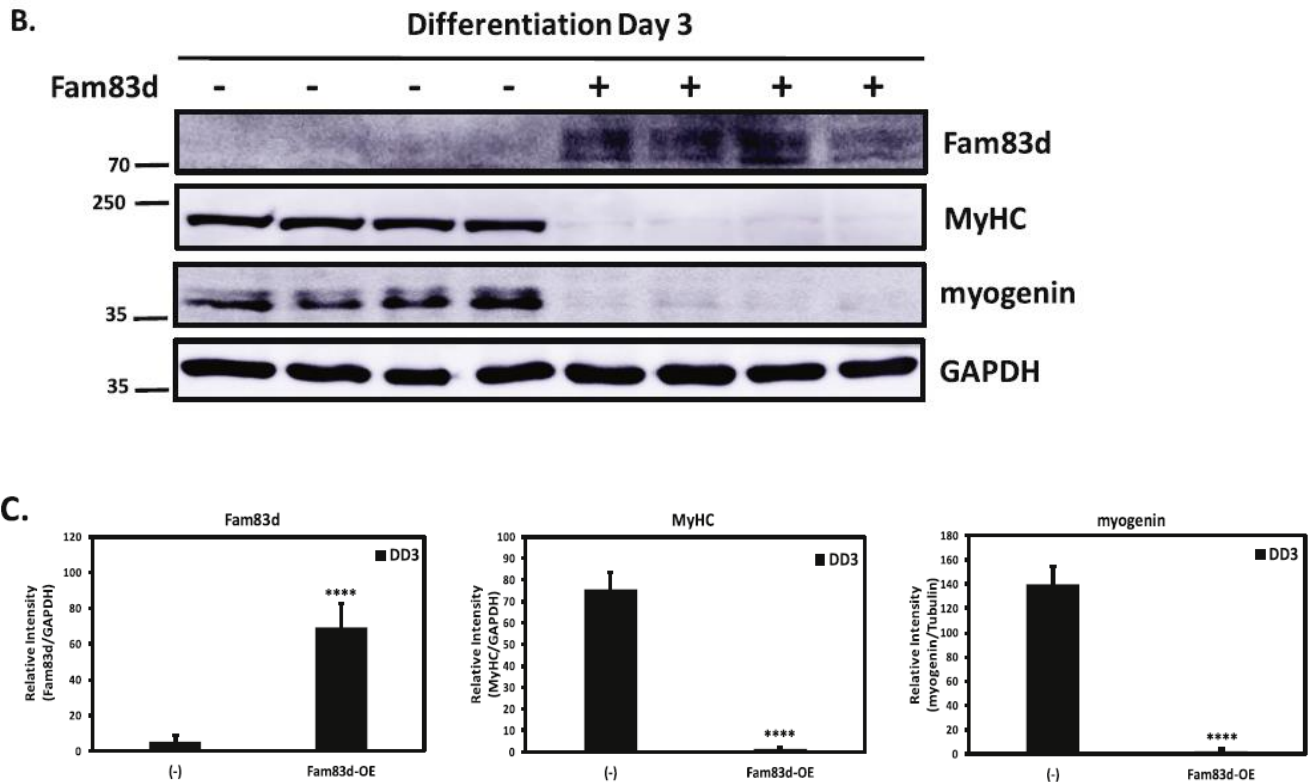
Figure 12. Ectopic expression of Fam83d attenuates muscle cell differentiation. C_2C_{12} cells were transfected with a Fam83d-myc-Flag expression plasmid or mock transfected followed by Western blot analysis. (A) Western blot analysis of Fam83d, Myosin Heavy Chain (MyHC), and myogenin using protein homogenates from proliferating (PD) and differentiated (DD) C_2C_{12} cells harvested over a 5-day differentiation time course. Cells were maintained in proliferation media (10% serum) and harvested 2 days post-plating and the remaining cells were then switched to differentiation media (2% serum) and harvested at 1, 3 and 5-days post-media change. GAPDH was analyzed to confirm equal protein loading. The experiments were repeated at least three times and the Western blots shown are representative examples of the results obtained. (B) C_2C_{12} cells were transfected with a Fam83d-myc-Flag expression plasmid or mock transfected in biological quadruplicates and cell lysates were then analyzed by Western blot for Fam83d, MyHC, and myogenin. Cells were maintained in proliferation media then switched to differentiation media (2% serum) for 3 days. GAPDH and α-tubulin was analyzed to confirm equal protein loading. The experiment was performed in quadruplicate (n = 4), repeated at least three times, and the blots shown are representative examples of the results obtained. (C) Quantification of the Western blot band intensities for Fam83d, MyHC, and myogenin. Relative intensity of each band was corrected to either GAPDH (shown) or α-tubulin band intensities for each corresponding biological replicate. Significant differences between control cells compared to cells ectopically expressing Fam83d-myc-Flag, (****: P < .0001).

Fam83d overexpression attenuates MAP kinase signaling

33

To determine if Fam83d overexpression impacts MAP kinase signaling, C_2C_{12} cells were transfected with a pSEAP-Pro-AP-1 reporter construct in combination with increasing concentrations of a wild-type Fam83d-myc-Flag expression plasmid (Fam83d-myc-Flag WT). Growth media was sampled 24 h post-transfection to evaluate SEAP levels in proliferating myoblasts and the AP-1 reporter showed significant activity at this timepoint in control cells, while Fam83d overexpression significantly reduced reporter activity in a dose-dependent manner (Fig. 13A). To confirm that Fam83d ectopic expression negatively regulates the MAP kinase signaling pathway, C_2C_{12} mouse cells were harvested over a differentiation time course, as well as, in biological quadruplicate at differentiation day 3 (DD3) as described above. Protein homogenates from cells ectopically expressing Fam83d were evaluated by Western blot to assess the effect that overexpression has on MAP kinase signaling. ERK1/2 phosphorylation levels decreased significantly in lysates isolated from cells overexpressing Fam83d at all differentiation time points assessed (Fig. 13B-D). To determine if Fam83d functions upstream of ERK1/2 in the MAP kinase signaling cascade, MEK1/2 and phosphorylated MEK1/2 levels were also evaluated by Western blot. Overexpression of Fam83d did not significant effect the level of whole MEK1/2 protein, but did show a small but significant inhibition of the phosphorylation status of MEK1/2 (p- MEK), suggesting that Fam83d likely influences MAP kinase signaling predominantly at the level of ERK1/2 in muscle cells (Fig. 13B-D). To investigate if a putative phospholipase D-like (PLD-like) motif is necessary for Fam83d inhibition of MAP kinase signaling, site-directed mutagenesis was used to modify two residues in the predicted catalytic pocket to create the Fam83d-H239N/K241Q double mutant. Interestingly, in contrast to wild-type Fam83d, overexpression of the Fam83d PLD-like motif mutant did not significantly inhibit the AP-1 reporter activity (Fig. 13A). To confirm that Fam83d-H293N/K241Q ectopic

expression does not negatively regulate the MAP kinase signaling pathway to the same level as wild-type Fam83d, C_2C_{12} cells were harvested in biological quadruplicate at DD3. Western blot analysis showed that overexpression of the Fam83d phospholipase D-like motif mutant had no significant effect on ERK1/2 protein or phosphorylation levels, in contrast to wild-type Fam83d (Fig. 13E and F).

A.

B.

C.

Differentiation Day 3

Fam83d: − − − − + + + +

p-ERK1/2

ERK1/2

p-MEK1/2

MEK1/2

D.

ERK1/2

p-ERK/ERK Ratio

MEK1/2

p-MEK/MEK Ratio

E.

Differentiation Day 3

Fam83d-H/K-Mut.: − − − − + + + +

Fam83d

p-ERK1/2

ERK1/2

GAPDH

36
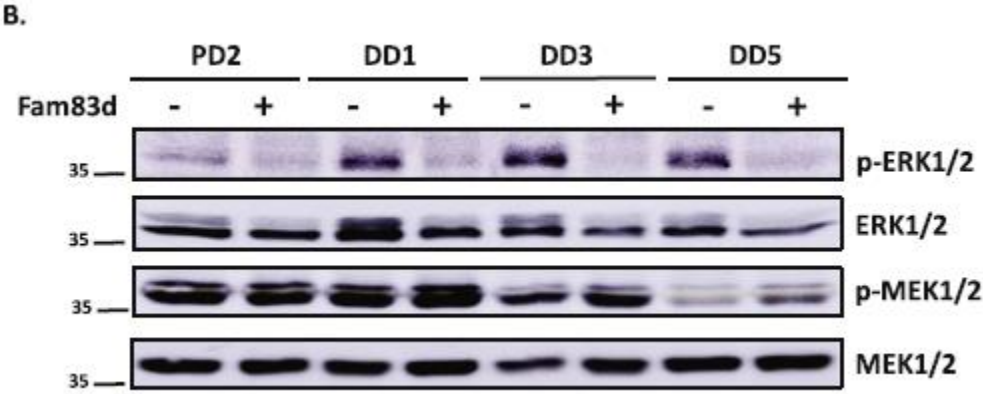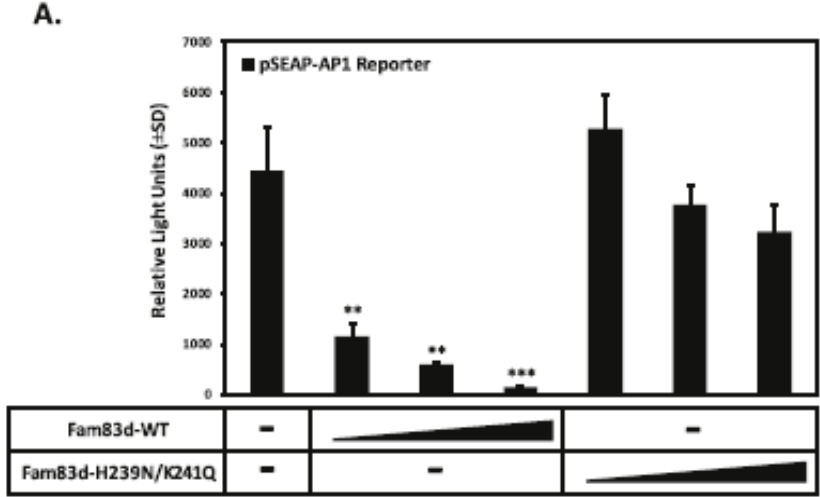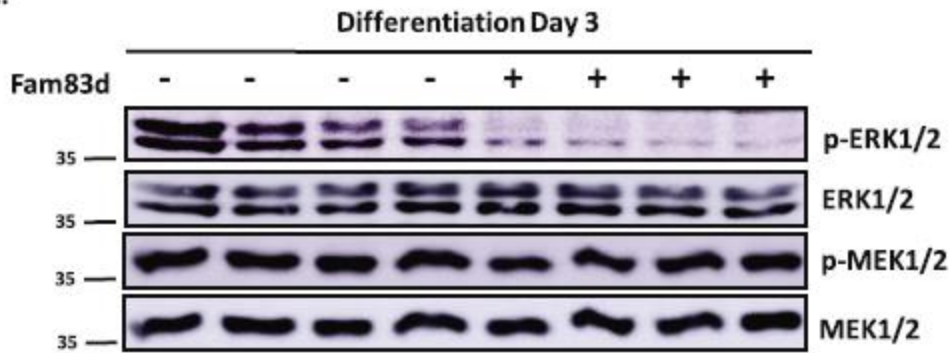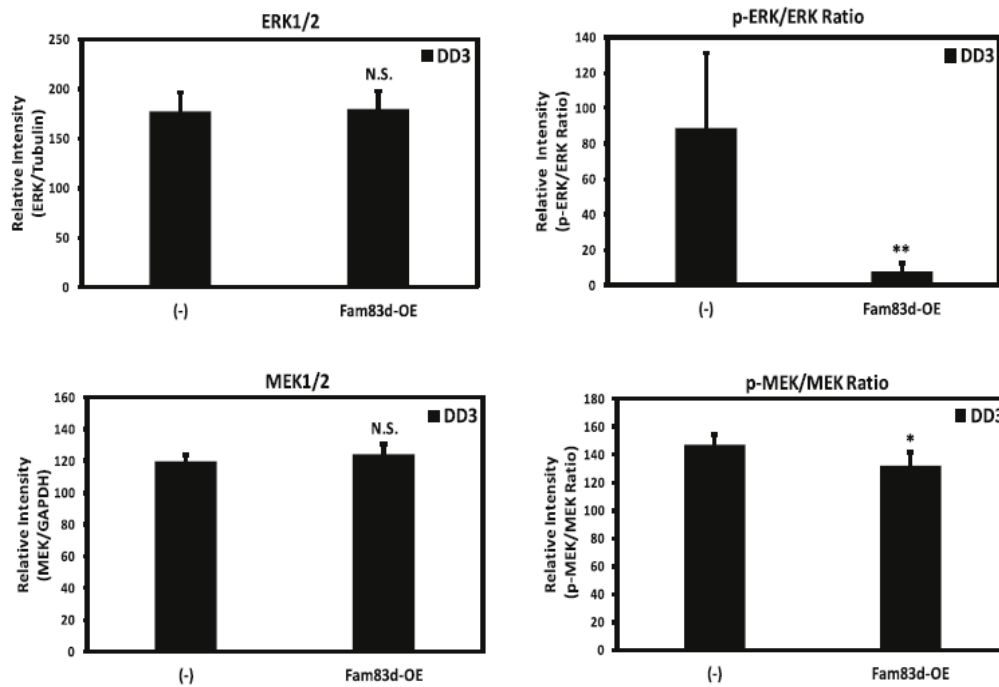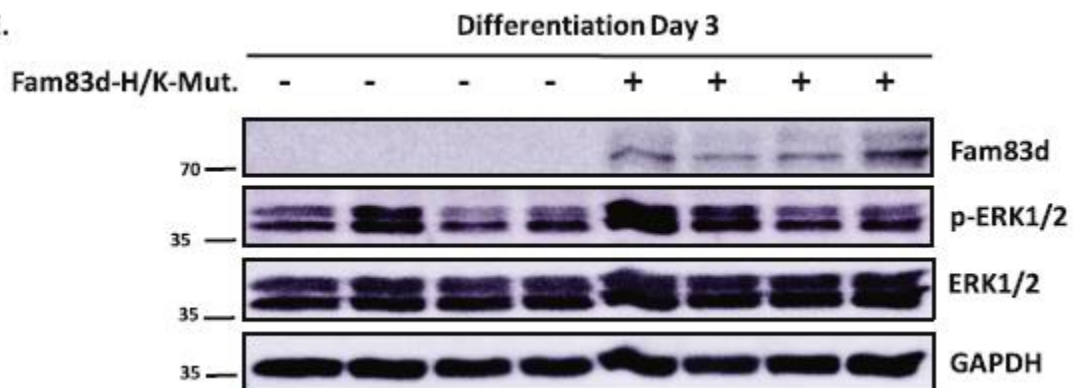
F.
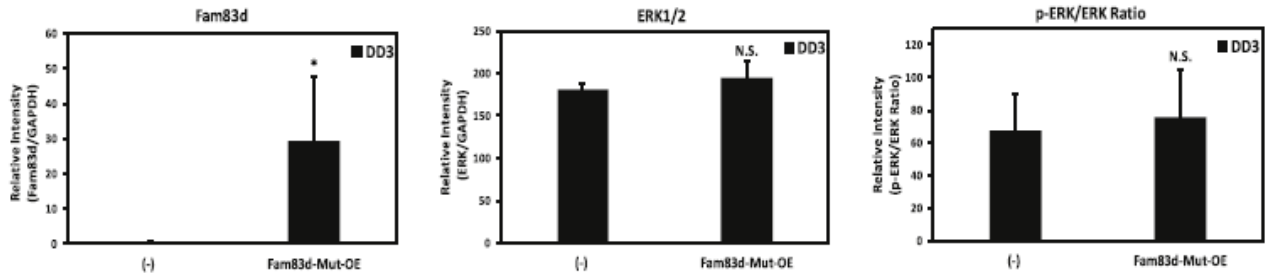
Figure 13. Fam83d overexpression inhibits AP-1 reporter activity and MAP kinase signaling. (A) C_2C_{12} cells were transfected with an AP-1 reporter plasmid and either a wild-type Fam83d or Fam83d-H239N/K241Q double mutant expression plasmid. The media was then assayed for SEAP activity 48 h (DD2) following the switch to differentiation media and SEAP numbers were normalized to β-galactosidase activity to correct for variations in transfection efficiency. Each condition was performed in triplicate and each experiment was repeated at least three times (n = 3). The graphs are of a representative experiment and values correspond to the mean relative light unit (RLU) values ±SD. Significant differences between the activities of the pSEAP2-AP-1-Pro reporter construct alone and in combination with Fam83d-WT or Fam83d-H239N/K241Q ectopic expression, (**: $P < .01$, ***: $P < .001$). (B) C_2C_{12} cells were transfected with a Fam83d-myc-Flag expression plasmid or mock transfected followed by Western blot analysis. Cells were maintained in proliferation media (10% serum) and harvested 2 days post-plating and the remaining cells were then switched to differentiation media (2% serum) and harvested 1, 3, and 5 days post-media change. Western blot analysis of phosphorylated-ERK1/2 (p-ERK1/2), pan-ERK1/2 (ERK1/2), phosphorylated-MEK1/2 (p-MEK1/2), and pan-MEK1/2 (MEK1/2) using protein homogenates from proliferating (PD2) and differentiated C_2C_{12} cells. The experiments were repeated at least three times (n = 3) and the Western blots shown are representative examples of the results obtained. (C) C_2C_{12} cells were transfected with a Fam83d-myc-Flag WT expression plasmid or mock transfected in biological quadruplicates. Western blot analysis of phosphorylated ERK1/2 (p-ERK1/2), pan-ERK1/2 (ERK1/2), phosphorylated-MEK1/2 (p-MEK1/2), and pan-MEK1/2 (MEK1/2) using protein homogenates from C_2C_{12} cells differentiated for 3 days. The experiment was performed in quadruplicate (n = 4), repeated at least three times, and the blots shown are representative examples of the results obtained. (D) Quantification of the Western blot band intensities were measured for pan-ERK1/2 and pan-MEK1/2 protein levels, as well as, the phospho-ERK1/2 to pan-ERK1/2 ratio and the phospho-MEK1/2 to pan-MEK ratios. Significant differences between control cells compared to cells ectopically expressing Fam83d, (*: $P < .05$, **: $P < .01$, N.S. = not significant). (E) C_2C_{12} cells were transfected with a Fam83d-H239N/K241Q expression plasmid or mock transfected in biological quadruplicates. Western blot analysis of Fam83d, phosphorylated-ERK1/2 (p-ERK1/2), pan-ERK1/2 (ERK1/2), phosphorylated-MEK1/2 (p- MEK1/2), and pan-MEK1/2 (MEK1/2) using protein homogenates from C_2C_{12} cells differentiated for 3 days. The experiment was performed in quadruplicate (n=4), repeated at least three times, and the blots shown are representative examples of the results obtained. (F) Quantification of the Western blot band intensities were measured for pan-ERK1/2 and the phospho-ERK1/2 to pan-ERK1/2 ratio. (N.S. = not significant).

Fam83d overexpression attenuates AKT signaling

The effect of Fam83d overexpression on AKT signaling was also evaluated by Western blot over

a differentiation time course, as well as, in biological quadruplicate at DD3. Overexpression of

Fam83d significantly reduced whole protein and phosphorylation levels of AKT at all time

points assessed (Fig. 14A-D). To further evaluate the effect of Fam83d on the AKT signaling

pathway, mTOR protein and phosphorylation levels were also investigated. Interestingly, at 3

days of differentiation, Fam83d overexpression had no significant effect on total mTOR protein

or phosphorylation of S2448, which is a primary target residue for AKT phosphorylation. GSK-

3β, another downstream target of AKT signaling, was also evaluated and no significant effect at

the whole protein level was observed in response to ectopic expression of Fam83d, while a small

but significant repression in phosphorylation levels in response to Fam83d overexpression was

observed (Fig. 14A-D).
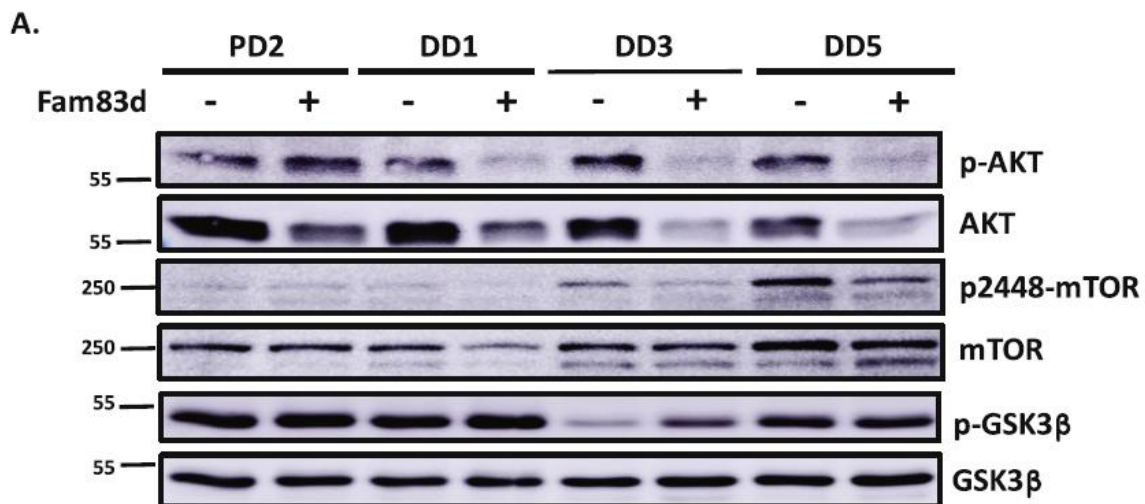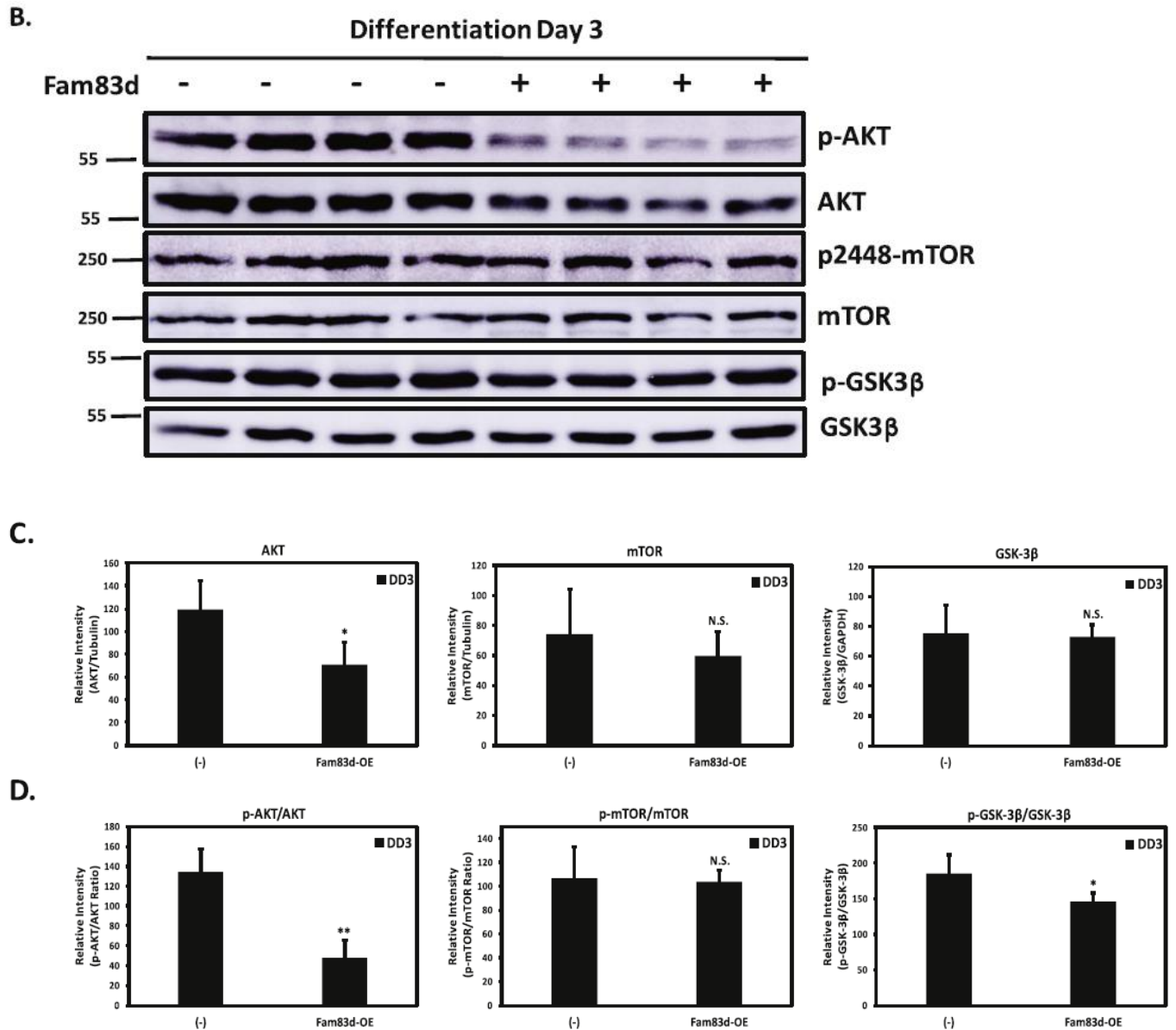
Figure 14. Ectopic expression of Fam83d inhibits AKT signaling in muscle cells. (A) C_2C_{12} cells were transfected with a Fam83d-myc-Flag expression plasmid or mock transfected. Cells were maintained in proliferation media (10% serum) and harvested 2 days post-plating and the remaining cells were then switched to differentiation media (2% serum) and harvested 1, 3, and 5 days post-media change. Western blot analysis of phosphorylated-AKT (p-AKT), pan-AKT (AKT), phosphorylated serine 2448-mTOR (p-S2448-mTOR), pan-mTOR (mTOR), phosphorylated-GSK-3β (p-GSK-3β), and pan-GSK-3β (GSK-3β) using protein homogenates from proliferating (PD2) and differentiated C_2C_{12} cells. These experiments were repeated at least three times (n = 3) and the Western blots shown are representative examples of the results obtained. (B) C_2C_{12} cells were transfected with a Fam83d-myc-Flag WT expression plasmid or mock transfected in biological quadruplicates. Western blot analysis of phosphorylated-AKT (p-AKT), pan-AKT (AKT), phosphorylated serine 2448 mTOR (p-S2448-mTOR), pan-mTOR (mTOR), phosphorylated-GSK-3β (p-GSK-3β), and pan-GSK-3β (GSK-3β) using protein

39

homogenates from C_2C_{12} cells differentiated for 3 days. The experiment was performed in quadruplicate (n =4), repeated at least three times, and the blots shown are representative examples of the results obtained. (C) Quantification of the Western blot band intensities were measured for AKT, mTOR, and GSK-3β. Relative intensity of each band was corrected to either GAPDH or α-tubulin band intensities for each corresponding biological replicate. Significant differences between control cells compared to cells ectopically expressing Fam83d-myc-Flag, (*: $P < .05$, N.S. = not significant). (D) Relative intensity of the phospho-AKT to pan-AKT ratio, the phospho-S2448-mTOR to pan-mTOR ratio, and the phospho-GSK-3β (p-GSK-3β) to pan-GSK-3β (GSK-3β) ratio. Significant differences between control cells compared to cells ectopically expressing Fam83d-myc-Flag, (*: $P < .05$, **: $P < .01$, N.S. = not significant).

Fam83d physically interacts with and destabilizes casein kinase 1α in muscle cells

Previous studies have demonstrated that Fam83 family members interact with casein kinase 1α (CSNK1α1) and HMMR (31, 32, 33, 34).To investigate if these interactions occur in muscle cells, co-immunoprecipitation (co-IP) was performed using protein lysates isolated from C_2C_{12} myoblasts transfected with a Fam83d-myc-Flag expression plasmid and harvested 24 h post-transfection. Immunoprecipitation of the Fam83d protein revealed a strong interaction with CSNK1α1 and HMMR (Fig. 15). To determine if the interactions between Fam83d and CSNK1α1 and Fam83d and HMMR are dependent on the putative phospholipase D-like (PLD) motif, lysates from C_2C_{12} cells overexpressing the Fam83d-H239N/K241Q mutant protein were also used for co-IP. Interestingly, mutation of the PLD-like motif significantly impaired the Fam83d/CSNK1α1 interaction, but did not affect the Fam83d/HMMR interaction (Fig. 15). Fam83d has also been shown previously to associate with Fbxw7 in colorectal cancer (30) and breast cancer (22) but co-immunoprecipitation showed no evidence of a direct interaction between Fam83d and Fbxw7 in skeletal muscle cells (Fig. 15).
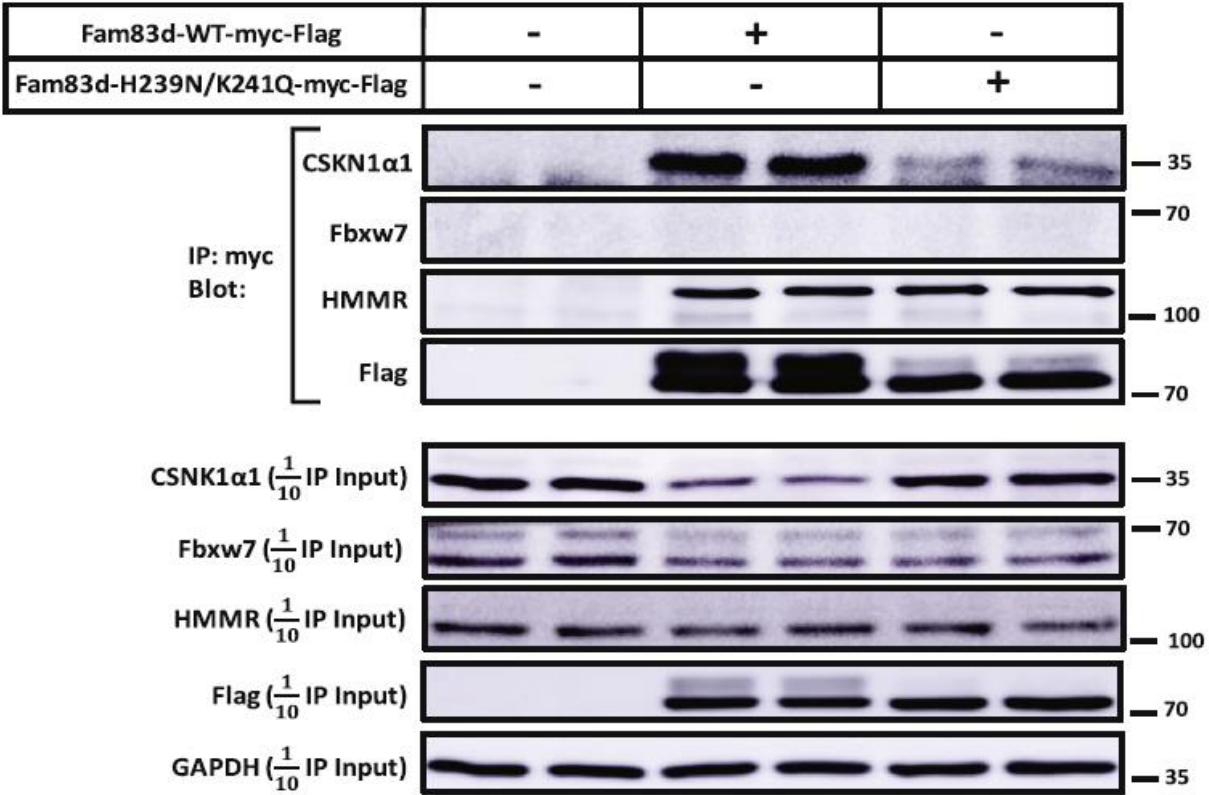
Figure 15. Fam83d physically interacts with casein kinase 1α. Fam83d directly interacts with casein kinase Iα and HMMR but not Fbxw7 in muscle cells. Immunoprecipitation (IP) of Fam83d from control C_2C_{12} cells and cells overexpressing wild-type Fam83d-myc- Flag or Fam83d-myc-Flag-H239N/K241Q double mutant followed by Western blotting for casein kinase Iα, Fbxw7, HMMR, or Fam83d-Flag (top four panels). Western blot analysis confirmed relatively equal casein kinase Iα, Fbxw7, HMMR, Fam83d, and GAPDH in cell lysates from control C_2C_{12} cells and cells overexpressing Fam83d-WT or Fam83d-H239N/K241Q (bottom five panels).

To further investigate the affect Fam83d might have on CSNK1α1, HMMR, and Fbxw7 stability, protein lysates from cells harvested over a differentiation time course and in biological quadruplicates at DD3 were evaluated by Western blot. Overexpression of Fam83d-WT significantly reduced CSNK1α1 protein levels at PD2 but did not appear to effect stability during differentiation (Fig. 16A-C). In contrast, Fbxw7 and HMMR protein levels showed significant elevation in response to Fam83d-WT ectopic expression later in differentiation (Fig. 16A-C).
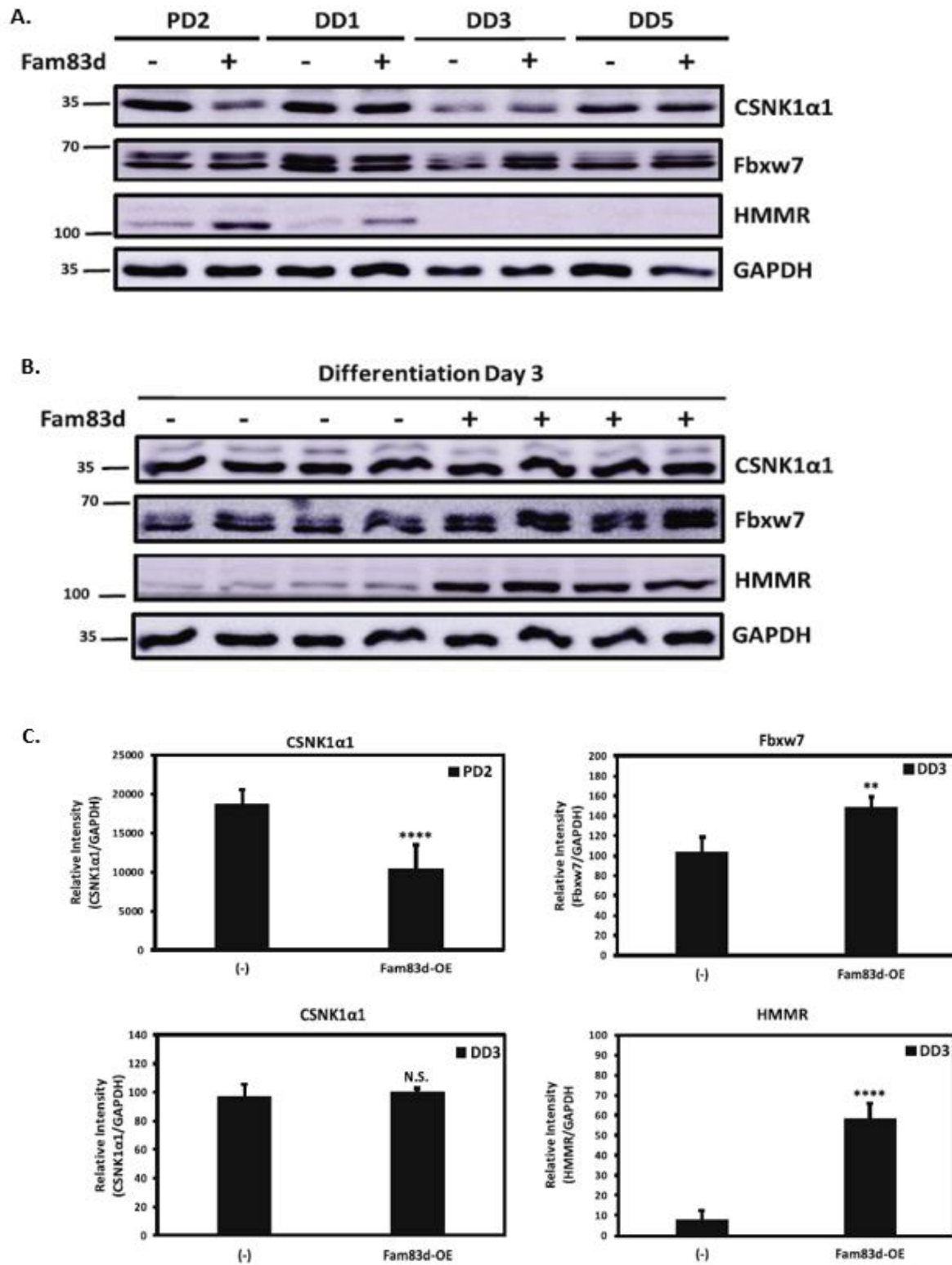
Figure 16. Overexpression of Fam83d destabilizes casein kinase 1α. (A) C₂C₁₂ cells were
transfected with a Fam83d-myc-Flag expression plasmid or mock transfected. Western blot

analysis of casein kinase Iα, Fbxw7, and HMMR using protein homogenates from proliferating (PD2) and differentiated (DD1, DD3, and DD5) C_2C_{12} cells. The experiments were repeated at least three times (n = 3) and the Western blots shown are representative examples of the results obtained. GAPDH was analyzed to confirm equal protein loading. (B) C_2C_{12} cells were transfected with a wild-type Fam83d-myc-Flag expression plasmid or mock transfected in biological quadruplicates. Western blot analysis of casein kinase Iα, Fbxw7, and HMMR using protein homogenates from C_2C_{12} cells differentiated for 3 days. The experiment was performed in quadruplicate (n = 4), repeated at least three times, and the blots shown are representative examples of the results obtained. GAPDH was analyzed to confirm equal protein loading. (C) Quantification of the Western blot band intensities measured from part C. Significant differences between control cells and cells ectopically expressing Fam83d, (**: $P < .01$, ****: $P < .0001$, N.S. = not significant).

To determine if the PLD-like motif plays a role in CSNK1α1, HMMR, and Fbxw7 protein stability, the Fam83d-H239N/K241Q mutant was overexpressed in cultured muscle cells and harvested in biological quadruplicates at DD3. In contrast to wild-type Fam83d, Fam83d-H239N/ K241Q overexpression resulted in significantly elevated levels of CSNK1α1, while Fbxw7 levels remained unchanged compared to control cells (Fig.17A and B)). Furthermore, as described above, AKT protein levels were found to be significantly repressed in response to ectopic expression of wild-type Fam83d (Fig. 14B and C). Therefore, AKT protein levels were also assessed using lysates harvested from cells ectopically expressing the Fam83d double mutant and no significant change in expression of AKT was observed (Fig. 17A and B). Interestingly, HMMR protein levels were elevated in cells overexpressing either Fam83d-WT (Fig. 16B and C) or Fam83d-H239N/K241Q (Fig. 17A and B). These results suggest that the mechanism by which Fam83d affects CSNK1α1, AKT, and Fbxw7 protein stability may depend on the putative phospholipase D-like motif, while stabilization of HMMR may be independent of the PLD-like motif.
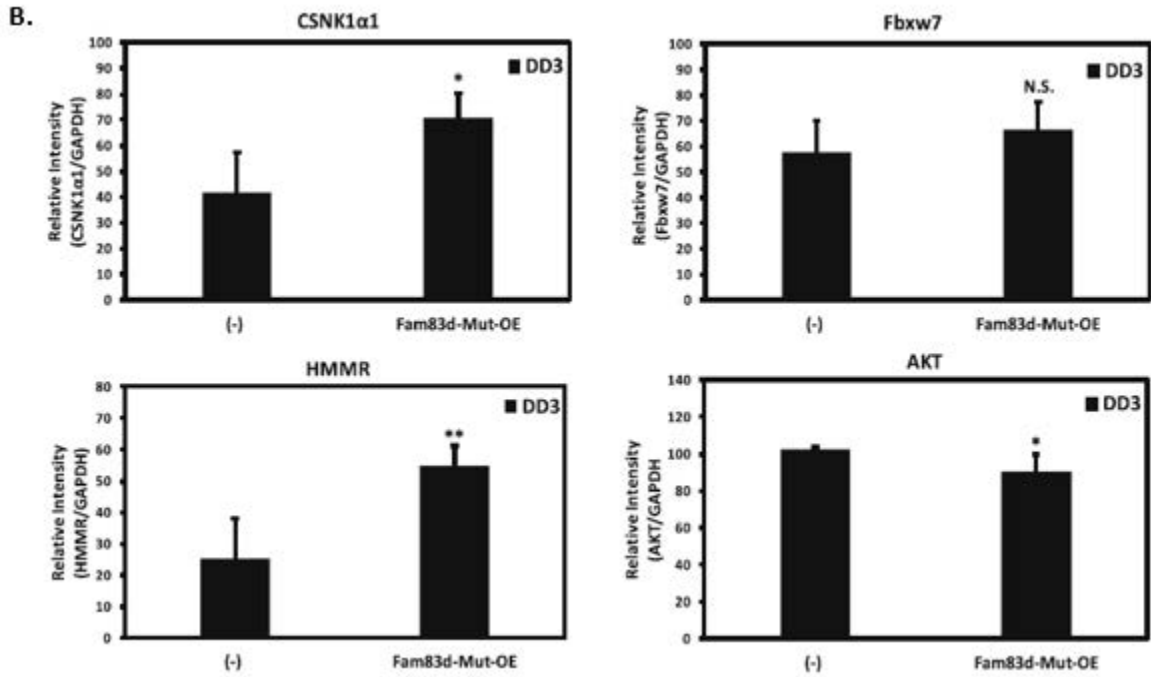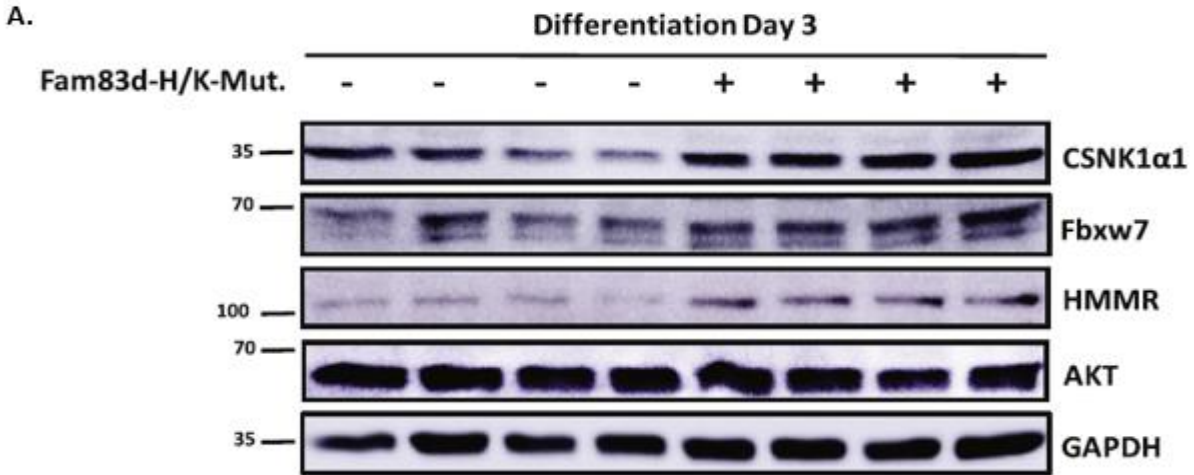
Figure 17. Fam83d effect on casein kinase 1α stability is PLD-like motif dependent. (A) C_2C_{12} cells were transfected with the Fam83d-H239N/K241Q double mutant expression plasmid or mock transfected in biological quadruplicates. Western blot analysis of casein kinase Iα, Fbxw7, HMMR, and AKT using protein homogenates from C_2C_{12} cells differentiated for 3 days. The experiment was performed in quadruplicate (n = 4), repeated at least three times, and the blots shown are representative examples of the results obtained. GAPDH was analyzed to confirm equal protein loading. (B) Quantification of the Western blot band intensities measured from part A. Significant differences between control cells and cells ectopically expressing Fam83d-H239N/K241Q, (*: $P < .05$, N.S. = not significant).

Finally, to support the hypothesis that the putative PLD-like motif likely plays a role in

CSNK1α1 stability and ERK1/2 phosphorylation levels, a second Fam83d mutant, Fam83d-

F280A, was generated. Mutation of F280 has previously been shown to abolish the Fam83d-

CSNK1α1 interaction (32, 33). Co-immunoprecipitation assays demonstrate that the Fam83d-

F280A mutant has diminished CSNK1α1 binding ability in muscle cells (Fig. 18A).

Furthermore, unlike the Fam83d PLD-like motif mutant, overexpression of the Fam83d-F280A

mutant did not lead to increased levels of CSNK1α1 in differentiated C2C12 cells (Fig. 18B and

C). Additionally, ectopic expression of the Fam83d-F280A mutant caused significant repression

of ERK1/2 phosphorylation (Fig. 18B and C), which matches the results obtained for Fam83d-

WT (Fig. 13C and D), but not the Fam83d PLD-like motif mutant (Fig. 13E and F).

A.
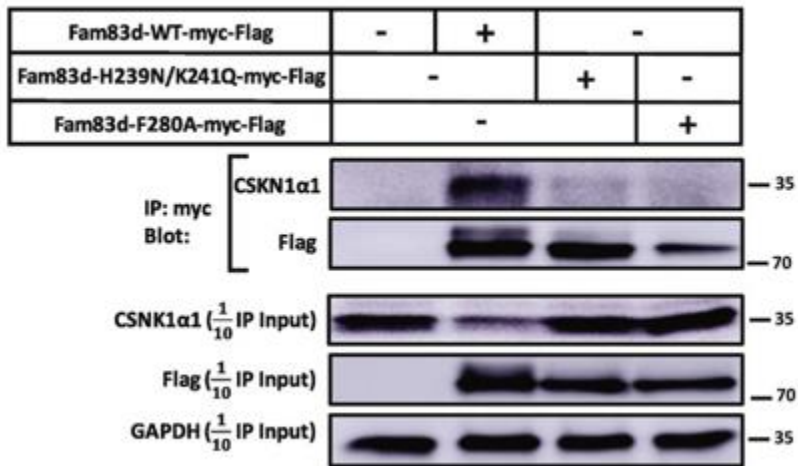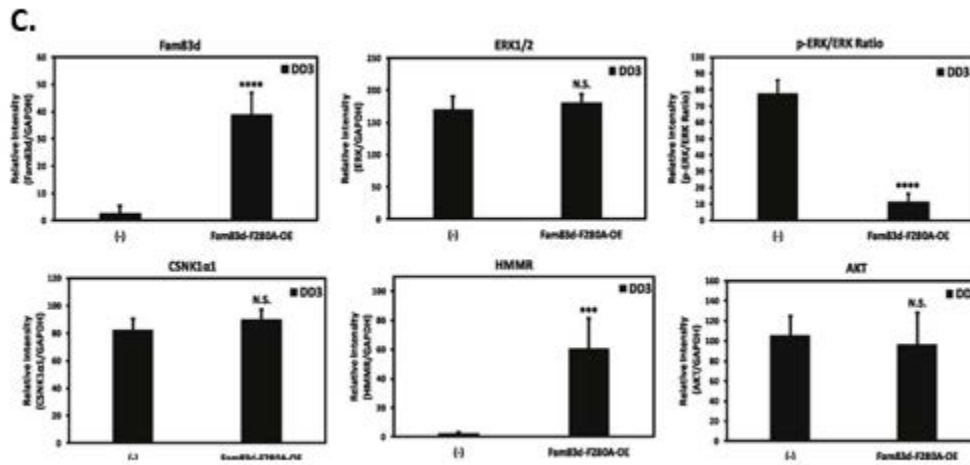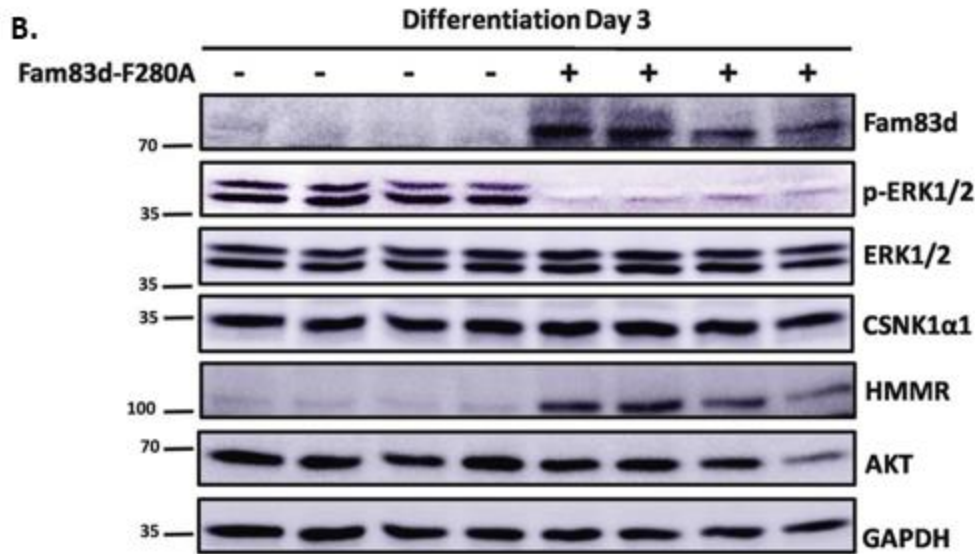
Figure 18. Fam83d-F280A mutant inhibits ERK1/2 phosphorylation and does not destabilize casein kinase 1α. (A) Fam83d-F280A does not interact with casein kinase Iα. Immunoprecipitation (IP) of Fam83d from control C2C12 cells and cells overexpressing wild-type Fam83d-myc-Flag, Fam83d-myc-Flag-H239N/K241Q double mutant, or Fam83d-myc-Flag-F280A mutant followed by Western blotting for casein kinase Iα or Fam83d-Flag (top two panels). Western blot analysis confirmed relatively equal casein kinase Iα, Fam83d, and GAPDH in cell lysates from control C2C12 cells and cells overexpressing Fam83d-myc-Flag WT, Fam83d-myc-Flag-H239N/K241Q, or Fam83d-myc-Flag-F280A (bottom three panels). (B) C2C12 cells were transfected with a Fam83d-myc-Flag-F280A mutant expression plasmid or mock transfected in biological quadruplicates. Western blot analysis of Fam83d, phospho-ERK1/2, pan-ERK1/2, CSNK1α1, HMMR, and AKT using protein homogenates from C2C12 cells differentiated for 3 days (DD3). The experiment was performed in quadruplicate (n = 4), repeated at least three times, and the blots shown are representative examples of the results obtained. GAPDH was analyzed to confirm equal protein loading. (C) Quantification of the

46

Western blot band intensities measured from part B. Significant differences between control cells compared to cells ectopically expressing Fam83d-myc-Flag-F280A, (***: P < .001, ****: P < .0001, N.S. = not significant).

Inhibition of ERK1/2 and MEK1/2 stabilizes Fam83d during muscle cell differentiation

As noted above, ectopic expression of Fam83d in C_2C_{12} results in a high level of expression during proliferation and then rapidly decreases as cells begin to differentiate (Fig. 9C and D). Since Fam83d inhibits the ERK1/2 branch of the MAP kinase signaling pathway, and inhibition of ERK1/2 or MEK1/2 causes pre-mature differentiation of C_2C_{12} cells, we evaluated if inhibition of ERK1/2 or MEK1/2 using small molecule inhibitors might impact Fam83d stability during muscle cell differentiation. To answer this question, C_2C_{12} cells were transfected with a Fam83d-myc-Flag expression plasmid and treated with increasing concentrations of either GSK1120212 (MEK inhibitor) or SCH772984 (ERK inhibitor) 24 h post-transfection and again at the switch to differentiation media. Cells were then harvested 24 h posttreatment and protein lysates were analyzed by Western blot. Fam83d protein levels were significantly elevated in response to both the MEK1/2 and ERK1/2 inhibitors (Fig. 19A-E). Furthermore, stabilization of Fam83d using the ERK1/2 and MEK1/2 inhibitors also resulted in significantly elevated levels of CSNK1α1 and AKT in muscle cells (Fig. 19B-E).
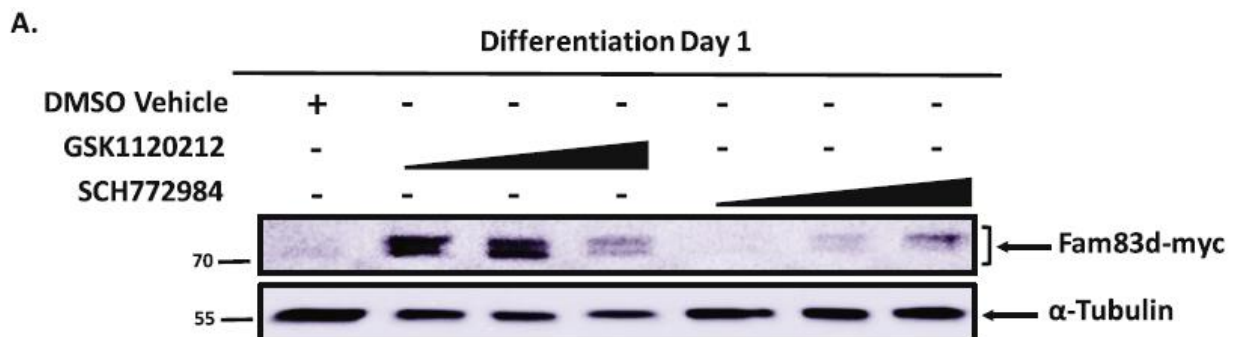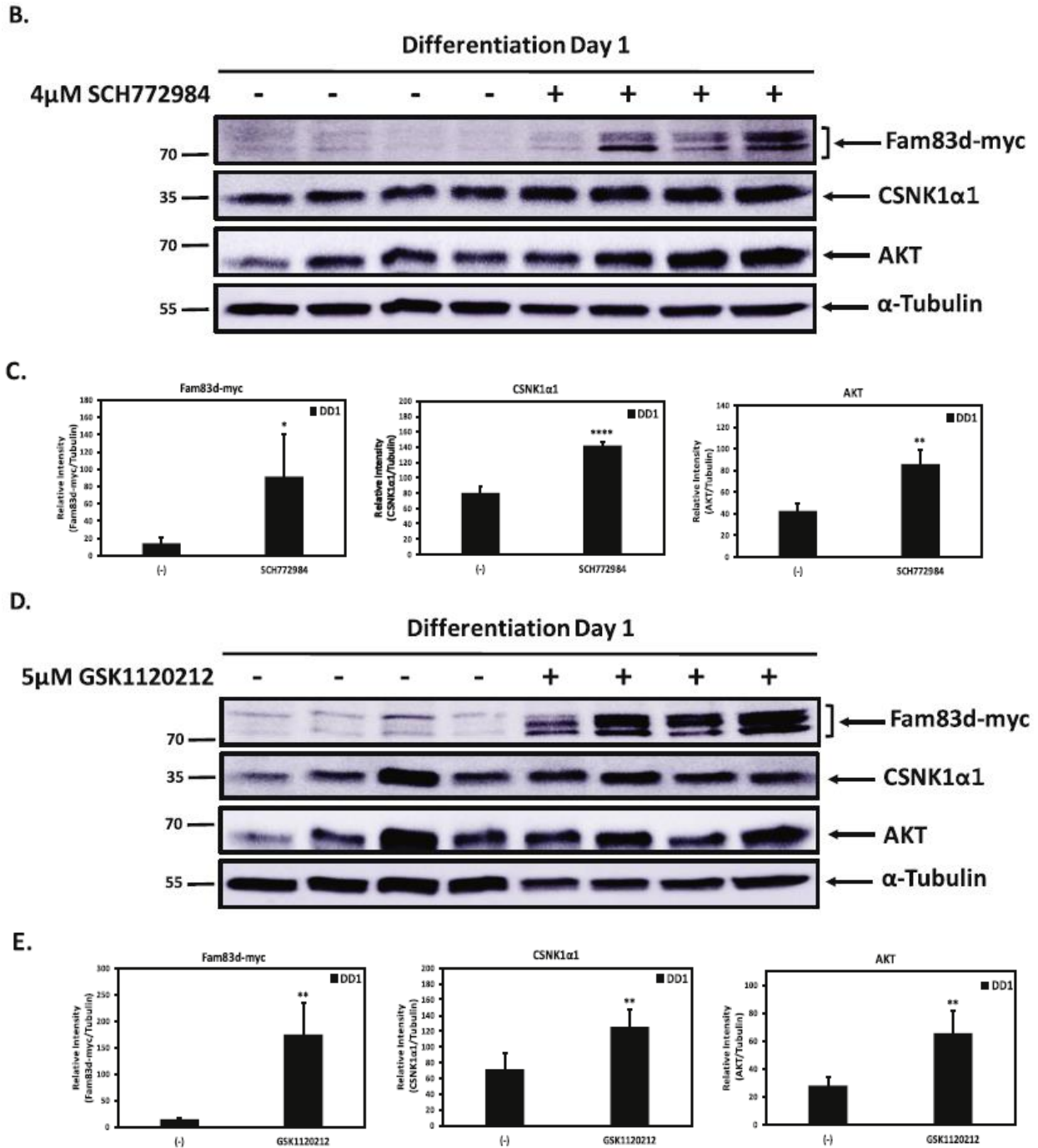
Figure 19. Inhibition of the MAP kinase signaling pathway stabilizes Fam83D. (A) C_2C_{12} cells were transfected with a wild-type Fam83d-myc-Flag expression plasmid and cells were then treated with either the MEK1/2 inhibitor GSK1120212 (2.5 µM, 5 µM or 10 µM) or the ERK1/2 inhibitor SCH772984 (1 µM. 2 µM or 4 µM) or vehicle alone 24 h post-transfection. Western blot analysis of Fam83d-myc-Flag using protein homogenates from cells differentiated for 1 day. α-tubulin was analyzed to confirm equal protein loading. (B) C_2C_{12} cells were transfected with a wild-type Fam83d-myc-Flag expression plasmid and then treated with either SCH772984 (4 µM) or vehicle alone 24 h post-transfection and differentiated for 1 day. Western blot analysis of Fam83d-myc-Flag, casein kinase Iα, and AKT using protein lysates from cells differentiated for

48

1 day. The experiment was performed in quadruplicate (n = 4), repeated at least three times, and the blots shown are representative examples of the results obtained. α-tubulin was analyzed to confirm equal protein loading. (C) Quantification of the Western blot band intensities measured from part B. Significant differences between control cells and cells treated with SCH772984, (*: $P < .05$, **: $P < .01$, ****: $P < .0001$). (D) C_2C_{12} cells were transfected with a wild-type Fam83d-myc-Flag expression plasmid and then treated with either GSK1120212 (5 μM) or vehicle alone 24 h post-transfection and differentiated for 1 day. Western blot analysis of Fam83d-myc-Flag, casein kinase Iα, and AKT using protein lysates from cells differentiated for 1 day. The experiment was performed in quadruplicate (n = 4), repeated at least three times, and the blots shown are representative examples of the results obtained. α-tubulin was analyzed to confirm equal protein loading. (E) Quantification of the Western blot band intensities measured from part D. Significant differences between control cells and cells treated with GSK1120212, (**: $P < .01$).

Discussion

Skeletal muscle is unique among body tissues due to its high degree of plasticity and its ability to regulate its size and mass (9, 35). Skeletal muscle mass is maintained by a balance between protein synthesis and protein degradation and when this balance is shifted toward protein degradation, atrophy occurs (35). This imbalance can be triggered by a wide range of physiological events including denervation, starvation, disease, disuse, and aging (9). While there has been much work focused on degradation pathways, such as the ubiquitin proteasome system, the molecular mechanisms that underly these disparate atrophy-inducing events remains unclear. Fam83d has been identified as a novel molecular component of the atrophy cascade as it is transcriptionally active in muscle and was found to be upregulated in response to neurogenic atrophy (5). Fam83d has been previously studied in a variety of cancer models but this is the first study to examine its role in muscle.

To characterize the expression and regulation of Fam83d in muscle, qPCR was conducted using cDNA generated from C_2C_{12} mouse myoblasts over a differentiation time course. These results showed that Fam83d is highly upregulated during myoblast proliferation and is significantly

down regulated as the cells proceed through differentiation. In addition, a Fam83d reporter gene was found to be highly active in proliferating muscle cells and was repressed by ectopic expression of MyoD, a myogenic regulator factor (MRFs) that is capable of binding canonical E-box elements such as those found in the proximal promoter region of Fam83d. Muscle development is a highly ordered process controlled by a concert of myogenic regulatory factors being expressed at specific stages of muscle cell development (36). Myf5 is the first MRF to be expressed in satellite cells, which commits them to the muscle cell lineage. MyoD expression follows shortly thereafter, in a semi-redundant role, to further push cells toward muscle cell development. Finally, as MyoD expression rises in proliferating myoblasts myogenin and MRF4 are transcriptionally activated, which subsequently promotes muscle cell differentiation and myotube formation (36). Therefore, the transcriptional repression of Fam83d during muscle differentiation is likely MRF-dependent and might be a necessary step in muscle development. In support of the qPCR data, endogenous Fam83d protein levels were found to decrease significantly as cultured muscle cells transitioned from proliferating myoblasts to differentiated myotubes.

Ectopic expression of myc-tagged Fam83d fusion protein was also found to be highly expressed during proliferation and then rapidly turned over, which matches the endogenous Fam83d expression pattern in muscle cells. Furthermore, treatment with MG132 stabilized Fam83d expression during differentiation suggesting Fam83d is actively degraded by the 26S proteasome as muscle cell differentiation progresses. These findings together suggest that Fam83d may have a muscle-specific role with a narrow window of activity during the proliferative stage of muscle development and is then transcriptionally downregulated and

proteolytically degraded as cells enter differentiation. This is in agreement with previous findings in several models of cancer where Fam83d was found to be a cell-cycle related gene and alterations in its expression effected cell proliferation (22, 25, 29, 30, 31). Additionally, Fam83d has previously been shown to be co-expressed with several mitosis-related genes (37).

To better understand the function of this gene in skeletal muscle, Fam83d was overexpressed and protein lysates were compared to those from control cells via Western blot. It was found that ectopic expression of Fam83d inhibited myogenic differentiation, as determined by significant decreases of both myogenin and myosin heavy chain at all time points of differentiation tested. It is important to note that C_2C_{12} cells proliferate as myoblasts until they reach a confluent monolayer and then fuse and differentiate into multinucleated myotubes on the culture plate under reduced serum conditions. Therefore, if Fam83d were driving C_2C_{12} cell proliferation as is observed in many cancer cell models, it would be expected that myoblasts overexpressing Fam83d would differentiate more quickly than cells not overexpressing Fam83d.

Furthermore, signaling pathways involved in myogenesis have been extensively studied and it is well established that perturbations in these pathways can impair, delay or prevent muscle cell differentiation and tissue development (11) One such pathway is the mitogen-activated protein (MAP) kinase pathway. This pathway has four canonical branches, including extracellular signal-regulated kinase 1/2 (ERK1/2), p38, c-Jun N terminal kinase (JNK), and ERK5 (10). As Fam83d overexpression significantly inhibits myogenic differentiation, we hypothesized it may be acting though inhibition of the MAP kinase pathway. Indeed, Fam83d overexpression significantly reduced ERK1/2 phosphorylation, while ERK1/2 protein levels were also reduced,

albeit to a lesser extent. Interestingly, MEK1/2 protein levels were not affected by Fam83d overexpression, while phosphorylation status of MEK1/2 was only mildly inhibited by Fam83d ectopic expression. To confirm that Fam83d-mediated inhibition of ERK1/2 phosphorylation results in a change in the MAPK signaling cascade, we evaluated the activity of the downstream transcription factor AP-1. When C_2C_{12} cells were transfected with increasing concentrations of Fam83d, we saw a corresponding decrease in the activity of an AP-1 reporter gene in a dose-dependent fashion. Taken together, this data suggests that Fam83d inhibits MAPK signaling specifically though the ERK1/2 branch by imposing its effects downstream of MEK1/2. Previous studies have also observed an effect of Fam83d on MAPK signaling. In hepatocellular carcinoma cell culture, Fam83d overexpression was shown to increase phosphorylation levels of both MEK1/2 and ERK1/2 (25). Another study investigating the role of Fam83d in ovarian cancer saw a similar increase in ERK1/2 phosphorylation when Fam83d was overexpressed in cell culture (38). The findings of this study provide further evidence for the involvement of Fam83d in the ERK branch of MAPK signaling but suggest the mechanism of that involvement may be different between skeletal muscle and various cancer types. This is not wholly unexpected as cancer represents an aberration of normal cell signaling. The ERK1/2 branch of the MAP kinase pathway is active during myoblast proliferation, decreases as cells differentiate, and then peaks again at terminal differentiation and during myoblast fusion (11). As Fam83d expression is highest during proliferation, it is possible that Fam83d is influencing this first phase of ERK1/2 activation. Since expression of both proteins decrease as cells enter differentiation, we evaluated the effect of MEK and ERK inhibition though the use of the small molecule inhibitors GSK1120212 or SCH772984, respectively. Data from this experiment revealed that inhibition of MEK or ERK was sufficient to significantly increased Fam83d levels during muscle cell

differentiation. This suggests there may be some coordination of protein turnover involving both Fam83d and the ERK1/2 branch of the MAPK signaling pathway as each appears to inhibit the other.

Another important molecular component of muscle development and growth is the AKT signaling pathway. AKT is a kinase that is activated in response to insulin signaling and can modulate the activity of several downstream targets, including mTOR and GSK-3β (11). Phosphorylation of mTOR by AKT is an activating event that leads to an increase in protein synthesis. GSK-3β has been shown to inhibit differentiation and hypertrophy and phosphorylation by AKT relieves this inhibition (11). To further elucidate the function of Fam83d, we investigated its possible role in the AKT pathway. Overexpression of Fam83d greatly reduced both total AKT protein levels, as well as, the amount of phosphorylated AKT in C_2C_{12} cells. Surprisingly, Fam83d overexpression did not significantly reduce mTOR phosphorylation at serine 2448, the primary site of AKT phosphorylation. Overexpression of Fam83d did not appear to effect GSK-3β protein levels, but did cause a small, but significant decrease in GSK-3β phosphorylation levels.

These data suggest Fam83d may have a role in negatively regulating AKT activity as part of the atrophy cascade. Interestingly, other investigations have also found Fam83d to be involved in AKT signaling (22, 29). A study looking at the role of Fam83d in breast cancer showed that overexpression of Fam83d increased the amount of mTOR phosphorylation (22). Another study investigating ovarian cancer also observed an increase in AKT and mTOR phosphorylation in response to Fam83d overexpression (29). As with the results from the effect of Fam83d on

ERK1/2 signaling, these results suggest that Fam83d is working via a different mechanism in skeletal muscle than in cancers.

Fam83d is one of an eight-member family of proteins that all have DUF1669 in common, which is a domain of unknown function located at the N-terminus of each protein. While the amino acid sequence of this highly conserved region provides few clues as to the function of the domain, it does contain an HxKxxxxD (HKD) motif that is characteristic of a phospholipase D-like (PLD-like) domain (39). Typically, proteins that have phospholipase D catalytic activity contain two PLD domains, and these domains interact to form the catalytic core within the protein (39). Fam83d contains only one such HKD motif and, to date, there is no evidence that Fam83d possess canonical PLD activity. A recent study found that DUF1669 was both necessary and sufficient for the association between Fam83 family members and members of the casein kinase 1 (CSNK1) family, which has resulted in a proposed renaming of DUF1669 to polypeptide anchor of casein kinase 1 (PACK1) (32). This same study demonstrated that different CSNK1 isoforms have affinity for specific Fam83 family members, and Fam83d was shown to associate specifically with CSNK1α1 and CSNK1α1-like (32).

To further elucidate the role of Fam83d in skeletal muscle, co-immunoprecipitation experiments using C_2C_{12} cells revealed that Fam83d does indeed associate with CSNK1α1. To investigate the mechanism of this interaction, site-directed mutagenesis was used to create a double mutation within the HKD motif resulting in the creation of the Fam83d- H239N/K241Q mutant (Fig. 11A, green asterisks signify mutated amino acids). Disruption of the HKD motif significantly diminished the interaction between Fam83d and CSNK1α1 in muscle cells. Interestingly,

overexpression of Fam83d-H238N/K241Q resulted in a significant increase in CSNK1α1 levels in differentiated myotubes, while overexpression of Fam38d-WT led to significant destabilization of CSNK1α1 in proliferating myoblasts. A recent study examined FAM83D and CSNK1α1 binding in the human osteosarcoma cell line U2OS by mutating two different amino acids also contained within DUF1669; F283A and D249A. Each of these substitutions on their own were sufficient to ablate the Fam83d/CSNK1α1 interaction (33). These results together suggest that the binding of CSNK1α1 to Fam83d likely involves numerous amino acids in the DUF1669 region and that mutation of any of these residues greatly disrupts the interaction between Fam83d and CSNK1α1. In the current study, we also generated a Fam83d-F280A mutant (equivalent to the human FAM83D-F283A mutation) and found that the Fam83d/CSNK1α1 interaction was significantly diminished. Interestingly, the Fam83d-F280A mutant did not stabilize CSNK1α1 in differentiated myotubes as was observed with Fam83d-H239N/K241Q double mutant overexpression. Furthermore, like wild-type Fam83d, the F280A mutant was still able to inhibit ERK1/2 phosphorylation, while the H239N/K241Q mutant was unable to inhibit ERK1/2 phosphorylation. These novel and intriguing observations suggest that the putative PLD-like domain may play a functional role in CSNK1α1 stability and ERK1/2 phosphorylation in muscle cells.

The discovery that Fam83d is induced in response to denervation furthers our understanding of the molecular genetic events of neurogenic atrophy. This study identifies Fam83d as having novel, muscle specific, expression and function. Fam83d is both transcriptionally active and highly expressed during myoblast proliferation and is rapidly downregulated and degraded as cells begin differentiation. Fam83d overexpression negatively regulates both the ERK1/2 branch

of MAP kinase signaling, as well as, AKT signaling. This regulation appears to involve the HKD motif located within DUF1669 at the N-terminal region of the protein and disruption of this motif reverses the negative effects. Fam83d also physically associates with and destabilizes CSNK1α1 in skeletal muscle and this association and destabilization is at least partially mediated by the HKD motif. Although further investigation is needed to elucidate the precise function of this gene, this study furthers our current understanding of the molecular and cellular events of muscle atrophy and suggests that Fam83d may play a functional role in muscle cell differentiation, development, and atrophy.

Chapter 3: Identification and Functional Analysis of Dual Specificity Phosphatase and Pro Isomerase Containing 1 (Dupd1) in Skeletal Muscle

Introduction

Overview of Dupd1

Dupd1 is categorized as an atypical dual specificity phosphatase (DUSP) capable of dephosphorylating both phosphotyrosine and phosphoserine/phosphothreonine residues within the same substrate (40). Dupd1 is evolutionarily conserved, sharing 87% identity with human and 91% identity with rat (41). In mice, Dupd1 is highly expressed in skeletal muscle, liver and adipose tissue (41). Interestingly, the human mRNA of Dupd1 has only been detected in skeletal muscle (http://www.proteinatlas.org/ENSG00000188716-DUPD1/tissue). When the open reading frame associated with Dupd1 was initially identified, it was predicted to include a proline isomerase and a DUSP region but further investigation showed the transcript does not include the proline isomerase, making dual specificity phosphatase and pro isomerase domain containing 1 a bit of a misnomer (41). Dupd1 was renamed to Dusp27 in a 2007 paper, causing confusion with another atypical DUSP that is identified by the same name (41). For clarity, the subject gene of this study will continue to be referred to as Dupd1 until the nomenclature has been definitively determined. Dupd1 has been the focus of few previous studies and its role in skeletal muscle atrophy is completely unknown. As a phosphatase, the role of Dupd1 may lie in modulation of intracellular signaling.

Materials and Methods

Cell Culture

The C$_2$C$_{12}$ immortalized mouse myoblast cell line was obtained from the American Type Culture Collection (Manassas, VA) and maintained in DMEM (Life 163 Technologies, Grand Island, NY) supplemented with 10% fetal bovine serum (FBS) (GE164 Healthcare HyClone Laboratories, Logan, UT), non-essential amino acids, gentamicin, penicillin and streptomycin (all from Life Technologies, Grand Island, NY). Cells were grown in a humidified chamber at 37ºC at 5% CO2. Cells were switched to DMEM supplemented with 2% serum, non-essential amino acids, gentamicin, penicillin and streptomycin 48 hours post-plating to stimulate myotube differentiation (Waddell, 2016).

RNA Isolation and cDNA synthesis

Total RNA was isolated from C$_2$C$_{12}$ myoblast cells using the RNeasy Mini Kit (Qiagen, Valencia, CA) according to the manufacturer's protocol. Purified RNA (1µg) was reverse-transcribed using Oligo-dT primers and Moloney Murine Leukemia Virus (M-MLV) Reverse Transcriptase according to the manufacturer's protocol (Life Technologies, Grand Island, NY)

Amplification and cloning of the full length Dupd1 cDNA

For the amplification of Dupd1 cDNA, gene-specific primer pairs were designed (see Table 1) using the gene sequences from *Mus musculus* (GenBank accession number: NM_001013826). PCR was performed according to the manufacturer's protocol (Life Technologies, Grand Island, NY) using Taq DNA polymerase, and template prepared by reverse transcription of RNA isolated from C$_2$C$_{12}$ cells as described above utilizing gene specific primer pairs (Table 1). Amplicons were cloned into the pGEM-T Easy vector (Promega, Madison, WI) according the manufacturer's protocol and sequenced using the Big Dye Sanger terminator sequencing method

(Eurofins MWG Operon, Huntsville, AL) to confirm amplification of the expected target and the absence of mutations. The Dupd1 cDNA was sub-cloned into the Xho1 and Bam HI restriction sites of pcDNA3.1 (+) (Life Technologies, Grand Island, NY) and sequenced to confirm correct orientation. The Dupd1 cDNA was also sub-cloned into the Xho1 and Bam HI restriction sites of the pEGFP-C3 expression plasmid (Clontech, Mountain View, CA) and sequenced to confirm correct orientation and in frame fusion with GFP. The Dupd1 cDNA fused to myc and DDDDK tags and cloned into the pCMV6-Entry vector was purchased from OriGene Technologies (Rockville, MD)..

Promoter cloning of the Dupd1 gene

Genomic DNA was isolated from C_2C_{12} cells using the DNeasy Blood and Tissue Kit (Qiagen, Valencia, CA) according to the manufacturer's protocol and used as template for the amplification of the proximal regulatory region of Dupd1. PCR was performed using Dupd1 promoter region-specific primer pairs (see Table 1) developed using mouse genomic sequences obtained from the Ensembl database (www.ensembl.org). PCR reactions were performed using Taq DNA polymerase and genomic mouse DNA according to the manufacturer's protocol (Life Technologies, Grand Island, NY). The PCR amplicons were cloned into the pGEM-T Easy vector (Promega,Madison,WI) according to the manufacturer's protocol and sequenced to confirm amplification of the predicted target region and the absence of mutations. The Dupd1 promoter fragments (~500, ~1000 and ~2000 base pairs) were sub-cloned into the Mlu I and Hind III sites of the pSEAP2-Basic reporter plasmid (Clontech, Mountain View, CA) to create the pSEAP-Dupd1-Pro500, the pSEAP-Dupd1-Pro1000 and the pSEAP-Dupd1-Pro2000 reporter plasmids and sequenced to confirm correct orientation.

Transfections

C_2C_{12} myoblast cells were plated into 12 well plates at a density of 75,000 cells/well in DMEM + 10% FBS (proliferation media) and cultured overnight. All conditions were assessed in triplicate. Transfections were performed utilizing Turbofect Transfection Reagent (Thermo Scientific, Rockford, IL) following the manufacturer's protocol. Media was refreshed 1 hour prior to transfection. 1 μg of total DNA (250 ng/well of reporter plasmid, 125 ng/well of β - galactosidase (β-gal) as the internal control plasmid, and empty pBluescript vector as filler DNA to 1 μg DNA/well) was allowed to complex with transfection reagent for 20 minutes prior to overlaying the cells. Following 24-hour incubation with the transfection reaction, the proliferation media was replaced with differentiation media (DMEM + 2% serum) and incubated for an additional 1-7 days until reporter assays were performed.

SEAP reporter gene assays

Growth media was collected from C_2C_{12} mouse myoblasts at 1-7 days after the switch to differentiation media post-transfection and tested for SEAP levels using the Phospha-Light SEAP Reporter Gene Assay Kit and following the manufacturer's instructions (Life Technologies, Grand Island, NY). The level of SEAP generated luminescence was assessed with a Synergy 2 microplate reader programmed for an endpoint read and a 2 s integration time. At the conclusion of the experiment, cells were lysed with Passive Lysis Buffer (Promega, Madison, WI), lysates were centrifuged to clear cell debris, and assessed for β-galactosidase (β-gal) activity. The SEAP activity numbers were corrected with β-gal activity numbers to adjust for any variation in transfection levels between wells.

Bioinformatic analysis of Dupd1

DNA sequences corresponding to the promoter regions of human, rat, and mouse Dupd1
(Ensembl Transcript ID: ENSG00000188716.5, ENSRNOG00000013034.5, and
ENSMUSG00000063821.6, respectively) starting at -2000 and including the first exon were
taken from the Ensembl database (www.ensembl.org) and analyzed using the Clustal Omega
multiple sequence alignment tool available on the EMBL-EBI website
(https://www.ebi.ac.uk/Tools/msa/clustalo/). The Clustal Omega alignment data was then
analyzed using Boxshade version 3.21 (http://www.ch.embnet.org/software/BOX_form.html)
that is available on the ExPASy (www.expasy.org) website. The polypeptide sequences for
human, mouse, and rat Dupd1 were also downloaded from Ensembl and aligned using the
Clustal Omega alignment tool and shaded with Boxshade as described for the promoter
sequences above.

Quantitative PCR

Total RNA was isolated from proliferating and differentiated C_2C_{12} cells as described above.
Purified total RNA (1.0 μg) was reverse-transcribed using the iScript cDNA Synthesis Kit
according to the manufacturer's protocol (Bio- Rad, Hercules, CA). cDNA amplification was
conducted using the iTaq Universal SYBR Green Reaction Supermix and gene specific primers
(see Table 1) according to the manufacturer's protocol (Bio-Rad, Hercules, CA). Samples were
analyzed using a CFX Connect Real-Time PCR Detection System (Bio-Rad, Hercules, CA) and
gene expression levels of Dupd1 at PD2, DD2 and DD7 were quantitated. Each timepoint was
performed in biological triplicates, each individual biological replicate was used for cDNA

synthesis in duplicate, and each cDNA synthesis replicate was analyzed in technical triplicates (three biological replicates × two cDNA synthesis replicates × three technical replicates = 18 individual reads per biological sample) and the experiment was repeated at least twice. Relative gene expression was calculated using the $2^{-\Delta\Delta Ct}$ Livak method and using GAPDH as the reference gene.

Protein purification and Western blot analysis

C_2C_{12} cells were cultured in 10 cm culture dishes and Dupd1 was exogenously expressed by transfecting the cells with the pCMV6-Dupd1-myc-DDK or pcDNA3.1-Dupd1 expression plasmid 24 h post-plating. The Dupd1 overexpression time course was collected by harvesting cells 48 h post-plating (PD2), as well as cells cultured for an additional 1, 3 or 5 days in differentiation media (DD1, DD3, DD5). The collected cells were spun down and kept at −80°C until cell homogenization and protein isolation was performed.

The harvested cells were incubated on ice for 30 min, with agitation every 10 minutes, in Universal Lysis Buffer (50 mM Tris, pH 7.5, 150 mM NaCl, 50 mM NaF, 0.5% NP-40), plus additions (1 mM PMSF, 1 mM DTT, 10 mM β-glycerophosphate, 2 mM sodium molbydate, and a protease inhibitor cocktail). Cell homogenates were centrifuged to clear cellular debris and protein concentrations were determined using the Quick Start Bradford 1× Dye Reagent (Bio-Rad, Hercules, CA) following the manufacturer's instructions.

Western blots were conducted using 75-100 μg of protein on a 10% sodium dodecyl sulfate polyacrylamide gel electrophoresis denaturing gel and then transferring overnight to

polyvinylidene fluoride membrane (EMD Millipore, Billerica, MA). Membranes were stained with Ponceau S to visualize equal protein loading and successful transfer and then incubated with blocking solution (5% w/v dry milk in tris-buffered saline with 0.05% Tween-20). Western blot membranes were incubated with antibodies listed in Table 2, followed by probing with an appropriate HRP-conjugated secondary antibody (Santa Cruz Biotechnology, Dallas, TX) and visualized using ECL substrate (Pierce/Thermo Fisher Scientific, Rockford, IL). Polyvinylidene difluoride (PVDF) membranes were stripped by incubating for 20-30 min in stripping buffer (10% SDS, 0.5 M tris-HCl pH 6.8 and β-mercaptoethanol) at 50°C, and then blocked, probed, and visualized again as described above. Western blot band intensity quantifications were conducted using the open access ImageJ software.

Confocal Fluorescence Microscopy

C_2C_{12} cells were plated on Cellvis (Sunnyvale, CA) 35 mm glass bottom dishes and transfected 24 h after cells were plated with either the pEGFP-C3 or pEGFP-Dupd1 plasmids duplexed with TurboFect Reagent (Thermo Fisher Scientific, Rockford, IL) as per the manufacturer's instructions. Before imaging, the cells were washed with phosphate buffered saline, fixed with paraformaldehyde dissolved in sodium cacodylate, and stained with DRAQ5 fluorescent DNA dye (Biostatus, Leicestershire, UK). The images were acquired using an Olympus Fluoview FV-1000 confocal fluorescent microscope equipped with Super Apochromat UPLSAPO 20X and Super Apochromat UPLSAPO 60XW objectives. Open access ImageJ software combined with the Open Microscopy Environment Bio-Formats plugin was used to analyze, merge, and save all images.

Co-immunoprecipitation

C_2C_{12} cells were grown in 10% FBS DMEM media and transfected with pCMV6-Dupd1-myc-DDK expression plasmid and harvested 24 hours post-transfection. Cells were lysed on ice for 30 minutes in ULB (+) (50 mM Tris, pH 7.5, 150 mM NaCl, 50 mM NaF, 0.5% NP-40, 1 mM PMSF, 1 mM DTT, 10 mM β-glycerophosphate, 2 mM sodium molbydate, and protease inhibitor cocktail). Homogenates were cleared by centrifugation and protein concentrations were quantified using the Quick Start Bradford 1X Dye Reagent (Bio-Rad, Hercules, CA) according to the manufacturer's protocol. 500 µg protein was diluted in ULB and precleared with protein A/G agarose beads (Pierce/Thermo Scientific, Rockford, IL) for 1 h at 4°C with constant end-over-end rotation. Beads were cleared from solution via centrifugation and the supernatant was incubated with 2 µg of anti-myc (60003-2-lg; ProteinTech, 318 Rosemont, IL) antibody for 4 h at 4°C with constant end-over-end rotation. Protein A/G agarose beads were added to solution and incubation was continued for 6 additional hours. Beads were cleared from solution via centrifugation and pelleted beads were washed 3X with ULB, and then boiled for 5 mins at 95°C. 50 µg of protein lysate was used for input control and SDS-PAGE was performed. Separated proteins were then transferred to a PVDF membrane and probed using the antibodies listed in Table 2. .

Statistics

Data are presented as the mean ± standard deviation (SD). Statistical analysis was conducted using a two-tailed t-test and a difference was considered statistically significant at a P value < 0.05.

Table 3. List of primers used in the Dupd1 study

Primer	Sequence (5'-3')
Dupd1-cDNA-F1	GCCTCGAGGCTGCCACACACCCTTCGGACTGG
Dupd1-cDNA-R1	GCGGATCCCCCCTACAGCCCTAGGTCACTGTCC
Dupd1-cDNA-F2	GCCTCGAGGGCTCCAAAATGGCATCAGGAGATA
Dupd1-cDNA-R2	GCGGATCCCCTTTTCCTTACCCAGATCCCCCTG
Dupd1-C146A-F	GATCCTGGTTCACGCTGCCATGGGCCG
Dupd1-C146A-R	CGGCCATGGCAGCGTGAACCAGGATC
Dupd1-pro500-F	GCACGCGTGAAGTGCTACCTGCACAGTGTTTGCCC
Dupd1-pro1000-F	GCACGCGTGCATACCCGTCAGACCATCACCACACC
Dupd1-pro2000-F	GCACGCGTCACTACTCCCAGGCCTCAGGGATTAGG
Dupd1-pro-R	GCAAGCTTCTGGCTGGGCTAAGAGGTACCAGTCCG
Dupd1-pro500-Ebox1-Mut-F	CATCCTGGCGGCCGCACGTCCTGTATCTGTGG
Dupd1-pro500-Ebox1-Mut-R	CCACAGATACAGGACGTGCGGCCGCCAGGATG
Dupd1-pro500-Ebox2-Mut-F	TCATTTTGCAAACGAACGCCACGGGTCTCC
Dupd1-pro500-Ebox2-Mut-R	GGAGACCCGTGGCGTTCGTTTGCAAAATGA
Dupd1-qpcr-F1	GCACACAGAAAGGAAAGAACC
Dupd1-qpc-R1	TACAGTAGTCCTCAGCATCTC
Dupd1-qpcr-F2	CACACGTCAATGAGGTCTGGC
Dupd1-qpc-R2	ATGGCCATGTCTCGGTAGTAG

Table 4. List of antibodies used in the Dupd1 study

Antibody	Source	Catalog #	Dilution
anti-Dusp27	Santa Cruz Biotechnology, Dallas, TX	Sc-515513	WB: 1:250
anti-myc	ProteinTech, Rosemont, IL	60003-2-lg	WB: 1:2000 IF: 1:50
anti-α-tubulin	Santa Cruz Biotechnology, Dallas, TX	sc-32293	WB: 1:1000
anti-Myosin Heavy Chain (MYH1/2/4/6)	Santa Cruz Biotechnology, Dallas, TX	sc-32732	WB: 1:1000
anti-myogenin	Santa Cruz Biotechnology, Dallas, TX	sc-12732	WB: 1:1000
anti-GAPDH	ProteinTech, Rosemont, IL	60004-1-lg	WB: 1:5000
anti-phospho-ERK	Santa Cruz Biotechnology, Dallas, TX	sc-7383	WB: 1:1000
anti-ERK	Santa Cruz Biotechnology, Dallas, TX	sc-94	WB: 1:1000
anti-Akt1-phospho-S473	ProteinTech, Rosemont, IL	66444-I-lg	WB: 1:2000
anti-Akt	ProteinTech, Rosemont, IL	60203-2-lg	WB: 1:5000
anti-phospho-mTOR-Ser2448	Cell Signaling Technology, Danvers, MA	5536	WB: 1:2000
anti-phospho-mTOR-Ser2481	Cell Signaling Technology, Danvers, MA	2974	WB: 1:2000
anti-mTOR	ProteinTech, Rosemont, IL	66888-1-lg	WB: 1:10000
anti-phospho-4E-BP1 (Thr37/46)	Cell Signaling Technology, Danvers, MA	2855	WB: 1:1000

anti-4EBP1	ProteinTech, Rosemont, IL	60246-1-lg	WB: 1:2000
Anti-phospho-p70 S6 Kinase (Thr389)	Cell Signaling Technology, Danvers, MA	9205	WB: 1:1000
Anti p70(S6K)	ProteinTech, Rosemont, IL	66638-1-lg	WB: 1:4000
anti-phospho-AMPKα (Thr172)	Cell Signaling Technology, Danvers, MA	2535	WB: 1:1000
anti-AMPK	ProteinTech, Rosemont, IL	18167-1-AP	WB: 1:2000
anti-phospho-Glucocorticoid receptor (Ser211)	Cell Signaling Technology, Danvers, MA	4161	WB: 1:1000
Anti-Glucocorticoid receptor	ProteinTech, Rosemont, IL	66904-1-lg	WB: 1:5000
Anti-GFP tag	ProteinTech, Rosemont, IL	66002-1-lg	WB: 1:5000
anti-DDK	ProteinTech, Rosemont, IL	20543-1-AP	WB: 1:5000
Mouse anti-rabbit IgG-HRP	Santa Cruz Biotechnology, Dallas, TX	sc-2357	WB: 1:5000
Rabbit anti-mouse IgG-HRP (H+L)	Thermo Scientific, Rockford, IL	PI31450	WB: 1:5000

Results

Dupd1 is upregulated during neurogenic skeletal muscle atrophy

RNA was isolated from control and denervated mouse gastrocnemius and soleus muscles as previously described (5) and an Illumina mouse-6 v1.1 microarray was performed at 3 days and 14 days post-denervation. Analysis of the microarray data submitted to the NCBI Gene Expression Omnibus (GEO) revealed a significant number of genes that show differential expression patterns in response to neurogenic muscle atrophy. Many of these genes have not previously been characterized in skeletal muscle nor implicated in atrophy. Dupd1 showed low basal levels of expression in control gastrocnemius and soleus muscles. However, in the denervated tissue, Dupd1 was shown to be significantly upregulated at day 3 and day 14 post-denervation as compared to control animals (Fig. 20A).

Dupd1 is composed of three coding and one non-coding exons, is located on chromosome 14 in

mice, and shows strong architectural conservation between mouse, rat, and human (Fig. 20B).
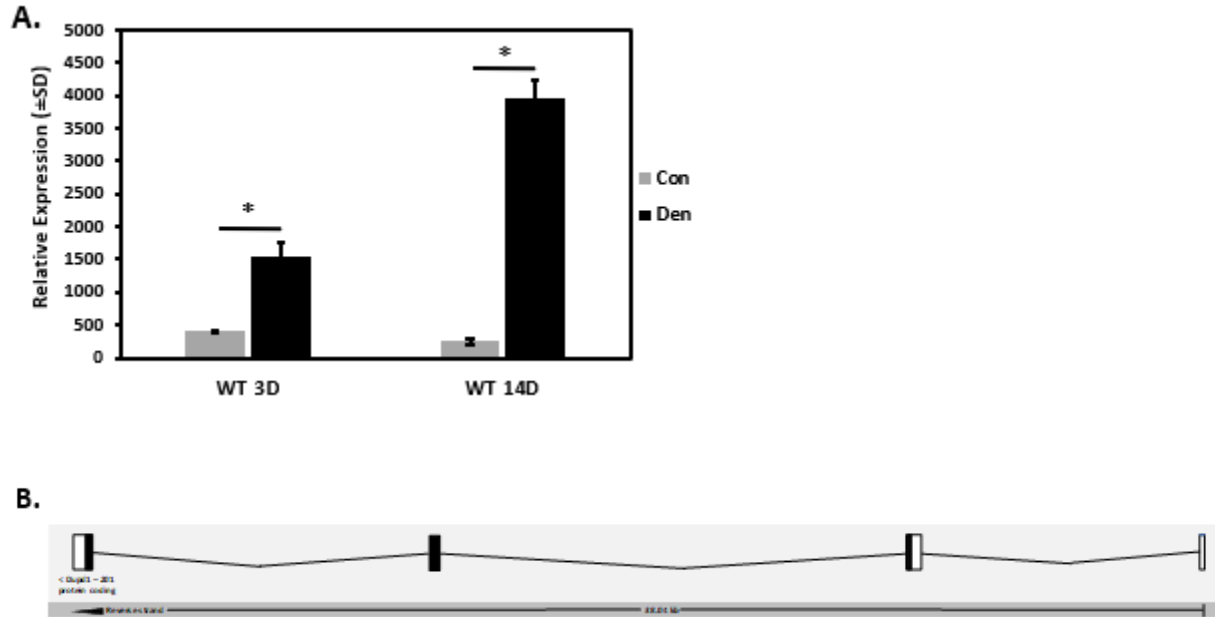
Figure 20. Dupd1 is upregulated during skeletal muscle atrophy. A) Whole genome expression analysis was conducted on triceps surae muscle from wild-type (WT) mice after 3 days (3D) and 14 days (14D) of denervation. Each condition represents the average expression from three animals and error bars represent ±SD. White bars, controls (Con); black bars, denervated (Den). Significant difference between denervated mice and control mice in the same group (**:P < .01). B) Schematic of the Dupd1 transcript in mouse. Darkened rectangles represent the exons containing the translated region, open rectangles represent exons containing the untranslated regions, and the lines connecting these rectangles represent introns

Dupd1 is expressed during late muscle cell differentiation

To measure the transcriptional activity of Dupd1, total RNA was harvested from C_2C_{12} mouse

myoblasts during proliferation (PD2), as well as an early (DD2) and late (DD7) differentiation

timepoints. cDNA synthesized from this RNA was used to conduct RT-qPCR using Dupd1

specific primers listed in Table 3. Two sets of primer pairs were utilized to compare expression

between an amplicon containing part of the non-coding first exon and an amplicon lacking any

of the non-coding first exon. The qPCR analysis showed Dupd1 mRNA levels to be substantially

higher during late differentiation compared to either proliferation or early differentiation

timepoints for both primer pairs (Fig. 21).
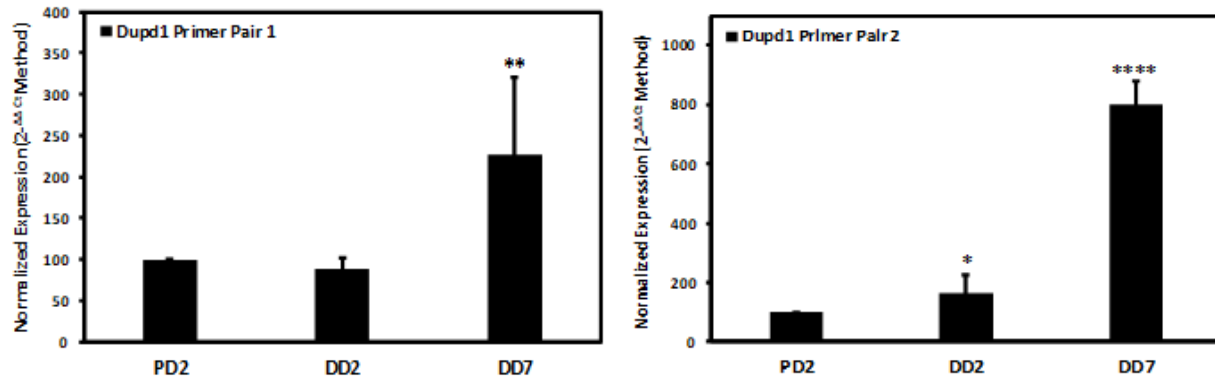
Figure 21. Dupd1 is significantly upregulated during muscle cell differentiation. Dupd1 mRNA increases significantly during late differentiation compared to either proliferation or early differentiation. Quantitative polymerase chain reaction (qPCR) utilizing cDNA generated from RNA isolated from C_2C_{12} cells harvested at proliferation day 2 (PD2), differentiation day 2 (DD2) and differentiation day 7 (DD7). Cells were maintained in proliferation media (10% serum) and harvested at 2 days post-plating and the remaining cells were switched to differentiation media (2% serum) and harvested at 2- and 7-days post-media change. Significant difference between Dupd1 expression in differentiated cells compared to Dupd1 expression in proliferating cells (*:P < .05, **:P < .01, ****:P< .0001).

Dupd1 is regulated by Myogenic Regulatory Factors

To evaluate how the proximal promoter region of Dupd1 is regulated within muscle cells,

approximately 500 and 1000 base pairs of the promoter were cloned using the primers listed in

Table 2. The fragments were then fused to a secreted alkaline phosphatase (SEAP) reporter

plasmid to create the pSEAP-Dupd1-Pro500 andpSEAP-Dupd1-Pro1000 reporter constructs. The

constructs were then transfected into C_2C_{12} mouse myoblasts and SEAP assays were preformed

48 hours after the change to differentiation media. Promoter activity was assessed by secreted

alkaline phosphatase activity. Both the 500 and 1000 base pair fragments show low endogenous

expression at DD2 (Fig. 22A). However, endogenous activity of the 500 and 1000 base pair

fragments were significantly upregulated at DD7 compared to the proliferation and early

differentiation timepoints, mirroring the endogenous mRNA expression as determined by qPCR (Fig. 22B). Interestingly, co-transfection with a MyoD or myogenin expression plasmid resulted in dramatic induction of both the 500 and 1000 bp promoter fragments (Fig. 22A). Myogenic regulatory factors, such as MyoD and myogenin, regulate gene transcription through interaction with E-box consensus elements found in the promotors of muscle-specific genes. Bioinformatic analysis of the first 500 base pairs of the promoter of Dupd1 revealed five such elements, two of which are conserved between humans and rodents (Fig. 22C). Site-directed mutagenesis was used to disrupt each of the two conserved E-box elements individually and in combination. Disruption of either E-box resulted in a dramatic blunting of the induction of the Dupd1-Pro500 seen with MyoD overexpression, while disruption of both E-boxes simultaneously eliminated the MyoD induction effect (Fig. 22D).
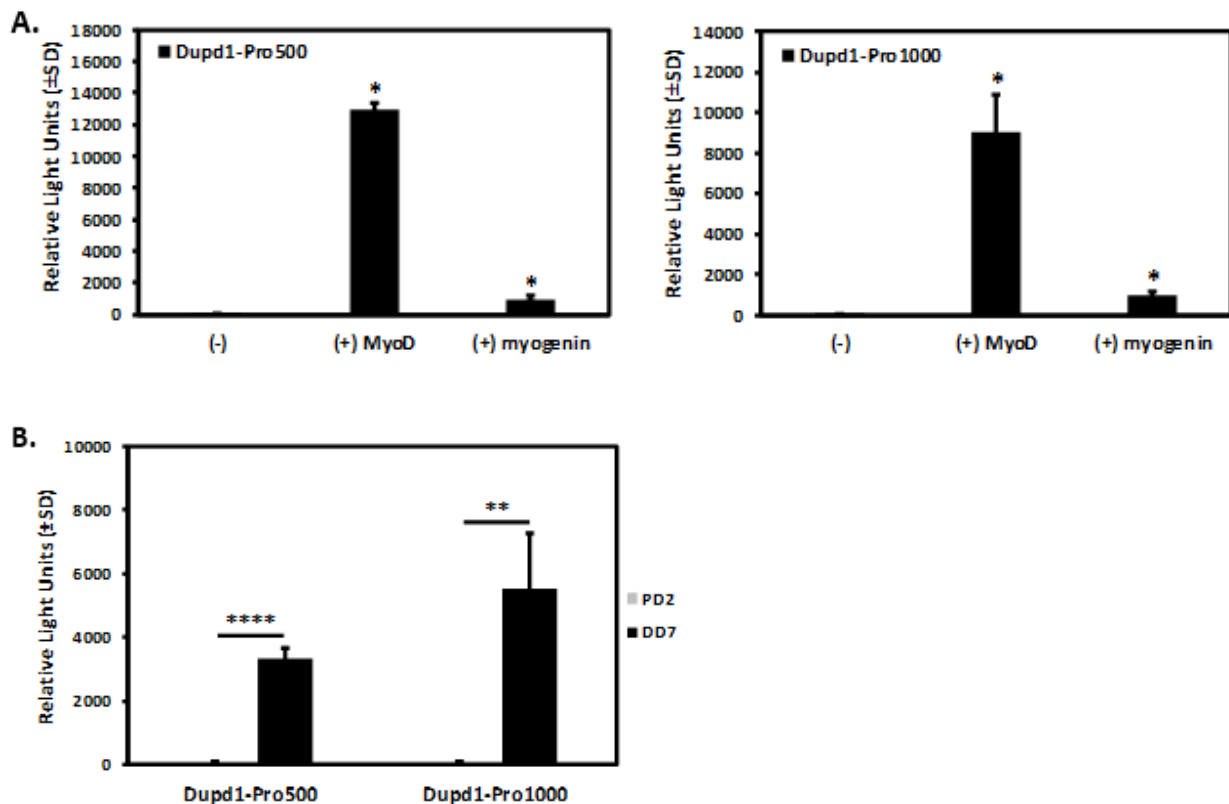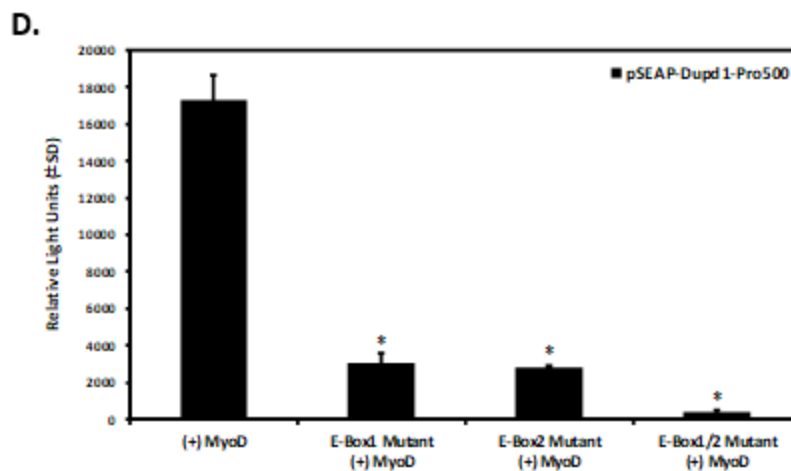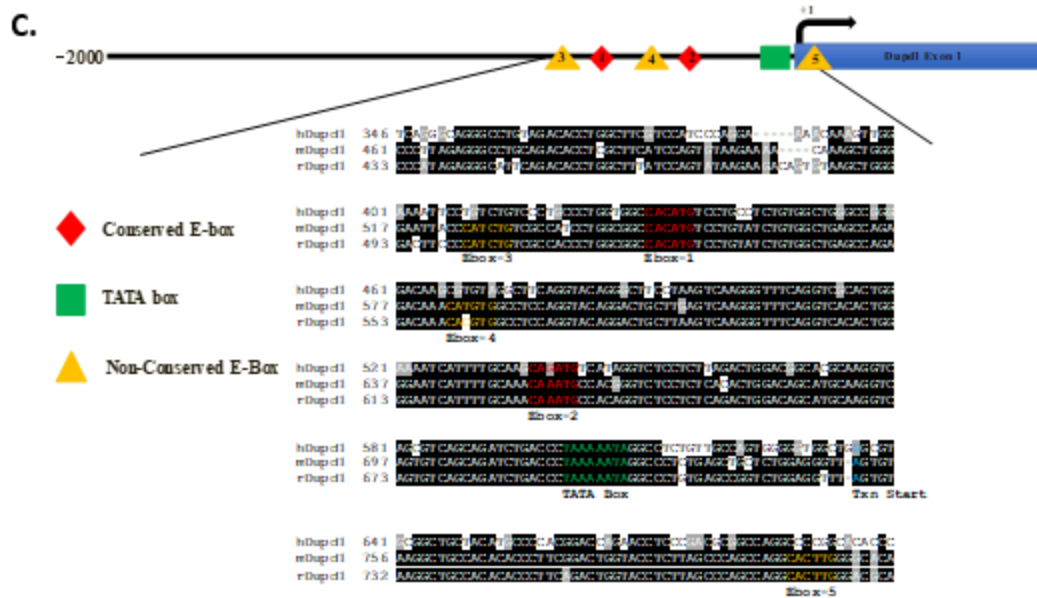
Figure 22. Cloning and analysis of the proximal regulatory region of the Dupd1 gene locus. (A) C_2C_{12} myoblasts were transfected with reporter plasmids containing 500 bp or 1000 bp of the Dupd1 promoter fused to the Secreted Alkaline Phosphatase (SEAP) reporter gene alone or in combination with either a MyoD or myogenin expression plasmid. Each condition was performed in triplicate and each experiment was repeated at least three times (n = 3). The graphs are of a representative experiment and values correspond to the mean relative light unit (RLU) values ±SD. Significant difference between the empty control reporter plasmid (pSEAP2-Basic) and the pSEAP2-Dupd1 reporter constructs, (*: P < .0001). Significant differences between the activities of the pSEAP2-Dupd1-Pro reporter constructs with and without MyoD or myogenin ectopic expression (B) C_2C_{12} myoblasts were transfected with a reporter plasmid containing the SEAP reporter gene fused to either 500 bp or 1000 bp of the Dupd1 proximal promoter or an empty reporter plasmid. Each condition was performed in triplicate and assays were performed at PD2 and DD7. Numbers correspond to the mean relative light unit (RLU) values ±SD. Significant difference between the reporter constructs activity at PD2 and reporter constructs activity at DD7 (*: P < .0001). (C) Schematic and sequence alignment of the Dupd1 regulatory

region. Promoter sequences from mouse, rat, and human Dupd1 (2000 base pairs upstream of the transcription start site (+1) through the first exon) were downloaded from the Ensembl database (www.ensembl.org) and aligned using the ClustalW algorithm. Approximate positions of putative transcription factor binding sites are indicated in the schematic of the Dupd1 regulatory region at the top. Putative consensus E-box elements 5′-CANNTG-3′ (Red diamond, conserved and yellow triangle, non-conserved) and TATA box (green square) are indicated. N represents any nucleotide. Conserved nucleotides are highlighted in black, transitions are highlighted in gray, and transversions are highlighted in white. (D) C_2C_{12} myoblasts were transfected with the pSEAP-Dupd1-Pro500 wild-type,pSEAP-Dupd1-Pro500-Ebox-1-Mutant, pSEAP-Dupd1-Pro500-Ebox-2-Mutant, or pSEAP-Dupd1-Pro500-Ebox-1/2-Mutant reporter plasmids. The media was then assayed for SEAP activity at 72 hours following the switch to differentiation media. All conditions were performed in triplicate and each experiment was repeated at least once. The graphs are of a representative experiment and numbers correspond to the mean relative light unit (RLU) values ± SD. Significant differences between the activities of the pSEAP-Dupd1-Pro500 wild-type reporter constructs and the pSEAP-Dupd1-Pro500-Ebox mutant reporter constructs, (*: $P < 0.001$).

Subcellular localization of Dupd1

Dupd1 is located on chromosome 14 in mice and encodes a protein of 220 amino acids with a predicted molecular weight of 27 kDa. It contains a phosphatase domain with an active catalytic motif (Fig. 23A). To further characterize Dupd1 in skeletal muscle, the cDNA was cloned and fused to a GFP plasmid to allow for analysis of subcellular localization by confocal fluorescent microscopy. C_2C_{12} cells were transfected with either an empty GFP expression plasmid or the Dupd1-cDNA-GFP expression plasmid and analyzed 24 hours post-transfection. The control GFP expression plasmid shows uniform GFP localization throughout the cell (Fig. 23B, Panels 1-3). Cells transfected with Dupd1 fused to GFP also showed ubiquitous distribution throughout the cell, (Fig. 23B, Panels 4-12). The Dupd1-GFP expression plasmid was sequenced to confirm Dupd1 inframe fusion with GFP and correct orientation. C_2C_{12} myoblasts were transfected with either an empty GFP expression plasmid or the Dupd1-GFP construct and protein lysates were used for Western blots.. Probing with an anti-GFP antibody demonstrated the correct shift in size in the Dupd1 containing plasmid compared to GFP alone. These findings together confirm that

the Dupd1-GFP expression plasmid is truly expressing GFP-tagged Dupd1 that localizes

throughout C$_2$C$_{12}$ mouse myoblasts (Fig. 23C).

A.

```
mDupd1    1  MASGDTKTSVKHAHLCAERLSY-REEEGLAEDYCTPGAFELERLFWKGSPQYTHVNEVWP
rDupd1    1  MASGDTKTSVKHAHPCAERLSY-QQEEGEAEDYCTPGAFELERLFWKGSPQYTHVNEVWP
hDupd1    1  MTSGEVKTSLKNAYSSARRLSPRMEEEGEBEDYCTPGAFELERLFWKGSPQYTHVNEVWP

mDupd1   60  RLHIGDEATALDRYGLQKAGFTHVLNAAHGRWNVDTGPDYYRDMAIEYHGVEADDVPTFD
rDupd1   60  RLHIGDEATALDRYGLQKAGFTHVLNAAHGRWNVDTGPDYYRDMAIEYHGVEADDVPTFD
hDupd1   61  RLYIGDEATALDRYRLQKAGFTHVLNAAHGRWNVDTGPDYYRDMDIQYHGVEADDLPTFD
                         Phosphatase Domain

mDupd1  120  LSIFFYSAAAFIDSALRDDHSKILVHCAMGRSRSATLVLAYIMIHKNMTLVDAIQQVARN
rDupd1  120  LSIFFYSAAAFIDSALQDDHSKILVHCAMGRSRSATLVLAYIMIHKNMTLVDAIQQVAKN
hDupd1  121  LSVFFYPAAAFIDRALSDDHSKILVHCVMGRSRSATLVLAYIMIHKDMTLVDAIQQVAKN
                         Active Motif

mDupd1  180  RCVLPNRGFLKQLRELDKQLVKQRRQAGPGDSDL--GL--
rDupd1  180  RCVLPNRGFLKQLRELDKQLVKQRRQAGPGAGEL--GL--
hDupd1  181  RCVLPNRGFLKQLRELDKQLVQQRRSQRQDGEEEDGREL
```
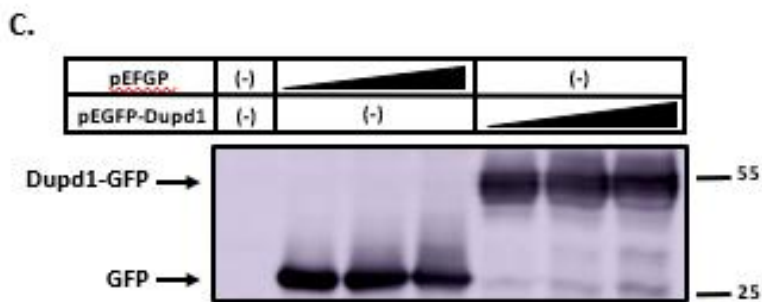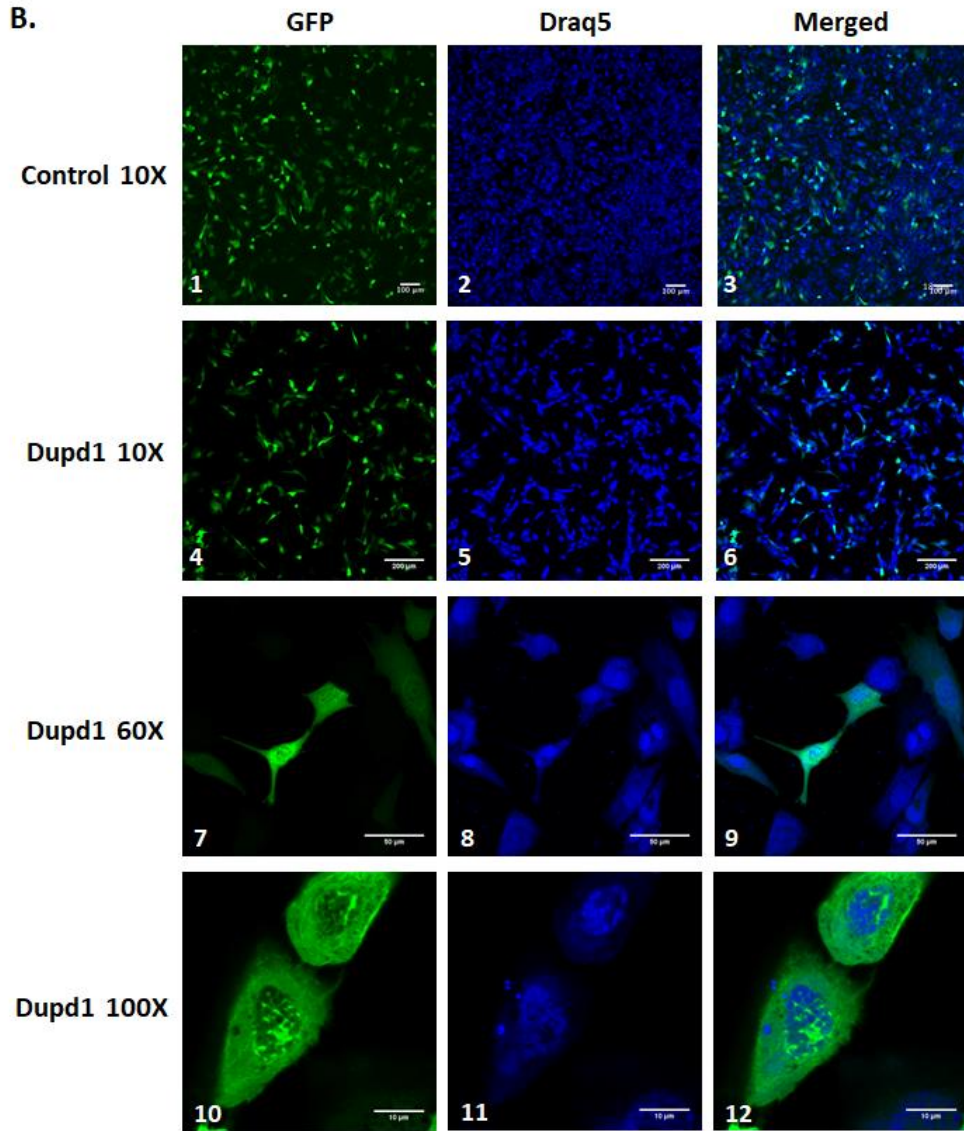
Figure 23. Dupd1 localizes to the cytoplasm and nucleus of myoblast cells. (A) Sequences of the mouse, rat, and human Dupd1 protein were downloaded from the Ensembl database and aligned using the ClustalW2 algorithm. Approximate position of the phosphatase domain is highlighted in green with the active motif within that domain highlighted in blue. (B) Proliferating C_2C_{12}

cells (PD2) transfected with the empty pEGFP-C3 expression vector were imaged at 10× (Panels 1–3) and uniform cellular localization of GFP was observed. Representative C_2C_{12} cells transfected with a pEGFP-Dupd1 expression plasmid were imaged at proliferation day 2 (PD2) at 10× (Panels 4–6), 60× (Panels 7–9), and 100× (Panels 10–12) and uniform cellular fluorescence was observed. Draq5, a cell permeable fluorescent DNA dye, was used to visualize cell nuclei. (C) NIH3T3 cells were transfected with either an empty pEGFP expression plasmid or pEGFP-Dupd1 expression plasmid. Cells were maintained in culture media and harvested 24 hours post-transfection. Protein samples (25 µg, 50 µg, and 100 µg) from each condition were used for Western blot analysis and membranes were probed with an anti-GFP antibody.

Ectopic expression of Dupd1 impairs muscle cell differentiation

To investigate whether Dupd1 has an impact on muscle cell differentiation, C_2C_{12} cells were transfected with a myc-tagged Dupd1 expression plasmid. Cells were then harvested, over a time course spanning proliferation (PD2) and several differentiation timepoints (DD1, DD3 and DD5). Protein was isolated from cells and evaluated for expression of myosin heavy chain (MyHC) and myogenin, canonical makers of muscle cell differentiation. Western blot analysis showed significantly lower levels of both myogenin and MyHC at all time points analyzed, with the greatest inhibition at DD3 (Fig. 24A). To quantify the amount of inhibition, Dupd1 was overexpressed in biological quadruplicate and harvested at day 3 of differentiation. Lysates were evaluated by Western blot and it was found that myogenin and MyHC expression were significantly reduced in samples ectopically expressing Dupd1 (Fig. 24B and C). Analysis with an anti-Flag antibody confirmed significant overexpression of Flag tagged Dupd1 in all transfected samples. GAPDH was used to confirm equal protein loading and it expression remained relatively constant between samples.
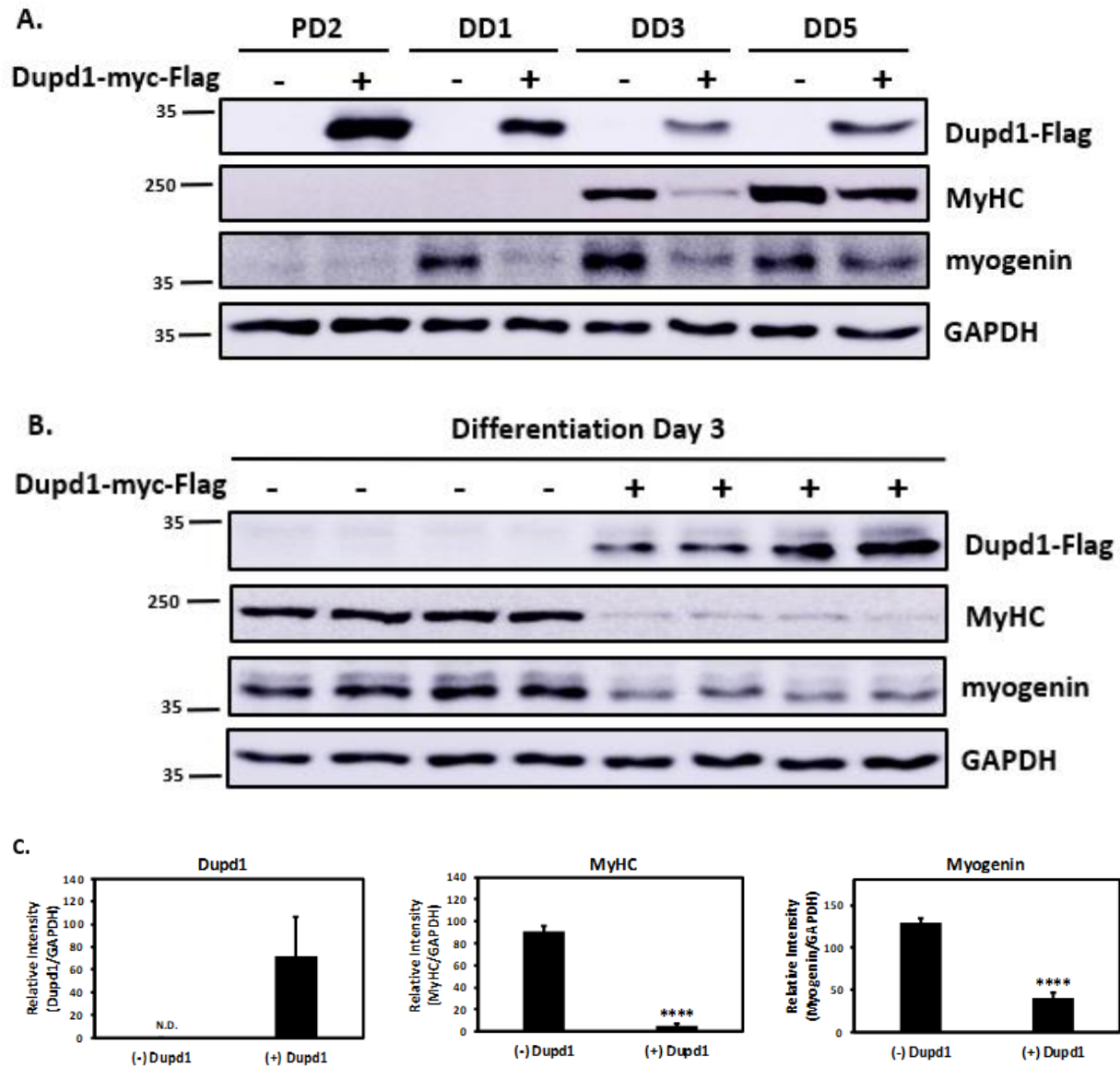
Figure 24. Ectopic expression of Dupd1 impairs muscle cell differentiation. C_2C_{12} cells were transfected with a Dupd1-myc-Flag expression plasmid or mock transfected followed by Western blot analysis. (A) Western blot analysis of Flag, Myosin Heavy Chain (MyHC), and myogenin using protein homogenates from proliferating (PD) and differentiated (DD) C_2C_{12} cells harvested over a 5-day differentiation time course. Cells were maintained in proliferation media (10% serum) and harvested 2 days post-plating and the remaining cells were then switched to differentiation media (2% serum) and harvested at 1, 3 and 5-days post-media change. GAPDH was analyzed to confirm equal protein loading. The experiments were repeated at least three times and the Western blots shown are representative examples of the results obtained. (B) C_2C_{12} cells were transfected with a Dupd1-myc-Flag expression plasmid or mock transfected in biological quadruplicates and cell lysates were then analyzed by Western blot for Flag, MyHC, and myogenin. Cells were maintained in proliferation media then switched to differentiation media (2% serum) for 3 days. GAPDH was analyzed to confirm equal protein loading. The experiment was performed in quadruplicate (n = 4). (C) Quantification of the

75

Western blot band intensities for Flag, MyHC, and myogenin in Part B. Relative intensity of each band was corrected to either GAPDH (shown) or α-tubulin band intensities for each corresponding biological replicate. Significant differences between control cells compared to cells ectopically expressing Dupd1-myc-Flag, (****: P < .0001).

Ectopic expression of Dupd1 attenuates MAP Kinase and AMPK protein expression

As Dupd1 was previously shown to effect MAP kinase signaling though modulation of the

ERK1/2 cascade in ovarian tissue, its potential role in this pathway in skeletal muscle was

investigated (45). C_2C_{12} cells were transfected with a reporter plasmid created by fusing the AP-

1 consensus element to a pSEAP-promoter plasmid in combination with increasing

concentrations of the pcDNA3.1-Dupd1 expression plasmid. SCH772984, a validated ERK1/2

inhibitor, was used as a positive control. Dupd1 overexpression repressed AP1 reporter activity

in a dose dependent fashion, with the highest concentration of Dupd1 expression plasmid

exhibiting a similar level of repression as SCH772984 (Fig. 25A). To further evaluate this effect,

Dupd1 was overexpressed in C_2C_{12} mouse myoblasts and harvested over a differentiation time

course, as well as in biological quadruplicate as described above, and protein homogenates from

these cells were evaluated by Western blot. Protein levels of ERK1/2 were not significantly

different in Dupd1 overexpression samples. However, overexpression of Dupd1 reduced levels

of ERK phosphorylation at all timepoints (Fig. 25B and C). Interestingly, Dupd1 seemed to

effect p42 phosphorylation levels more than p44 phosphorylation.
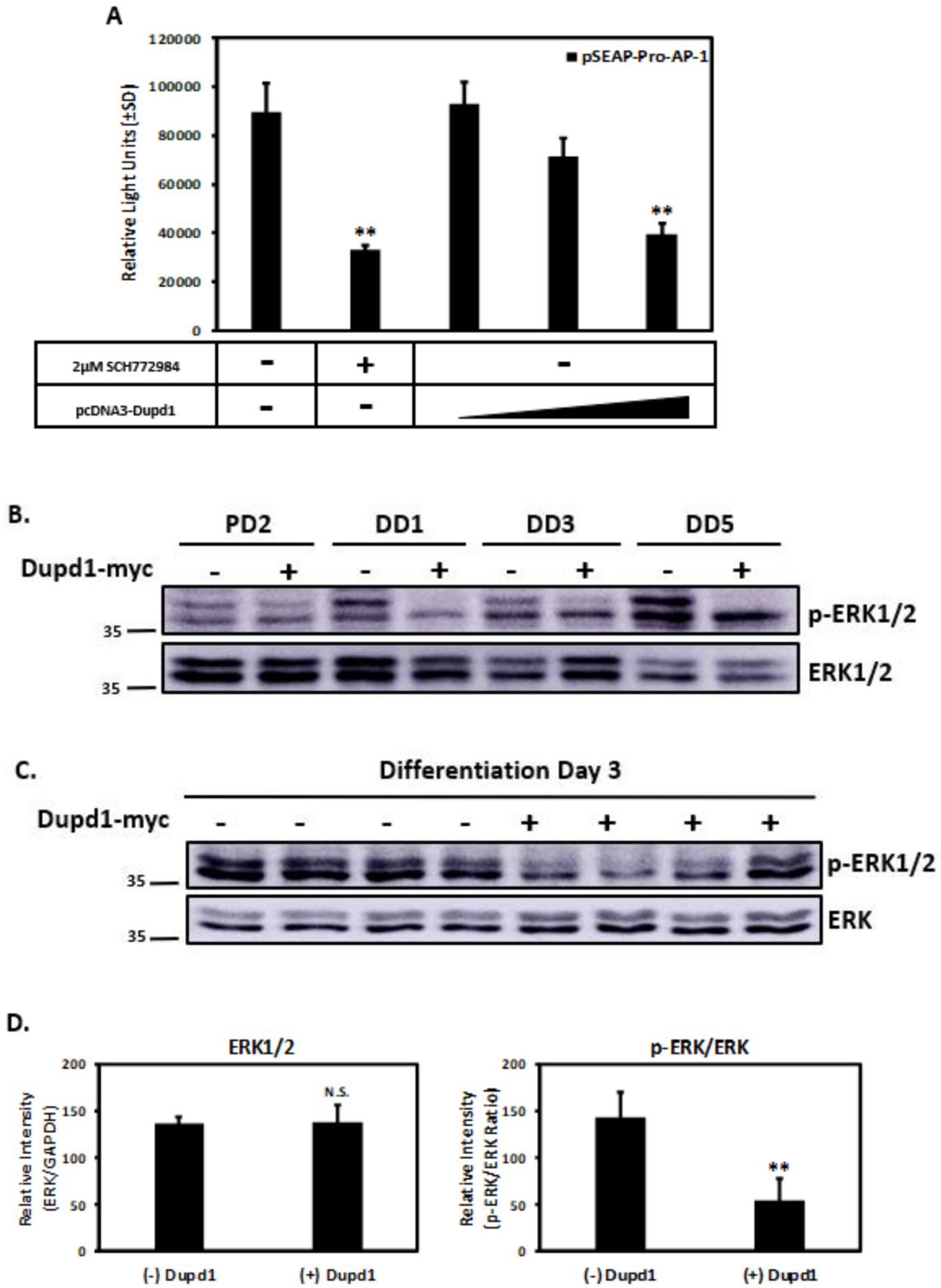
Figure 25. Ectopic expression of Dupd1 attenuates MAP Kinase signaling. (A) C_2C_{12} cells were transfected with an AP-1 reporter plasmid alone or in combination with 0.125 µg, 0.25 µg or

0.50 µg of the Dupd1-myc-Flag expression plasmid or treated with 2 µM of SCH772984, a validated ERK inhibitor. The media was then assayed for SEAP activity 48 h (DD2) following the switch to differentiation media and SEAP numbers were normalized to β-galactosidase activity to correct for variations in transfection efficiency. Each condition was performed in triplicate and each experiment was repeated at least three times (n = 3). The graphs are of a representative experiment and numbers correspond to the mean relative light unit (RLU) values ±SD. Significant differences between the activities of the pSEAP2-AP-1-Pro reporter construct alone and in combination with either 2 µM SCH772984 or 0.5 µg Dupd1-myc-Flag expression plasmid , (**: P < .01). (B) C_2C_{12} cells were transfected with a Dupd1-myc-Flag expression plasmid or mock transfected followed by Western blot analysis. Cells were maintained in proliferation media (10% serum) and harvested 2 days post-plating and the remaining cells were then switched to differentiation media (2% serum) and harvested 1, 3, and 5 days post-media change. Western blot analysis of phosphorylated-ERK1/2 (p-ERK1/2), pan-ERK1/2 (ERK1/2) using protein homogenates from proliferating (PD2) and differentiated C_2C_{12} cells. The experiments were repeated at least three times (n = 3) and the Western blots shown are representative examples of the results obtained. (C) C_2C_{12} cells were transfected with a Dupd1-myc-Flag WT expression plasmid or mock transfected in biological quadruplicates. Western blot analysis of phosphorylated ERK1/2 (p-ERK1/2) and pan-ERK1/2 (ERK1/2) using protein homogenates from C_2C_{12} cells differentiated for 3 days. The experiment was performed in quadruplicate (n = 4), repeated at least three times, and the blots shown are representative examples of the results obtained. (D) Quantification of the Western blot band intensities were measured for pan-ERK1/2 and the phospho-ERK1/2 to pan-ERK1/2 ratio Significant differences between control cells compared to cells ectopically expressing Dupd1, (**: P < .01, N.S. = not significant).

A previous study found Dupd1interacts with AMPK (42). To evaluate if this relationship exists in muscle cells, the effect of Dupd1 overexpression on AMPK protein levels was evaluated by Western blot over a differentiation time course and AMPK protein levels were found to be significantly lower in the Dupd1 overexpression samples at all time points (Fig. 26A). To quantify this difference, control cells and cells overexpressing Dupd1 were harvested at DD3 in biological quadruplicate, and AMKP protein levels were quantified, revealing a significant decrease in total AMPK protein. Interestingly, the amount of AMPK phosphorylation is relatively constant between control cells and Dupd1 overexpressing cells and, considering the decrease in total AMPK, a significant increase in the ratio of AMKP phosphorylation in response to Dusp1 overexpression was observed (Fig. 26B and C)
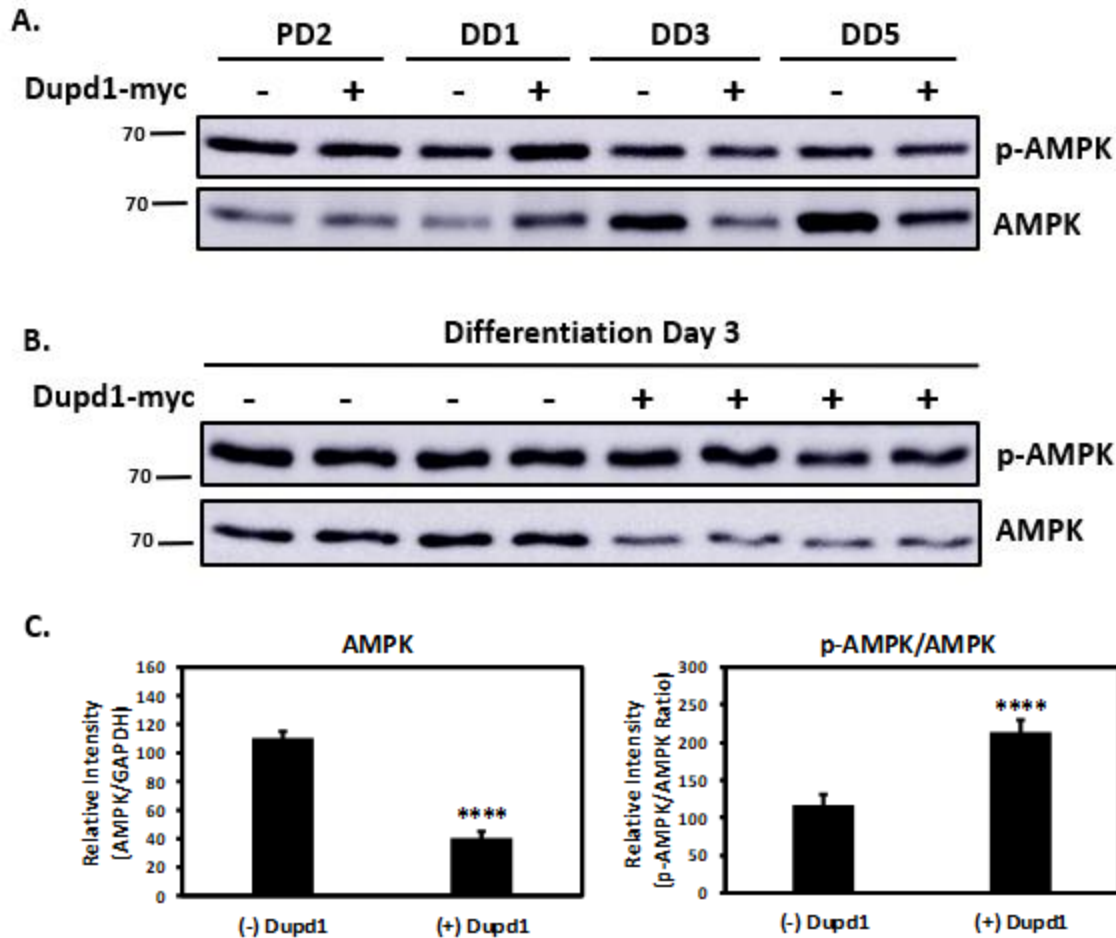
Figure 26. Ectopic expression of Dupd1 attenuates AMPK signaling. C_2C_{12} cells were transfected with a Dupd1-myc-Flag expression plasmid or mock transfected followed by Western blot analysis. Cells were maintained in proliferation media (10% serum) and harvested 2 days post-plating and the remaining cells were then switched to differentiation media (2% serum) and harvested 1, 3, and 5 days post-media change. Western blot analysis of phosphorylated-AMPK (p-AMPK) and pan-AMPK (AMPK) using protein homogenates from proliferating (PD2) and differentiated C_2C_{12} cells. The experiments were repeated at least three times (n = 3) and the Western blots shown are representative examples of the results obtained. (C) C_2C_{12} cells were transfected with a Dupd1-myc-Flag WT expression plasmid or mock transfected in biological quadruplicates. Western blot analysis of phosphorylated-AMPK (p-AMPK) andpan-AMPK (AMPK) using protein homogenates from cells differentiated for 3 days. The experiment was performed in quadruplicate (n = 4), repeated at least three times, and the blots shown are representative examples of the results obtained. (D) Quantification of the Western blot band intensities were measured for pan-AMPK and the phospho-AMPK to pan-AMPK ratio. Significant differences between control cells compared to cells ectopically expressing Dupd1, (****: P < .0001).

Dupd1 modulates glucocorticoid receptor signaling

79

As dexamethasone treatment was previously shown to affect Dupd1 expression in mouse skeletal muscle, the role of Dupd1 on glucocorticoid signaling was evaluated (5). C_2C_{12} mouse myoblasts were transfected with a reporter plasmid created by fusing four GRE consensus elements to a pSEAP-promoter plasmid in combination with increasing concentrations of the pcDNA3.1-Dupd1 expression plasmid. Additionally, cells were treated with dexamethasone at DD6 for 12 hours prior to the assay to induce the GR signaling pathway. Activity of the pSEAP-4X-GRE reporter plasmid increased with dexamethasone treatment, while Dupd1 overexpression significantly reduced this induction in a dose dependent manner (Fig. 27A). The proximal promoter region of MuRF1 contains a glucocorticoid response element (GRE), which has previously been shown to enhance transcription of MuRF1 in skeletal muscle (17). To evaluate if Dupd1 may be capable of regulating MuRF1, 500 base pairs of the proximal promoter region of MuRF1 was fused to the pSEAP2-Basic reporter plasmid and transfected into C_2C_{12} mouse myoblasts in combination with pcDNA3.1-Dupd1 expression plasmid followed by 12 h of dexamethasone treatment. Consistent with previous findings, dexamethasone significantly increased the activity of the pSEAP-MuRF1-Pro500 reporter. Overexpression of Dupd1 significantly blunted this dexamethasone-dependent induction (Fig. 27B).

B.

Figure 27. Dupd1 attenuates GR signaling. (A) C_2C_{12} cells were transfected with a pSEAP-4X-GRE reporter plasmid alone or in combination with 0.125 µg, 0.25 µg or 0.50 µg of the Dupd1-myc-Flag expression plasmid and 5 µM dexamethasone (Dex). The media was then assayed for SEAP activity 48 h (DD2) following the switch to differentiation media and SEAP numbers were normalized to β-galactosidase activity to correct for variations in transfection efficiency. Each condition was performed in triplicate and each experiment was repeated at least three times (n = 3). The graphs are of a representative experiment and numbers correspond to the mean relative light unit (RLU) values ±SD. (B) C_2C_{12} cells were transfected with a MuRF1-Pro500 SEAP reporter plasmid alone, with 5 µM Dex or in combination the Dupd1-myc-Flag expression plasmid and Dex. SEAP activity was measured at DD2.

As noted previously, Dupd1 expression was repressed in rat muscle tissue following 72 hours of dexamethasone treatment as evidenced by microarray (5). To assess if glucocorticoids can transcriptionally regulate Dupd1 in muscle cells, C_2C_{12} mouse myoblasts were grown in culture, switched to differentiation media and then allowed to differentiate for six days. Starting at day six, cells were treated with dexamethasone for 72 hours and then harvested. Total RNA isolates were used to generate cDNA and qPCR was conducted to compare Dupd1 transcript levels between control and dexamethasone treated cells (Fig. 28). Results demonstrate a significant increase in Dupd1 mRNA levels following dexamethasone treatment.
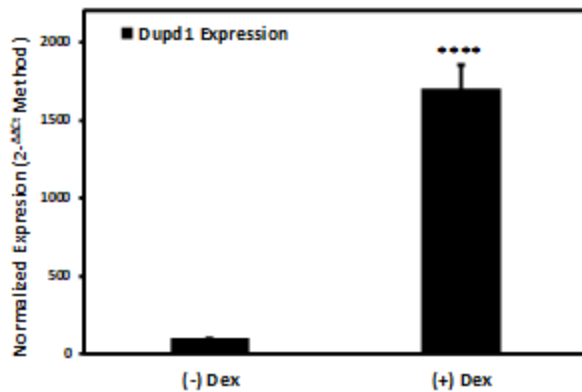
Figure 28. Dexamethsone treatment enhances Dupd1 mRNA expression. Quantitative polymerase chain reaction (qPCR) utilizing cDNA generated from RNA isolated from C_2C_{12} cells harvested at differentiation day 7 (DD7) with or without 72 h Dex. Cells were maintained in proliferation media (10% serum) and 2 days post-plating were switched to differentiation media (2% serum). Significant difference between endogenous Dupd1 expression compared to Dupd1 expression in dexamethasone treated cells (****:$P < .0001$).

To further investigate the relationship between Dupd1 and GR, Dupd1 was overexpressed in C_2C_{12} mouse myoblasts and harvested over a differentiation time course and protein homogenates from these cells were evaluated by Western blot. Interestingly, Dupd1 overexpression increased GR protein levels and phosphorylation status at all differentiation time points (Fig. 29A). To quantify this difference, control cells and cells overexpressing Dupd1 were harvested at DD5 in biological quadruplicate. Quantification revealed that Dupd1 overexpression significantly increases total GR protein levels, as well as GR phosphorylation. Comparison between GR protein levels and phosphorylation status indicated that not only is there an increase in GR protein levels, but there is also a significant rise in GR phosphorylation in response to Dupd1 overexpression (Fig. 29B and C). Since GR exists within a chaperone complex while in the cytoplasm, the level of one of the major components of this complex, heat shock protein 90 (HSP90), was also evaluated in biological quadruplicate at DD5 (Fig. 29B and C). Dupd1 overexpression appears to have no effect on the levels of HSP90 (Fig. 29B and C).
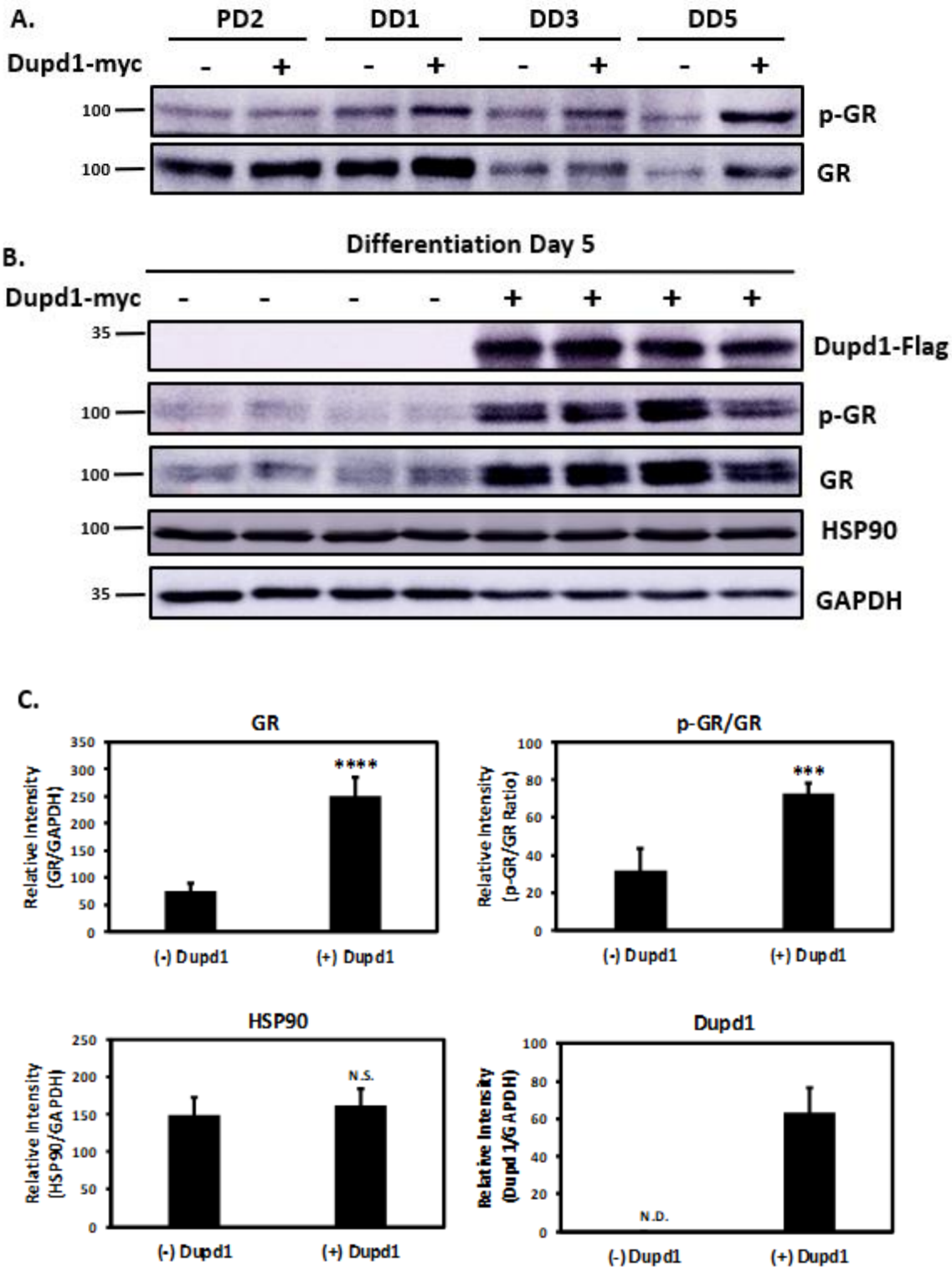
Figure 29. Dupd1 overexpression increases GR protein and phosphorylation levels. (A) C$_2$C$_{12}$ cells were transfected with a Dupd1-myc-Flag expression plasmid or mock transfected followed by Western blot analysis. Cells were maintained in proliferation media (10% serum) and harvested 2 days post-plating and the remaining cells were then switched to differentiation media

(2% serum) and harvested 1, 3, and 5 days post-media change. Western blot analysis of phosphorylated-GR (p-GR) and pan-GR (GR) using protein homogenates from proliferating (PD2) and differentiated C_2C_{12} cells. The experiments were repeated at least three times (n = 3) and the Western blots shown are representative examples of the results obtained. (B) C_2C_{12} cells were transfected with a Dupd1-myc-Flag WT expression plasmid or mock transfected in biological quadruplicates. Western blot analysis of Flag (Dupd1-Flag), phosphorylated-GR (p-GR), pan-GR (GR), and heat shock protein 90 (HSP90) using protein homogenates from C_2C_{12} cells differentiated for 3 days. The experiment was performed in quadruplicate (n = 4), repeated at least three times, and the blots shown are representative examples of the results obtained. GAPDH was used to confirm equal protein loading. (C) Quantification of the Western blot band intensities were measured for pan-GR, the phospho-GR to pan-GR ratio, HSP90, and Flag (Dupd1). Significant differences between control cells compared to cells ectopically expressing Dupd1 (**: P < .01, N.S. = not significant).

Discussion

Skeletal muscle is a uniquely dynamic tissue and has remarkable ability to regulate its size and mass (9, 35). Skeletal muscle mass is maintained through a balance of protein synthesis and protein degradation and when this balance is shifted toward protein degradation, atrophy occurs (35). A wide range of events are capable of inducing this imbalance including denervation, starvation, disease, disuse, and aging (9). Much of the research in recent years has focused on degradation pathways, such as the ubiquitin proteasome system (UPS), however, the molecular mechanisms that underly these disparate atrophy-inducing events remain unclear. Dupd1 has been identified as a novel molecular component of the atrophy cascade as it is transcriptionally active in muscle and has been observed to be upregulated in response to neurogenic atrophy (5). There have been few previous studies that have focused on Dupd1 and this is the first to evaluate its role in the context of skeletal muscle atrophy.

To characterize the regulation and expression of Dupd1 in muscle, qPCR was conducted using cDNA from C_2C_{12} mouse myoblasts over a differentiation time course. These results showed that

Dupd1 is highly upregulated during late differentiation as compared to either proliferation or early differentiation. Additionally, the proximal promotor region was found to have endogenous expression that mirrors the transcription profile identified by qPCR. The promoter has low endogenous activity during cell proliferation but is highly upregulated during late differentiation. Additionally, even when endogenous activity is low the promotor has been shown to be highly inducible by myogenic regulatory factors (MRFs), specifically MyoD, and to a lesser extent, myogenin. MRFs can modulate activity of muscle-specific genes by binding of Ebox elements, of which there are two conserved Eboxes located in the proximal promoter region of Dupd1 (43). Disruption of either of these conserved Ebox sequences significantly diminishes the MyoD dependent induction and disruption of both all but ablates MRF-mediated induction. MyoD and myogenin are both is upregulated during muscle cell differentiation and act as a markers of myogenic commitment to the skeletal muscle lineage (43). Notably, MyoD and myognin are also significantly upregulated during neurogenic skeletal muscle atrophy, which may play a role in the upregulation of Dupd1 during both these processes (44). These findings together suggest that Dupd1 has a muscle-specific role and is highly sensitive to changes in the muscle cell environment.

Dupd1 is shown here to have a dramatic negative impact on muscle cell differentiation as evidenced by a stark decrease in both myosin heavy chain (MyHC) and myogenin protein levels, both canonical markers of differentiation in skeletal muscle. To further explore this effect, we evaluated the potential role of Dupd1 in several signaling pathways important for muscle cell growth and development. Dupd1 was previously shown to effect MAPK signaling though interaction with both the ERK1/2 and p38 branches of the pathway in ovary tissue (45). In the

current study, we find Dupd1 overexpression to inhibit MAPK signaling as evidenced by

decreases in AP-1 reporter activity in C_2C_{12} mouse myoblasts. Furthermore, Western blot

analysis demonstrated that ERK1/2 phosphorylation was also inhibited by Dupd1

overexpression. Interestingly, it appears there is a preference for dephosphorylation of ERK2

(p42) over ERK1 (p44), as shown by an increased effect on the level of phosphorylation

observed for the 42 kDa band compared to the signal to 44 kDa (Fig. 25B and C). Direct

interaction between ERK1/2 and Dupd1 and p38 and Dupd1 was demonstrated by co-

immunoprecipitation using the ovarian cell line GG-CL (45). This interaction was not found in

C_2C_{12} mouse myoblasts nor did Dupd1 overexpression have any significant effect on p38 protein

levels or its phosphorylation status (data not shown). Additionally, the effect of Dupd1

overexpression on ERK1/2 phosphorylation appears more moderate than effects in the ovary

(45). Taken together this suggests that the effect exerted by Dupd1 on MAPK signaling in

skeletal muscle may be less robust in skeletal muscle than in the ovary. Rather than a direct

physical interaction and potential dephosphorylation event, the effect observed in skeletal muscle

may be a result of a downstream affect or an effect on another signaling pathway that

tangentially regulates ERK1/2 signaling.

AMP-activated protein kinase (AMPK) is a master regulator of energy homeostasis in virtually

all eukaryotic cell types and is highly conserved across animals, plants, and yeast (46). As

skeletal muscle plays a large role in metabolic homeostasis it is not surprising that AMPK is

highly expressed in this tissue (46). AMPK is regulated by a wide variety of upstream signals

and, through phosphorylation of a variety of transcription factors and co-factors, influences many

pathways involved with both protein synthesis and protein degradation (46). Many residues on

AMPK are capable of being phosphorylated and one of the key residues for active kinase activity is Threonine 172 (47). AMPK becomes activated, primarily though phosphorylation of T172, in response to cellular stress and in turn activates pathways aimed at conserving existing ATP reserves, as well as increasing the supply of ATP (47). The current study demonstrates that Dudp1 overexpression significantly reduces AMPK protein levels while simultaneously increasing the proportionate amount of phosphorylation of T172. This increase in relative phosphorylation may be a compensatory mechanism in response to decreased protein levels or the result of a Dupd1-mediated dephosphorylation event that destabilizes hypophosphorylated AMPK in muscle cells. Interestingly, AMPK has also been previously shown to down regulate glucocorticoid receptor (GR) signaling, specifically through increasing phosphorylation at serine 211 on GR (48).

Glucocorticoids (GC) are key metabolic regulators in skeletal muscle (19). Increases in GCs decrease protein synthesis and increase protein degradation leading to skeletal muscle atrophy (19). A previous study identified Dupd1 and being downregulated 7.2-fold in mouse triceps surae (TS) complexes during skeletal muscle atrophy induced by three days of systemic treatment with dexamethasone, a synthetic glucocorticoid. (5). The current study demonstrated that a Dupd1 reporter gene is transcriptionally upregulated by dexamethasone treatment, which is mirrored by RT-qPCR data showing that Dupd1 is upregulated in differentiated C_2C_{12} cells in response to dexamethasone treatment. The discrepancy between the previous microarray study and the findings shown here highlight the complexity of atrophy signaling and the possibility of signaling pathway crosstalk that might be absent in a cell culture model. Despite these differences, evaluation in cell culture still provides valuable insights into muscle-specific

responses. Dupd1 overexpression has a dramatic effect on the glucocorticoid receptor. Total GR protein levels are significantly increased and phosphorylation of S211 is also increased. In many tissues, phosphorylation of S211 leads to a conformational change resulting in increased binding to glucocorticoid response elements (GRE) (49). However, in neuronal cells, liver cells, skeletal muscle, and adipose tissue, phosphorylation of the S211site has been shown to decrease signaling (48). This latter outcome is what was observed in C_2C_{12} cells in response to overexpression of Dupd1, which resulted in an attenuation of the transcriptional activity of both the apSEAP-4X-GRE reporter construct and a MuRF1-Pro500 reporter construct containing a fragment of the MuRF1 promoter that includes a canonical GRE.

Inactive glucocorticoid receptors reside in the cytoplasm bound in heat shock protein 90 (HSP90) chaperone complexes (50). GR is activated by binding with glucocorticoids which results in disassociation from the chaperone complex and translocation to the nucleus (50). Once in the nucleus several GR-mediated responses are possible. GR may homodimerize and bind to GRE consensus elements, enhancing transcription of the genes they are associated with (20). Ligand-bound GR may also bind other transcription factors such as AP-1 or NF-κB to modulate their transcriptional activity (20). Additionally, monomeric GR may bind negative GREs (nGRE), resulting in transcriptional inhibition (20). Phosphorylation of GR either pre- or post-ligand binding plays a role in determining which of these pathways GR will participate in (20). As a phosphatase, Dupd1 likely plays a role in the dynamic phosphorylation landscape regulating GR activity, resulting in the significant results described by this study. As a transcription factor, GR can have wide-ranging effects on the cellular signaling environment (51). GR can affect MAPK signaling though interaction with AP-1, as previously mentioned, and has also been

shown to inhibit ERK phosphorylation (51). It is possible that the reduction in ERK phosphorylation described in the current study is a result of downstream GR effects rather than direct dephosphorylation by Dupd1.

The finding that Dupd1 expression is affected by multiple atrophy inducing stimuli furthers our understanding of the complex molecular signaling network that underlies this debilitating condition. This study demonstrates that Dupd1 overexpression dramatically inhibits muscle cell differentiation, possibly as a result of its effect on the multiple signaling pathways examined here. When Dupd1 was first characterized, it was predicted to be involved in the regulation of energy metabolism, based on its tissue expression profile (41). The current study supports that initial prediction by implicating Dupd1 as modulating two major pathways important for metabolic homeostasis; glucocorticoid receptor and AMP-activated protein kinase signaling. Although the precise molecular mechanisms responsible for the function of Dupd1 remains unclear, this study reveals Dupd1 as potentially having a role in muscle cell differentiation, development, and atrophy, as well as identifies it as a novel modulator of GR activity.

References

1. Bodine SC, Baehr LM. 2014. Skeletal muscle atrophy and the E3 ubiquitin ligases MuRF1 and MAFbx/atrogin-1. *American Journal of Physiology - Endocrinology and Metabolism*. 307: LE469-E484.

2. Bodine SC, Latres E, Baumhueter S, et al. 2001. Identification of ubiquitin ligases required for skeletal muscle atrophy. *Science Signaling*. 294(5547):1704-1707.

3. McKinnell IW, Rudnicki MA. 2004. Molecular mechanisms of muscle atrophy. *Cell*. 119(7): 907-910.

4. Dodd, R. 2011. Ubiquitylation [open access image]. Attribution: By Roger Dodd at the English Language Wikipedia, CC BY---SA 3.0, https://commons.wikimedia.org/w/index.php?curid=7677277

5. Furlow JD, Watson ML, Waddell DS, et al. 2013. Altered gene expression patterns in muscle ring finger 1 null mice during denervation and dexamethasone induced muscle atrophy. *Physiological genomics*. 45:1168-1185.

6. Dilworth FJ, Singh K. 2013. Differential Modulation of cell cycle progression distinguishes members of the myogenic regulatory family of transcription factors. *FEBS Journal*. 280:3991---4003.

7. Londhe, P., Davie, J. 2011. Sequential association of myogenic regulatory factors and E proteins at muscle---specific genes. *Skeletal Muscle*. 1:14.

8. Moresi V, Williams AH, Meadows E, et al. 2010. Myogenin and Class II HDACs control neurogenic muscle atrophy by inducing E3 ubiquitin ligases. *Cell*. 143(1): 35-45.

9. Sandri M . Signaling in muscle atrophy and hypertrophy. Physiology: 2008; 23: 160 70. doi:10.1152/physiol.00041.2007

10. A.M. Bennett, N.K. Tonks, Regulation of distinct stages of skeletal muscle differentiation by mitogen-activated protein kinases, Science 278 (5341) (1997) 1288–1291.

11. Knight J, Kothary R. 2011. The myogenic kinome: protein kinases critical to mammalian skeletal myogenesis. *Skeletal Muscle*. 1:29

12. Adi A, Bin-Abbas B, Wu N and Rosenthal S. 2002. Early Stimulation and Late Inhibition of Extracellular Signal-Regulated Kinase 1/2 Phosphorylation by IGF-I: A Potential Mechanism Mediating the Switch in IGF-I Action on Skeletal Muscle Cell Differentiation. *Endocrinology*. 143(2):511–516

13. Penna F, Costamagna D, Fanzani A, Bonelli G, Baccino F, Costelli P. Muscle Wasting and Impaired Myogenesis in Tumor Bearing Mice Are Prevented by ERK Inhibition. PLoS One. 2010. Volume 5, Issue 10:e1360

14. Raman M, Chen W and Cobb MH. Differential regulation and properties of MAPKs. Oncogene. 2007. 26, 3100–3112

15. Zhang X, Tang N, Hadden T, Rishi A. 2011. Akt, FoxO and regulation of apoptosis. *Biochimica et Biophysica Acta.* 1813: 1978–1986

16. Schiaffino S and Mammucar C. Regulation of skeletal muscle growth by the IGF1-Akt/PKB pathway: insights from genetic models. Skeletal Muscle. 2011. Vol 1:4

17. Waddell D, Baehr L, Brandt J, Johnsen S, Reichardt H, Furlow J, Bodine S. 2008. The glucocorticoid receptor and FOXO1 synergistically activate the skeletal muscle atrophy-associated MuRF1 gene. *American Journal of Physiology-Endocrinology and Metabolism.* 295: E785–E797

18. Schakman O, Kalista S, Barbé C, Loumaye A, Thissen J. Glucocorticoid-induced skeletal muscle atrophy. The International Journal of Biochemistry & Cell Biology. 2013. 45:2163– 2172

19. Kuo T, Harris C , Wang J-C. Metabolic functions of glucocorticoid receptor in skeletal muscle. Molecular and Cellular Endocrinology. 2013.380: 79–88

20. Liberman A, Antunica-Noguerol M, Arzt E. Modulation of the Glucocorticoid Receptor Activity by Post-Translational Modifications. Nuclear Receptor Research. 2014. Vol. 1, Article ID 101086, 15 pages

21. Cipriano R, Miskimen KL, Bryson BL, Foy CR, Bartel CA, Jackson MW. Conserved oncogenic behavior of the FAM83 family regulates MAPK signaling in human cancer. Molecular cancer research: MCR. 2014; 12:1156-1165.

22. Wang Z, Liu Y, Zhang P, Zhang W, Wang W, Curr K, Wei G, Mao JH. FAM83D promotes cell proliferation and motility by downregulating tumor suppressor gene FBXW7. Oncotarget. 2013; 4:2476-2486. doi: 10.18632/ oncotarget.1581.

23. Walian P.J. , Hang B, Mao J.H., Prognostic significance of FAM83D gene expression across human cancer types, Oncotarget 7 (3) (2016) 3332–3340.

24. Liao W, Liu W, Liu X, Yuan Q, Ou Y, Qi Y, Huang W, Wang Y, Huang J. Upregulation of FAM83D affects the proliferation and invasion of hepatocellular carcinoma, Oncotarget: 2015; 6 (27): 24132–24147.

25. Wang D, Han S, Peng R, Wang X, Yang X, Yang R, Jiao C, Ding D, Ji G, Li X. FAM83D activates the MEK/ERK signaling pathway and promotes cell proliferation in

hepatocellular carcinoma. Biochemical and Biophysical Research Communications: 2015; 458: 313-320

26. Shi R, Sun J, Sun Q, Zhang Q, Xia W, Dong G, Wang A, Jiang F, Xu L. Upregulation of FAM83D promotes malignant phenotypes of lung adenocarcinoma by regulating cell cycle, Am. J. Cancer Res: 2016; 6 (11): 2587– 2598.

27. Inamura K, Shimoji T, Ninomiya H, Hiramatsu M, Okui M, Satoh Y, Okumura S, Nakagawa K, Noda T, Fukayama M, Ishikawa Y. A metastatic signature in entire lung adenocarcinomas irrespective of morphological heterogeneity. Human pathology. 2007; 38:702-709.

28. Ramakrishna M, Williams LH, Boyle SE, Bearfoot JL, Sridhar A, Speed TP, Gorringe KL, Campbell IG. Identification of candidate growth promoting genes in ovarian cancer through integrated copy number and expression analysis. PloS one. 2010; 5:e9983.

29. Zhu H., Diao S., Lim V., Hu L., Hu J. FAM83D inhibits autophagy and promotes proliferation and invasion of ovarian cancer cells via PI3K/AKT/mTOR pathway. Acta Biochim Biophys Sin. 2019, 1–8. doi: 10.1093/abbs/gmz028

30. Mu Y, Zou H, Chen B, Fan Y, Luo S. FAM83D knockdown regulates proliferation, migration and invasion of colorectal cancer through inhibiting FBXW7/Notch-1 signaling pathway. Biomedicine & Pharmacotherapy: 2017; 90: 548–554

31. Huang M, Ma X, Shi H, Hu L, Fan Z, Pang L, Zhu P, Yang X, Xu W, Liu B, Zhu Z and Li C. FAM83D, a microtubule-associated protein, promotes tumor growth and progression of human gastric cancer. Oncotarget. 2017. Vol. 8, (No. 43), pp: 74479-74493

32. Fulcher L, Bozatzi P, Tachie-Menson T, Wu K, Cummins T, Bufton J, Pinkas D, Dunbar K, Shrestha S, Wood N, Weidlich S, Macartney T, Varghese J, Gourlay R, Campbell D, Dingwell K, Smith J, Bullock A, and Sapkota G. The DUF1669 domain of FAM83 family proteins anchor Casein Kinase 1 isoforms. 2018. Sci Signal. ; 11(531): . doi:10.1126/scisignal.aao2341.

33. Fulcher L, He Z, Mei L, Macartney T, Wood N, Prescott A, Whigham A, Varghese J, Gourlay R, Ball G, Clarke R, Campbell D, Maxwell C, Sapkota G. FAM83D directs protein kinase CK1α to the mitotic spindle for proper spindle positioning. EMBO Reports. 2019. 20(9): e47495 https://doi.org/10.15252/embr.201847495

34. Dunsch A, Hammond D, Lloyd J, Schermelleh L, Gruneberg U, Barr F. Dynein light chain 1 and a spindle-associated adaptor promote dynein asymmetry and spindle orientation. Journal of Cell Biology. 2012.Vol. 198 No. 61039–1054

35. Jackman RW, and Kandarian SC. The molecular basis of skeletal muscle atrophy. Am J Physiol Cell Physiol: 2004; 287: C834-843

36. Bentzinger C, Wang Y, Rudnicki M. Building Muscle: Molecular Regulation of Myogenesis. Cold Spring Harb. Perspect. Biol. 2012.4:a008342

37. Varisli,L. Meta-analysis of the expression of the mitosis-related gene Fam83D. Oncology Letters. 2012. 4(6)1335–1340.

38. Zhang Q, Yu S, Lok S, Wong A, Jiao Y, Lee L. FAM83D promotes ovarian cancer progression and its potential application in diagnosis of invasive ovarian cancer, Journal of Cellular and Molecular Medicine.2019. 23(7)4569–4581.

39. Selvy P, Lavieri R, Lindsley C, Brown A. Phospholipase D: Enzymology, Functionality, and Chemical Modulation. Chemical Reviews. 2011. (111) 6064-6119

40. Bayón Y. and Alonso A. 2010. Atypical DUSPs: 19 phosphatases in search of a role. Emerging *Signaling Pathways in Tumor Biology.* 2010: 185-208

41. Friedberg I, Nika K, Tautz L, Saito K, Cerignoli F, Friedberg I, Godzik A, Mustelin T. 2007. Identification and characterization of DUSP27, a novel dual-specific protein phosphatase. *Federation of European Biochemical Societies Letters.* 581: 2527–2533

42. Geng T, Liu Y, Xu Y, Jiang Y, Zhang N, Wang Z, Carmichael G, Taylor H, Li D, Huang Y. H19 lncRNA Promotes Skeletal Muscle Insulin Sensitivity in Part by Targeting AMPK. Diabetes. 2018. 67:2183–2198

43. Singh, K., Dilworth, F.J., 2013. Differential modulation of cell cycle progression distinguishes members of the myogenic regulatory factor family of transcription factors. FEBS J. 280, 3991–4003.

44. Merlie JP, Mudd J, Cheng TC, Olson EN. Myogenin and acetylcholine receptor alpha gene promoters mediate transcriptional regulation in response to motor innervation. The Journal of Biological Chemistry. 1994. 269: 2461-7.

45. Devi Y, Seibold A, Shehu S, Maizels E, Halperin J, Le J, Binart N, Bao L, Gibori G. Inhibition of MAPK by Prolactin Signaling through the Short Form of Its Receptor in the Ovary and Decidua. *The Journal of Biological Chemistry*. 2010. VOL. 286, NO. 9, pp. 7609–7618

46. Garcia D and Shaw R. AMPK: Mechanisms of Cellular Energy Sensing and Restoration of Metabolic Balance. Molecular Cell. 2017. Volume 66, Issue 6: Pages 789-800

47. Stein S, Woods A, Jones N, Davidson M, and Carling D. The regulation of AMP-activated protein kinase by phosphorylation. Biochemical Journal. 2000. 345: 437-443

48. Nader N, Ng SS, Lambrou GI, et al. AMPK regulates metabolic actions of glucocorticoids by phosphorylating the glucocorticoid receptor through p38 MAPK. *Mol Endocrinol*. 2010;24(9):1748–1764. doi:10.1210/me.2010-0192

49. Galliher-Beckley A. and Cidlowski J. Emerging Roles of Glucocorticoid Receptor Phosphorylation in Modulating Glucocorticoid Hormone Action in Health and Disease. IUBMB Life. 2009. 61(10): 979–986

50. Kadmiel M and Cidlowski J. Glucocorticoid receptor signaling in health and disease. Trends in Pharmacological Sciences. 2013. Vol. 34, No. 9:518- 530.

51. Beck I, Berghe W, Vermeulen L, Yamamoto K, Haegeman G, Bosscher K. Crosstalk in Inflammation: The Interplay of Glucocorticoid Receptor-Based Mechanisms and Kinases and Phosphatases. Endocrine Reviews. 2009. December 30(7):830–882